ISTANBUL TECHNICAL UNIVERSITY ★ GRADUATE SCHOOL OF SCIENCE ENGINEERING AND TECHNOLOGY

DIRECT SYNTHESIS OF PARAFFINS FROM COMBINED FISCHER TROPSCH AND HYDROCRACKING

M.Sc. THESIS

Yusuf TANUĞUR

Department of Chemical Engineering

Chemical Engineering Programme

Thesis Advisor: Prof. Dr. A. Nursen İPEKOĞLU

JANUARY 2012

ISTANBUL TECHNICAL UNIVERSITY ★ GRADUATE SCHOOL OF SCIENCE ENGINEERING AND TECHNOLOGY

DIRECT SYNTHESIS OF PARAFFINS FROM COMBINED FISCHER TROPSCH AND HYDROCRACKING

M.Sc. THESIS

Yusuf TANUĞUR
(506091058)

Department of Chemical Engineering

Chemical Engineering Programme

Thesis Advisor: Prof. Dr. A. Nursen İPEKOĞLU

JANUARY 2012

İSTANBUL TEKNİK ÜNİVERSİTESİ ★ FEN BİLİMLERİ ENSTİTÜSÜ

PARAFİNLERİN FİSCHER-TROPSCH VE HİDROKRAKİNG BİRLEŞİK YÖNTEMİ İLE DOĞRUDAN SENTEZİ

YÜKSEK LİSANS TEZİ

Yusuf TANUĞUR
(506091058)

Kimya Mühendisliği Anabilimdalı

Kimya Mühendisliği Programı

Tez Danışmanı: Prof. Dr. A. Nursen İPEKOĞLU

OCAK 2012

Yusuf TANUĞUR, a **M.Sc.** student of ITU **Graduate School of Science Engineering and Technology** student ID **506091058**, successfully defended the **thesis** entitled "**DIRECT SYNTHESIS OF PARAFFINS FROM COMBINED FISCHER TROPSCH AND HYDROCRACKING**", which he prepared after fulfilling the requirements specified in the associated legislations, before the jury whose signatures are below.

Thesis Advisor :	**Prof. Dr. A. Nursen İPEKOĞLU** Istanbul Technical University	.....
Jury Members :	**Prof. Dr. Ayşe AKSOY** Istanbul Technical University	.....
	Assist. Prof. Dr. Sibel KABAKCI Yalova University	.....

Date of Submission : 19 December 2011
Date of Defense : 25 January 2012

To my Parents,

FOREWORD

I would like to gratefully thank to my supervisor Prof. Dr. A. Nursen İPEKOĞLU for her supervision, support and guidance during my MSc. study and also I would like to express my sincere thanks for her patience during the editing of this dissertation.

I would like to acknowledge my gratitute to Prof. Dr. Filiz KARAOSMANOĞLU for her help and guidance through the analysis of this study results and her support in determining the the direction of this study.

For his support, advice and guidance through the experimental study at University of Cape Town, I would like to express my special thanks to Prof. Jack Q. C. FLETCHER without whom this study would not be possible.

I would like to acknowledge my special thanks to Dr. Roald BROSIUS for his guidance and patience in practially everything about this study; operation of the experimental setup, conduction of the experiments and for his encouraging ideas.

A special thanks to University of Cape Town Chemical Engineering Department for the use of their facilities and other sources and also I would like to express my regards for all staff members in University of Cape Town for their helpfulness and kindness and to my collegues in UCT for providing entertaining environment during the study.

I would like to express my most grateful thanks to YÖK (The Council of Higher Education) for its financial support by providing scholarship during my study visit in South Africa.

I would like to thank to Yalova University Energy System Engineering Department for providing perfect study environment and encouraging efforts which made this study possible.

Last of all, I would like to express my thanks to my parents for their support, patience and love during this study and my friends for their help, patience and keeping me concentrated and willing during this Msc study.

December 2011

Yusuf TANUĞUR
Chemical Engineer

TABLE OF CONTENTS

Page

ABBREVIATIONS

[Ar]	: Peak Area of Argon in the sample
$[Ar]_c$	: Peak Area of Ar in the calibration sample
[CO]	: Peak Area of CO in the sample
$[CO]_c$	: Peak Area of CO in the calibration sample
A_{C16}	: Peak Area of C16
A_i	: Peak Area of Species i
ASF	: Anderson Schulz Flory Distribution
C16	: n-hexadecane
CFTH	: Combined Fischer Tropsch and Hydrocracking
FID	: Flame Ionizer Detector
FT	: Fischer Tropsch
GC	: Gas Chromatography
GHSV	: Gas Hourly Space Velocity
GTL	: Gas to Liquid
HTFT	: High Temperature Fischer Tropsch Synthesis
IEA	: International Energy Agency
LTFT	: Low Temperature Fischer Tropsch Synthesis
MFI	: Mordenite Framework Inverted
Mtoe	: Million tonnes oil equivalent
PFD	: Process Flow Diagram
$S(C_i)$	: Carbon Selectivity of Species i
$S(CO_2)$	: Selectivity of Carbon monoxide
SASOL	: South African Coal and Oil (Suid Afrikaanse Steenkool en Olie)
Syngas	: Synthesis Gas
TCD	: Thermal Conductivity Detector
TKI	: Turkish Coal Enterprise (Türkiye Kömür İşletmeleri)
TOS	: Time on Stream
TTK	: Turkish Hard Coal Enterprise (Türkiye Taş Kömürü Kurumu)
UCT	: University of Cape Town
WGS	: Water Gas Shift Reaction
WHSV	: Weight Hourly Space Velocity
w/w	: Weight percentage
ZSM-5	: Zeolite Socony Mobile

LIST OF TABLES

Page

LIST OF FIGURES

Page

DIRECT SYNTHESIS OF PARAFFINS FROM COMBINED FISCHER TROPSCH AND HYDROCRACKING

SUMMARY

Coal can be used directly by combustion or with thermal conversion secondary energy sources can ve produced from coal. There different types of thermal conversion methods and gasification is one of the most important type of thermal conversion technology. Synthesis gas (H_2 and CO mixture) is one of the most important main products of gasification process. It can be used in chemical industry in addition to that it can be used for alternative fuel production. Synthesis can be further transformed into gasoline and diesel fuel hydrocarbons via Fischer-Tropsch Synthesis. However Fischer-Tropsch Synthesis has very wide range of hydrocarbon distribution. Thus product upgrading is necessary for synthesis of desired hydrocarbons. Hydrocracking can be applied for cracking the long chain hydrocarbons into desired ranged hydrocarbons. But hydrocracking process increases the investment and operation cost. One of the suggested methods for lowering the cost and upgrading the system is Combined Fischer-Tropsch and Hydrocracking Synthesis. Direct production of paraffins from synthesis gas can be done by Combined Fischer-Tropsch and Hydrocracking Synthesis. In this study, performance analysis of two different hydrocracking catalysts under low temperature Fischer-Tropsch synthesis conditions were examined. Pt/HMFI and Pd/HMFI bifunctional catalysts were selected for the comparison of the performance. Also two different metal loading on these cataylsts were applied in order to see whether the effect of metal loading could overcome the effect of low temperature Fischer Tropsch conditions. CO and H_2O were fed to the reactors as these compounds constitutes Fischer-Tropsch synthesis environment. Selectivities and n-hexadecane conversion rates of two different catalysts were compared under deactivating effects of CO and H_2O. Pd/HMFI bifunctional catalyst was chosen for hydrocracking part of the combined catalyst for combined synthesis experiments as it showed better performance under Fischer-Tropsch synthesis conditions and CO and H_2O environment. Cobalt and Pd/HMFI catalysts were mixed and direct synthesis of paraffins from syngas was done under low temperature Fischer-Tropsch synthesis conditions. Total paraffin, total olefin and methane selectivities were examined for different synthesis gas velocity and Pd loadings. At the experimental conditions, significant increase in total paraffin selectivity was observed. Methane selectivity at higher Pd loadings was lowered in comparison with standard Fischer Tropsch synthesis. Total olefin selectivity for both metal loadings were suppressed.Higher Pd loading on the combined catalyst showed higher CO conversion rates and overcame the effects of Fischer-Tropsch synthesis ambient conditions. In addition to that lowering synthesis gas velocity increased the CO conversion rates as the residence time in the reactors were increased. Thus very similar composition to diesel hydrocarbons was achieved. Besides it was observed that Combined Fischer-Tropsch and Hydrocracking can be applied to produce gasoline range hydrocarbons.

PARAFİNLERİN FİSCHER-TROPSCH VE HİDROKRAKİNG BİRLEŞİK YÖNTEMİ İLE DOĞRUDAN SENTEZİ

ÖZET

Günümüz dünyasında enerji sektörü pek çok sorunla karşılaşmaktadır. Dünya nüfusunun yaklaşık olarak %20'sinin elektrik enerjisine erişimi sağlanamamaktadır. Tüm gelişmiş ülkelerin güvenilir enerji kaynaklarına sahip olduğu düşünülürse, güvenilir enerji kaynaklarının sağlanamadığı bir dünyada ekonomik gelişme ve ilerlemeden bahsedilemez. Ucuz ve güvenilir enerji kaynaklarına erişim sürdürülebilir kalkınmanın temel şartlarından biridir. Bu nedenle şu anda kullanılabilir olan enerji teknolojilerinden tam olarak faydalanmak, daha geliştirmek ve yeni enerji kaynaklarının kullanımını desteklemek dünya üzerindeki her toplum için kaçınılımazdır. Kömür, son ikiyüz senedir insanlığın en temel enerji kaynaklarından biri olmuştur. 1800'lerin Avrupasında buhar makinelerinin gelişimi ve buna ek olarak kömürün kullanımının artması sanayi devriminin başlangıcı olarak sayılmaktadır. Kömürün yakılarak buhar eldesinde kullanılmasının yanısıra, ısınma amaçlı yoğun olarak kullanıldığı dönemler de olmuştur. Kömür 2011 yılı itibariyle dünyada birincil enerji arzının %30'unu, toplan elektrik üretiminin %41'lik kısmını oluşturmaktadır. Ayrıca kimya endüstrisi için önemli bir hammadde olan kömür, pek çok prosesde hammadde olarak kullanılabilmektedir. Fakat kömürün çevresel etkileri, kömür kullanımını bazı yönlerden kısıtlamaktadır. Kömür kullanımı ile oluşabilecek çevresel zararların en aza indirilmesini sağlayacak teknolojilerin geliştirilmesi bir seçenekten öte zorunluluk haline gelmiştir. Ayrıca dünyadaki mevcut kömür rezervlerinin 100-150 sene daha bitmeyeceğinin tahmin edilmesi, kömürün gelecekte önemini koruyacağını göstermektedir. Kömürün diğer fosil yakıtlarla karşılaştırıldığında dünya üzerindeki dağılımı daha eşittir. Bu nedenle her ülke için enerji konusunda dışa bağımlılıktan kurtulmanın önemli bir aşamasını kömürün enerji kaynağı olarak kullanılması oluşturmaktadır.

Kömür doğrudan yakılarak enerji kaynağı olarak kullanılabileceği gibi, ısıl dönüşüm teknolojileri ile de ikincil enerji kaynaklarına dönüştürülebilir. Isıl dönüşüm teknolojisi olarak piroliz, sıvılaştırma ve gazlaştırma gösterilebilir. Bu yöntemler ile kömürden ikincil enerji kaynaklarının üretiminin gerçekleştirilmesinin yanı sıra kimya endüstrisinde kullanılan çok farklı kimyasalların eldesi de mümkündür. Gazlaştırma ısıl dönüşüm teknolojileri arasında önemli bir yer tutmaktadır. Gazlaştırmanın temel amacı kömür, biyokütle gibi organik kaynaklardan CO ve H_2 gazlarını içeren sentez gazı elde etmektir. Gazlaştırma ile elde edilen sentez gazı kimya endüstrisinde kullanılabileceği gibi farklı oranlarda CO ve H_2 içeren sentez gazı Fischer-Tropsch sentezi ile benzin veya motorin hidrokarbonlarına dönüşümü de yapılabilir. Fischer-Tropsch sentezi uzun zamandır bilinen ve uygulanan bir teknolojidir. 1930'ların Almanya'sında geliştirilen bu yöntem daha sonraları başta Güney Afrika olmak üzere çeşitli ülkelerde uygulama alanı bulmuştur. Fischer-Tropsch sentezi farklı sıcaklık aralıklarında uygulanabilir. Düşük sıcaklıktaki uygulamalar genelde motorin hidrokarbonlarının üretiminde kullanılırken, yüksek

sıcaklık Fischer-Tropsch sentezi daha çok benzin hidrokarbonlarının üretiminde uygulanmaktadır. Fakat sıcaklık ve diğer proses parametreleri ne olursa olsun Fischer-Tropsch sentezi sonucunda ortaya geniş bir aralıkta ve farklı tipte hidrokarbonların bulunduğu karışım ortaya çıkmaktadır. Bu nedenle istenilen faydalı son ürünlere ulaşmak için Fischer-Tropsch sentezi ürünlerinin, ürün iyileştirme işlemine tabii tutulması gerekmektedir. Bu geniş aralıktaki hidrokarbon karışımından benzin ve motorin hidrokarbonlarına geçişinin Hidrokraking ile sağlanması mümkündür. Hidrokraking yöntemi petrol rafinerilerinde çok sık olarak kullanılmaktadır. Fischer-Tropsch sentezi içinde uygulanan bir yöntemdir. Sentez gazından motorin veya benzin elde edilirken prosese eklenecek her bir işlem aşaması ek maliyet gerektirmektedir. Bu maliyet probleminin çözümlerinden biri Birleşik Fischer-Tropsch ve Hidrokraking Sentezi uygulanmasıdır. Parafinlerin sentez gazından doğrudan üretiminde, Fischer-Tropsch ve Hidrokraking işlemlerinin birleştirilmesi, yatırım ve işletme maliyetlerini önemli oranda düşürecektir. Fischer-Tropsch ve Hidrokraking proseslerinin birleştirilmesi iki farklı tip katalizörün bir arada kullanılması ile mümkün olmaktadır.

Bu çalışmada Birleşik Fischer-Tropsch ve Hidrokraking sentezi ile motorin parafinlerinin üretimi amaçlanmıştır. Bu amaçla deneysel çalışma iki aşamada yürütülmüş ilk aşama olarak Birleşik Fischer-Tropsch ve Hidrokraking sentezi için Hidrokraking işlevini görecek iki tip katalizörün Fischer-Tropsch sentezi şartlarında performans analizi yapılmıştır. Deneysel çalışma sırasında Platin/HMFI ve Paladyum/HMFI katalizörleri test edilmiştir. Performans analizi sabit yataklı iki adet silindirik reaktörde gerçekleştirilmiştir. Deney düzeneği bu reaktörlerin yanı sıra analiz için olması gerekli olan buharlaştırıcı, gaz kromatografi, sıcaklığın ve basıncın kontrol edildiği düzenekler ve kütle akış kontrol cihazlarından oluşmaktadır. Reaktör yapılan deneyler sırasında sürekli olarak çalıştırılmıştır. Sürekli yapılan deneyler nedeniyle gaz kromatografi cihazı analiz için sisteme doğrudan bağlanmıştır. Gaz kromatografi analizi için iki farklı detektör ve cihaz kullanılmıştır. Seçiciklik hesabı için FID, karbonmonoksit dönüşüm oranının belirlenmesi için TCD tipi gaz detektörler kullanılmıştır. Reaktör çıkış akımı buharlaştırıcıda gaz haline geçmekte daha sonra bu gaz karışımı gaz kromatografi cihazına beslenmektedir. Yapılan deneysel çalışmada, deneysel çalışmanın tekrarlanabilirliğini artırmak ve daha güvenilir sonuçlar almak için katalizör reaktör içerisinde yatışkın bir sıcaklık profilinin elde edildiği bir noktaya yerleştirilmiştir ayrıca bu bölge dışarısında kalan kısımlar inert madde ile doldurulmuştur. Reaktörde sıcaklığı kontrol edebilmek ve ısı kayıplarını engellemek için reaktör yalıtım malzemesi ile kaplanmıştır. Katalizörün sabit sıcaklık bölgesine yerleştirmek dışında, reaktöre beslenen n-hekzadekanın akış debisinin de sabit olması gerekmektir. Bu amaçla deneysel çalışmaya başlamadan önce akış debisi, reaktöre katalizör yüklemeden boş olarak çalıştırılmıştır. Reaktör çıkışında n-hekzadekan debisi zamana bağlı olarak kontrol edilmiş, debinin değişmediği durum sağlandıktan sonra deneylere geçilmiştir. Analiz sırasında her iki katalizör için n-hekzadekan dönüşüm oranları ve seçicilikler karşılaştırılmıştır. n-hekzadekan dönüşüm oranının Fischer Tropsch sentezi ortamında yani karbonmonoksit ve suyun bulunduğu ortamda değişimi katalizörün seçiminde en etkili faktör olarak kullanılmıştır. Bu maddelerin birlikte beslendiği ortamda n-hekzadekan dönüşüm oranının düşüşü katalizörün aktivitesini kaybettiğini gösterir. Bu nedenle yüksek dönüşüm oranı veren katalizör yapılacak birleşik Fischer Tropsch sentezi ve hidrokraking için uygun olacaktır. Platin/HMFI katalizörü karbonmonoksit ortamında katalitik aktivitesini büyük oranda kaybetmiştir. Karbonmonoksit beslemesinin durdurulması katalitik aktivitenin geri kazanılmasını sağlamamıştır.

Platin/HMFI katalizör su ortamında ise tüm aktivitesini kaybetmiştir. n-hekzadekan dönüşümü tamamen durmuştur. Bu karşın Paladyum/HMFI çift etkili katalizörü karbonmonoksit ve su ortamında aktivitesini bir miktar kaybetmesine rağmen n-hekzadekan dönüşüm oranlarındaki düşüş Platin/HMFI katalizöründe olduğu kadar büyük olmamıştır. Bu analiz sonucunda çift işlevli Paladyum/HMFI katalizörü kombine sentez için seçilmiştir. Bunun nedeni Paladyum/HMFI katalizörünün, Platin/HMFI katalizörüne göre daha yüksek karbonmonoksit ve su toleransı göstermesidir. Paladyum/HMFI zeoliti katalizöründe paladyum metali büyük hidrokarbonların hidrojen ile daha sonraki reaksiyonlar için aktive olmasını sağlar. Zeolit kısım ise hidrokraking ve izomerizasyon olayının gerçekleştiği kısımdır. Deneysel çalışmanın ikinci aşamasında, seçilen bu katalizör daha sonra Pd/HMFI katalizörü Kobalt katalizörü ile fiziksel olarak karıştırılarak, Düşük Sıcaklık Fischer-Tropsch Sentezi şartlarında, sentez gazından doğrudan motorin parafinlerinin üretimi amaçlanmıştır. Doğrudan motorin parafinleri eldesi için kullanılan deney düzeneği hidrokraking çalışmasında kullanılan sistem ile aynıdır. Deney sistemine karbonmonoksit ve hidrojen gazı beslenerek, kobalt katalizörü yardımı ile Fischer Tropsch sentezi ürünleri elde edilmiştir. Bu ürünleri eş zamanlı olarak hidrokraking katalizörü üzerinde daha kısa hidrokarbonlara dönüştürülmüş ve izomerleşmiştir. Elde edilen sonuçlar metan, toplam olefin ve toplam parafin seçicilikleri bakımından tartışılmıştır. Ayrıca hidrokraking deneylerinden farklı olarak karbonmonoksit dönüşüm oranı katalizörün zamana karşı deaktivasyonunu incelemede kullanılmıştır. Bunların yanında iki farklı Paladyum yüklemesinin karbonmonoksit dönüşüm oranı ve seçicilikler üstündeki etkisi incelenmiştir. Deneyler sırasında dört farklı sentez gazı debisinde çalışılmış, reaktörde kalma süresinin birleşik fischer tropsch ve hidrokraking üzerindeki etkisi incelenmiştir. Birleşik Fischer Tropsch ve Hidrokraking sonuçları ile karşılaştırma yapılabilmesi için reaktörlerin birine sadece kobalt katalizörü yüklenmiştir. Yapılan karşılaştırmalar sonucunda reaktörde kalma süresinin artması ile karbonmonoksit dönüşümünün arttığı gözlemlenmiştir. Reaktörde kalma süresinin toplam parafin ve toplam olefin seçiciliği üzerinde etkisi küçük olmuştur. Bunun yanında metan seçiciliği reaktörde kalma süresi ile azalma göstermiştir. Birleşik Fischer Tropsch ve Hidrokraking sonucunda, Fischer Tropsch sentezi için yüzde yirmi mertebelerinde olan metan seçiciliği yüksek Paladyum yüklemesinde yüzde on mertebelerine indirilmiştir. Fischer Tropsch katalizörüne hidrokraking katalizörünün eklenmesi izomerleşmiş ürünlerin seçiciliğinde artışa neden olmuştur. Deneysel çalışma sırasında Fischer Tropsch sentezi ile üretilen en uzun karbon zincirli hidrokarbonda on sekiz karbon atomu bulunan ürün elde edilmiştir. Hidrokraking katalizörünün katılması ile birlikte zincir boyu on iki karbonlu hidrokarbonlara düşmüştür. Ayrıca Fischer Tropsch sentezi ile yoğun miktarda olefin elde edilmiştir. Birleşik Fischer Tropsch ve Hidrokraking ile olefinlerin parafinlere dönüşümü sağlanmıştır. Bu çalışmada denenen koşullar sonucunda, toplam parafin seçiciliğinde önemli oranda artış gözlemlenmiş, motorin hidrokarbonlarına oldukça yakın ürün bileşimi elde edilmiştir. Farklı Paladyum yüklemesinin ürün seçicilikleri üstünde etkisi olmuştur. Metan seçiciliği yüksek miktardaki metal yüklemesi için daha fazla olmuş buna karşılık düşük Paladyum yüklemesinde metan seçiciliğin daha fazla olduğu gözlemlenmiştir. Ayrıca daha fazla Paladyum yüklemesinin karbonmonoksit dönüşüm oranını artırdığı gözlemlenmiştir. Ürün bileşimi olarak daha az olefin ve daha çok parafin içeren bir karışım elde edilmiştir. Ayrıca izomer ürünlerin seçiciliklerinde artış gözlemlenmiş bu da dizel ürün yanında birleşik Fischer Tropsch ve Hidrokraking sentezinin motorin hidrokarbonlarının üretiminde de kullanılabileceğini göstermiştir.

1. INTRODUCTION

The global energy system has many challenges. Currently nearly 20 % of the world population, 1.4 billion people have no access to electricity. Without proper energy production and distribution, economical development is not possible. Affordable, reliable and secure energy sources will promote sustainable economical development. As providing 30 % of total primary supply and 41 % of total electricity generation in the world, coal plays crucial role in energy policies and economy of the world. With its reserves believed not to deplete in next 100-150 years, coal will keep its importance in the future. Not only for energy production, but also usage of coal in many types of industries makes coal crucial and inevitable resource. Neglecting coal in future energy policies is not possible as stable coal prices, secure supply chain and fairly distribution around the world make coal reliable energy source. Minimizing any negative impacts of coal usage and maximizing the advantages of coal will provide prosperity to world.

Beside from its direct usages like combustion, thermal conversion technologies can also be applied to coal. Gasification is one of the important thermal conversion processes and it is widely used commercially around the world. Basically gasification is the process where carbon atoms transform synthesis gas (syngas) which is a mixture of H_2 and CO. Syngas can be directly burned in order to produce heat and eventually electricity or it can go further transformation in which different range of hydrocarbons synthesized.

Named after its founders, Fischer-Tropsch Synthesis is the method of conversion of syngas to oil based gasoline, diesel fuel hydrocarbons. Currently there are several examples of industrial FT facilities around the world. Sasol (Suid Afrikaanse Steenkool en Olie), a South Africa based company, is operating four FT facilities in South Africa. Plant in Sasolburg is operational since 1955 and using coal as feedstock. In addition to that plant, there are two more plants in Secunda and they are also using coal for syngas production. Last plant of Sasol in South Africa is in Mossel Bay and it is a gas to liquid (GTL) facility. Outside of South Africa, Sasol is

operating a GTL facility in collaboration with Qatar Petroleum in Qatar. Beside from SASOL plants, Shell has opened a GTL facility in Malaysia, Bintulu in 1993. Chevron is planning to open a GTL plant in Escravos, Nigeria. It is expected to start production of synthetic fuels in 2013.

Due to the nature of FT synthesis, products range from methane to heavy waxes. So in order to produce desired range hydrocarbons, products of FT synthesis should be further upgraded to desired product spectrum. One of the products upgrading method is Hydrocracking (HC). HC is the process where long hydrocarbons get cracked to shorter ones. After the HC, FT products are in desired range of diesel or gasoline fuel. However implying a HC step to FT synthesis increases the total investment and operation cost.

Combined Fischer Tropsch and Hydrocracking (CFTH) synthesis is a possible upgrade in which FT and HC reactions occurred simultaneously at single stage. By CFTH, paraffins for diesel fuels can be directly synthesized. Thus investment an operation costs can be significantly lowered.

Aim of the this study is to compare different bifunctional HC catalysts performance under Low Temperature Fischer-Tropsch (LTFT) synthesis conditions and eventually produce paraffins for diesel fuel from CFTH reactions by using the selected HC and FT catalyst. Performance of two bifunctional HC catalysts under LTFT synthesis conditions were compared for their conversion rates and selectivities. After the performance tests, HC catalyst was combined with FT catalyst. Direct synthesis of Paraffins from syngas was done with combined catalyst. Results of direct synthesis were examined for their paraffins, olefins and methane selectivities.

2. THEORETICAL STUDY

In this chapter theoretical study is briefly presented under the following titles:

- World Energy Outlook
- Turkey Energy Statistics and Coal
- Coal as Energy Source
- Fischer Tropsch Synthesis
- Hydrocracking
- Literature Review

2.1 World Energy Outlook

According to IEA Key World Energy Statistics 2011, between 1973 and 2009 total primary energy supply has risen from 6,111 Mtoe (Million tonnes oil equivalent) to 12,150 Mtoe. Figure 2.1 shows the total primary energy supply by fuels between 1971 and 2009. Fossil fuels are still the main source of energy. In 2009 total oil consumption is at the first place with 4,095 Mtoe. Oil is followed by coal with 3299 Mtoe. Shares of different fuels in energy production are given in Figure 2.2 [1].

Between years 1973 and 2009, usage of oil as an energy source decreased from 46 % to 32.8 % due to increase in usage of natural gas and coal. Coal usage percentage has increased from 24.6 % to 27.2 %. Nearly half of the total production of coal is come from China. China is followed by OECD countries with 23.7 % of total production. Figure 2.3 shows the hard coal production distribution for different regions.

According to IEA, world total coal demand will be shifted towards non-OECD countries. In IEA projection of 2035 US and EU coal demand will be decreased due to new legislations concerning CO_2 emissions. On the other hand, China and India will make nearly 60 % of total coal demand alone in 2035 [2]. According to Bundesanstalt für Geowissenschaften und Rohstoffe (BGR) coal reserves stand for nearly 77 % of total non-renewable resources which will supply the coal demand for 150 years if the same production and consumption trends continue [3].

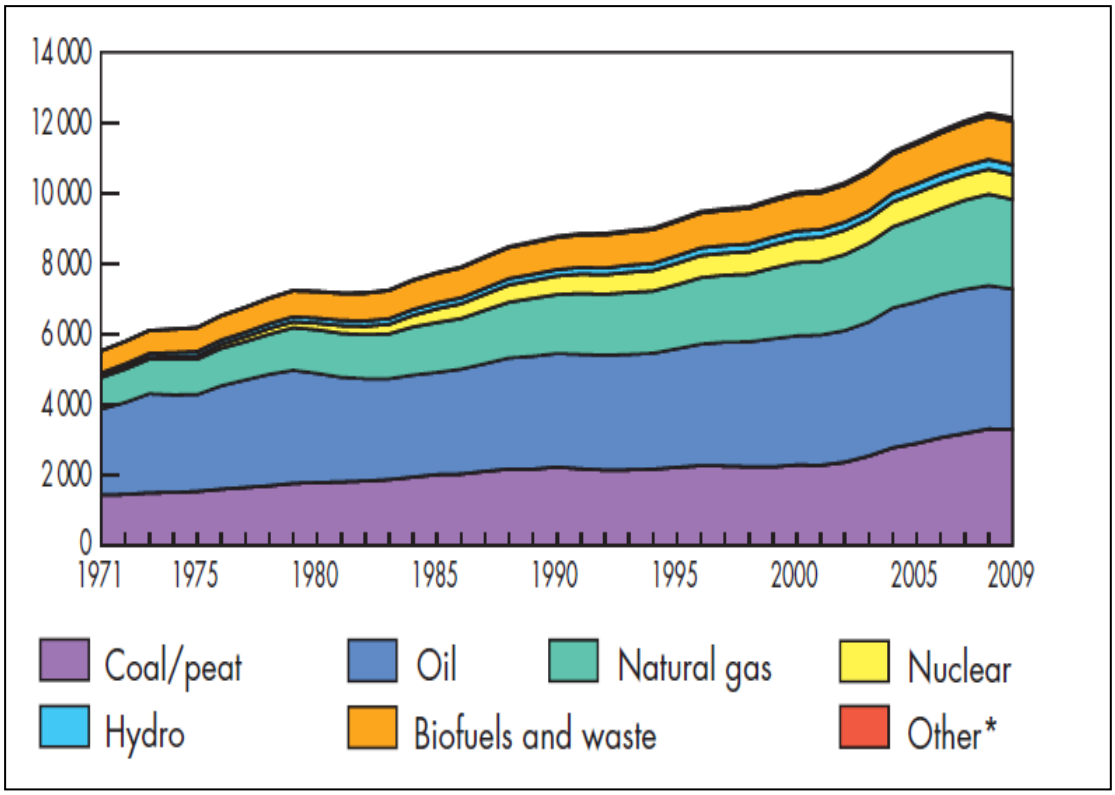

Figure 2.1 : Primary energy demands for different energy sources between 1971 2009 (Other includes; solar, wind, geothermal etc.) [1].

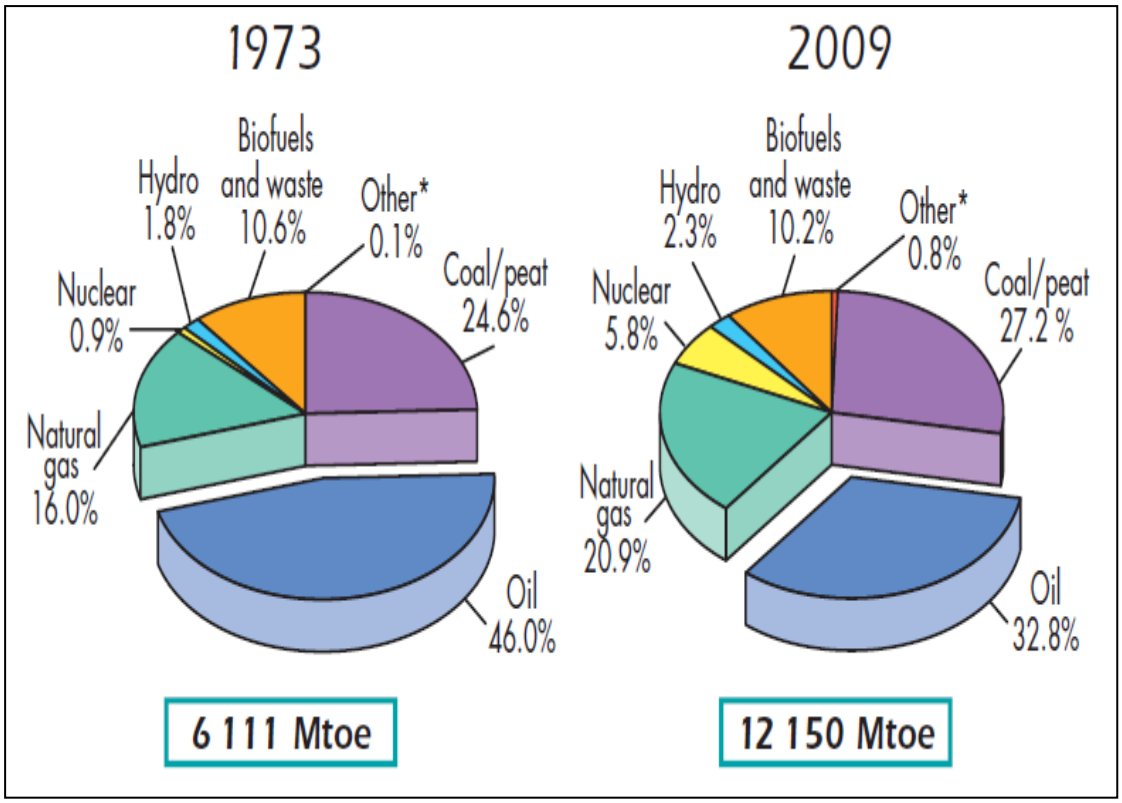

Figure 2.2 : Shares of different energy sources in 1973 and 2009 (Other includes solar, wind geothermal etc.) [1].

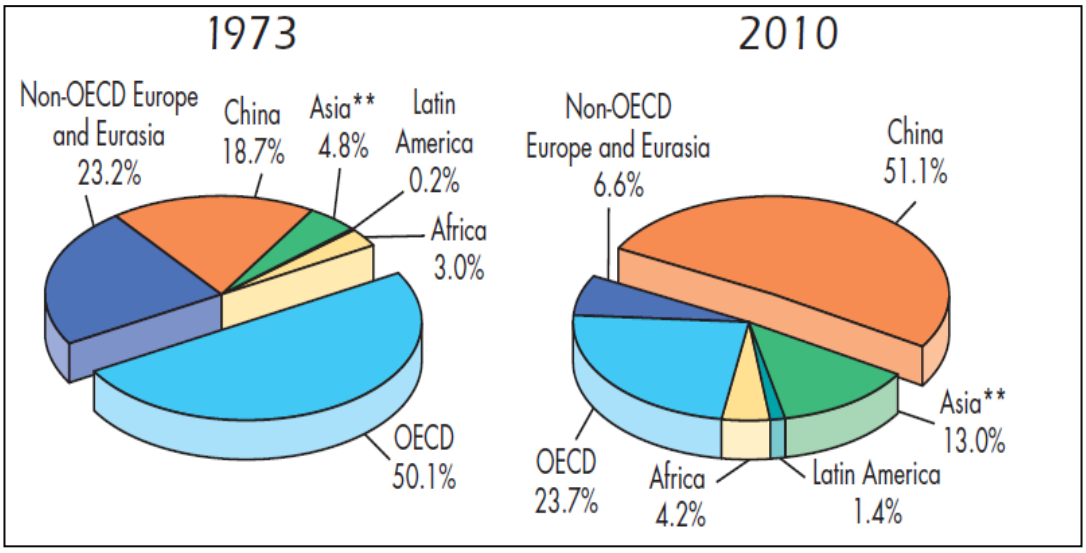

Figure 2.3 : Hard coal production for different regions(**: China excluded) [1].

2.2 Turkey Energy Statistics and Coal

In 2010, Turkey total primary energy demand is 109,266 toe. Figure 2.4 shows the shares of different primary energy sources demand of Turkey in 2010. Fossil resources accounts for 91 % of total demand. Oil, Natural gas are the main energy sources in Turkey. Nearly half of the total demand of oil comes from transportation sector. On the other hand natural gas is widely used for electricity production and heating [4,5].

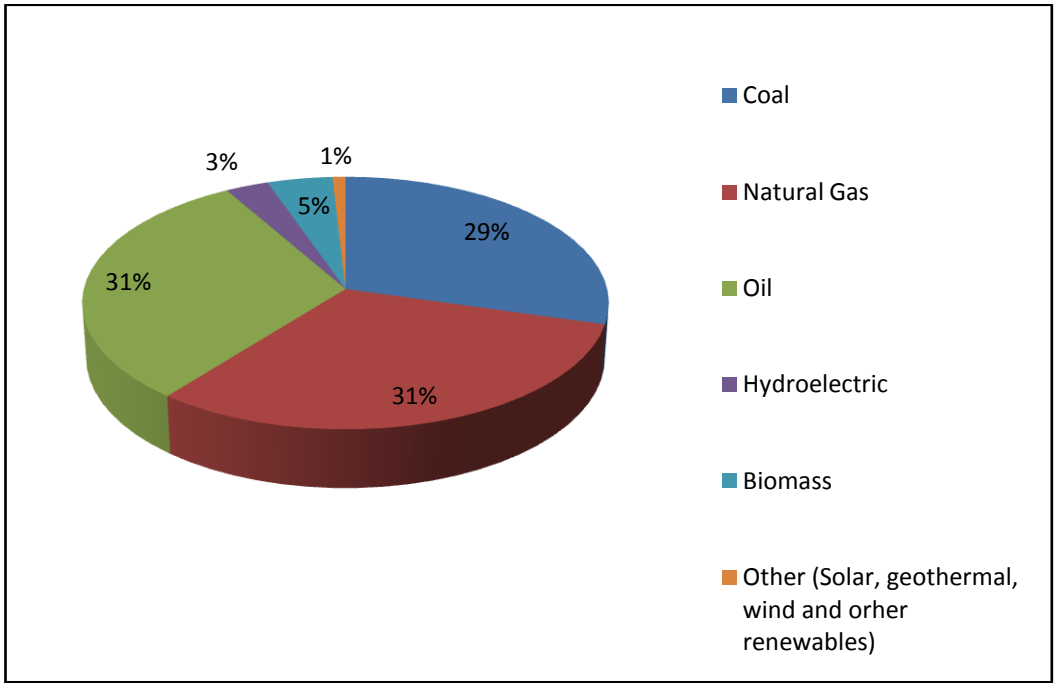

Figure 2.4 : Distribution of different primary energy sources in Turkey [4].

Nearly 98 % of natural gas and oil sources were imported in 2010. 90% of bituminous coal sources were imported from different countries. So totally nearly 75 % of energy sources are imported and 25 % is national product. In other word Turkey is dependent on other countries in energy area [4,5].

In Turkey coal mining started in 8th November 1829. Retired sailor Uzun Mehmet (Mehmet the Long) was the first person who found coal in Anatolia. However there is no certain knowledge about the exploration of lignite in Turkey. Lingite usage in Ottoman Era started in the late period of the empire. Between years 1914 and 1918 lignite mining facilities started near Soma. Later during First World War Lignite was intensively used as a fuel in Ottoman navy. In Republic Era lignite mining has been developed over the all country. From Ottoman times to late Turkish Republic coal gas was used in the largest cities of Turkey like Istanbul, Izmir and Ankara. First Coal Gas production facilities In Turkey were opened in Istanbul in 1887 and 1891 [6].

Two state owned enterprises govern the coal mining in Turkey. TKI (Turkish Coal Enterprise) is responsible for lignite mining and TTK (Turkish Hard Coal Enterprise) is the sole body for mining of hard coal.

According to TKI data, total lignite reserve is about 2.5 billion tones [7]. Table 2.1 is given to show the distribution of national reserves.

Table 2.1 : Distribution of Turkish national lignite reserves [7].

Location	Reserves (Million Tonnes)	Percentage (%)
Soma	623	23.5
Tavşanlı	276	10.5
Milas	267	10
Yatağan	152	5.8
Seyitömer	180	6.9
Ilgın	424	16
Orhaneli	97	3.7
Çan	79	2.9
Silopi	73	2.7
Other	474	18
Total	2648	100

Beside from Turkey's lignite reserves there is also a significant bituminous coal reserves can be found in Turkey. The largest part of the bituminous coal reserves are

in the Zonguldak region. In total 887.7 million tonnes bituminous coal reserves are available in Turkey. According to TTK, hard coal reserves in Turkey are distributed as shown in Table 2.2 [8].

Table 2.2 : Hard coal reserves of Turkey (Amounts are in million tonnes) [8].

Reserve Type	Bituminous				Semi Bituimous	Non Bitumious	Total
	Kozlu	Üzülmez	Karadon	Total	Armutçuk	Amasra	
Measured	2.35	1.38	5.61	9.34	1.10	0.41	10.85
Indicated	67.70	136.14	131.46	335.30	9.03	170.83	515.15
Hypothetical	40.54	94.34	159.16	294.04	15.86	115.05	424.95
Speculative	47.98	74.02	117.03	239.03	7.88	121.54	368.45
Total	158.55	305.89	413.26	887.70	33.88	407.83	1319.40

Lignite resources that are used in Turkey are all national product. In 2010, total 155505 toe lignite is used as primary energy resource. Nearly 60 % of lignite was used in electricity production sector. Rest was used in industry and domestic heating. However, Turkey imported most of its hard coal demand. 15479 toe hard coal was demanded in 2010 and 13,734 Mtoe hard coal were imported from several countries. Half of the hard coal demand was due to electricity production sector and the rest was used in industry mainly in steel and cement production sector. Turkey is 8th largest coal importer in the world. This relatively high import rate is due to larger steel production sector. Turkey's steel production is 29Mt in year 2010.This production amount makes Turkey being ranked as 10th largest steel producer in the world [4,9,10].

2.3 Coal as Energy Resource

Since from the ancient times organic materials are used for energy production. After the discovery of fire, wood became the first fuel for humankind. And just before the industrial revolution coal became the major fuel. During industrial age coal was excessively used as an energy source. Also another usage of coal was for lighting and heating in large cities in 19th and early 20th by coal gas which is the product of coal gasification. Coal can be transformed into energy by direct combustion, co-combustion (mixture with other resources like biomass) and thermal conversion technologies. Thermal conversion technologies are consisting of pyrolysis, liquefaction and gasification [11,12,13].

The gasification of coal is the chemical or physical transformation to produce gaseous products that are combustible. Since 1970's, gasification process has an important role. By the end of 2008 world wide syngas capacity is about 57 GW_{th} and in 2014 it is planned to have gasification capacity about 158 GW_{th} [12,13]. Figure 2.5 shows the possible products that can be produced via gasification.

Main target of gasification process is to process syngas which is a mixture of H_2 and CO gases. During the process of gasification of solid carbon, whether in the form of coal, coke or char, the principle chemical reactions are those involving carbon, carbon monoxide, carbon dioxide, hydrogen, water (or steam) and methane. Reactions that occurs during the gasification given in Table 2.3.

Table 2.3 : Reactions in gasification process [12].

Reactions	Reaction Equation	Reaction Enthalpy	Reaction Number
Combustion Reactions	$C + ½O_2 = CO$	-111 MJ/kmol	2.1
	$CO + ½O_2 = CO_2$	-283 MJ/Kmol	2.2
	$H_2 + ½O_2 = H_2O$	-242 MJ/Kmol	2.3
Boudard Reaction	$C + CO_2 \leftrightarrow 2CO$	+172 MJ/kmol	2.4
Water-gas Reaction	$C + H_2O \leftrightarrow CO + H_2$	+131 MJ/kmol	2.5
Methanation Reaction	$C + 2H_2 \leftrightarrow CH_4$	-75 MJ/kmol	2.6
CO shift Reaction	$CO + H_2O \leftrightarrow CO_2 + H_2$	-41 MJ/kmol	2.7
Steam Methane Reforming Reactions	$CH_4 + H_2O \leftrightarrow CO + 3H_2$	+206 MJ/kmol	2.8

Reactions 2.1, 2.2 and 2.3 are not considered to determine syngas compositions at equilibrium. 2.4, 2.5 and 2.6 reactions are sufficient for determination. Considering where the carbon conversion is complete, by subtraction 2.4 from 2.5 and 2.5 from 2.6 , 2.7 and 2.8 reactions are obtained respectively. Most gasification process relies on balances between reactions 2.1 and 2.5. Overall reaction can be written as in equation 2.1.

$$C_nH_m + n/2O_2 = nCO + m/2H_2 \quad \textbf{(2.1)}$$

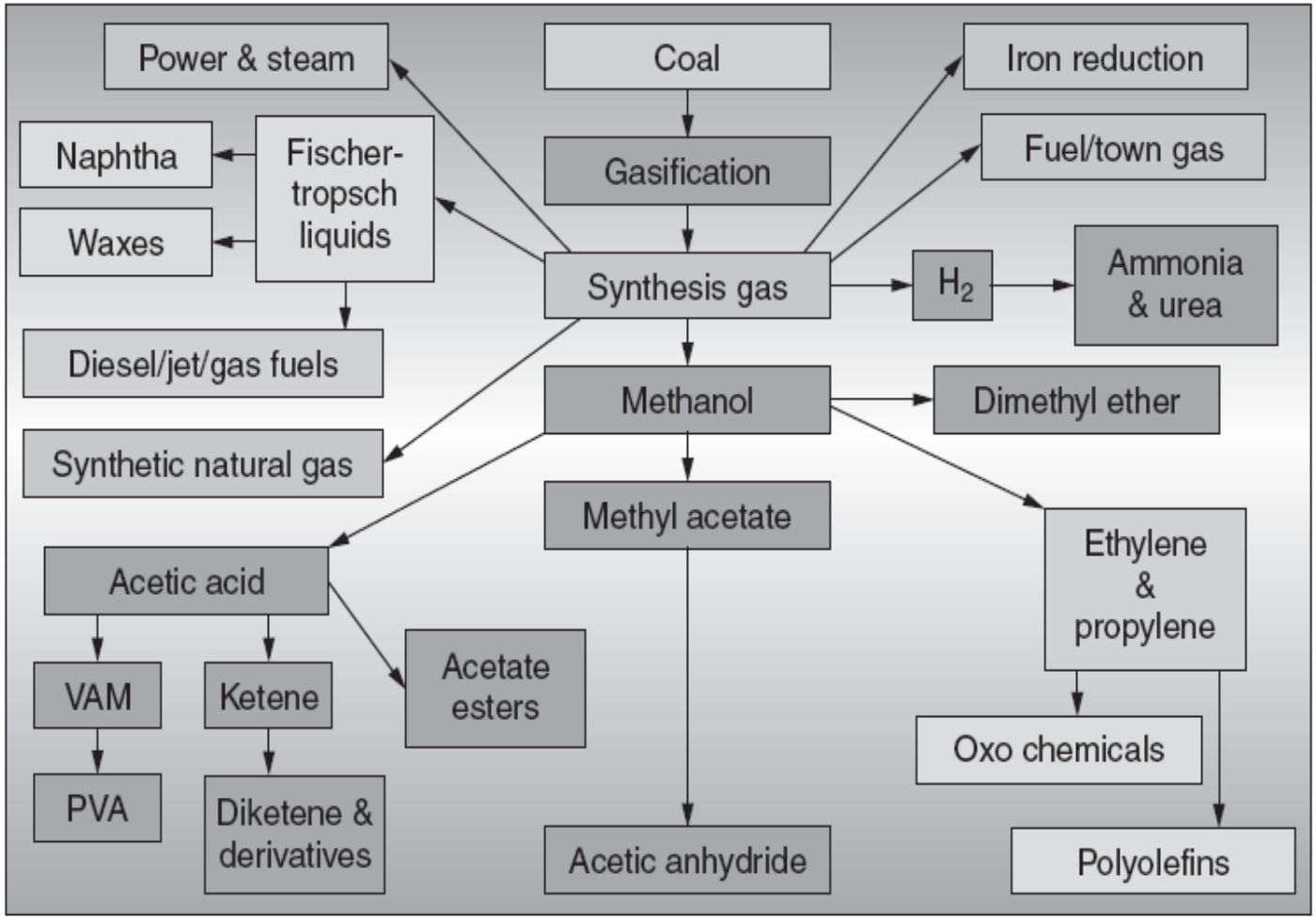

Figure 2.5 : Products of coal gasification (VAM: Vinyl acetate, PVA: Polyvinyl acetate) [14].

where

- for gas, as pure methane, m =4 and n =1, hence m/n = 4
- for oil, m/n ≈ 2, hence m =2 and n =1
- for coal, m/n ≈ 1, hence m = 1 and n = 1.

Gasification temperatures are in all cases so high that, thermodynamically as well as in practice, no hydrocarbons other than methane can be present in any appreciable quantity [12].

Syngas compositions for FT synthesis can vary with the temperature and the catalyst that are used during the process. For Co based FT, H_2/CO ratio is about 2.15 in order to assure higher conversion while in Fe based FT for 230°C typical H_2/CO ratio is about 1.7 [15].

2.4 Fischer-Tropsch Synthesis

FT synthesis is the catalytic conversion of synthesis gas (H_2/CO mixture) over a metallic catalyst yielding long chain hydrocarbons. Historic development of FT starts with production of methane from hydrogen and carbon monoxide over nickel, iron and cobalt catalyst by Sabatier and Sanderens in 1902. In 1923 , German scientists Dr. Franz Fischer and Hans Tropsch reported the use of alkalized iron catalyst to produce liquid hydrocarbons rich in oxygenated compound which is termed as the synthol process Commercialization of FT technology began in 1934 when Ruhrchemie A.G. undertook the industrial development of FT process. The first FT industrial operation went in operation in 1936 and at the end of 1940 over 1 million tons of FT liquids were produced. Licensed by Ruhrchemie, four facilities in Japan, as well as a plant in France and in Manchuria, were in service. After World War II, liquid fuels derived from coal were not profitable. The only new production facilities were in South Africa, for political reasons, built starting in 1950 in Sasolburg. During 60’s and 70’s due to cheap and abundant oil prices , interest in FT synthesis decreased. However latest environmental issues and increasing oil prices increased the attention on FT technologies [16,17].

The FT synthesis is, in principle, a carbon chain building process, where methylene groups are attached to the carbon chain [18]. The actual reactions that occur have been, and remain, a matter of controversy, as it has been the last century since 1930’s.

The overall FT process is described by the following chemical equations which are given in Table 2.4 [19].

CH_4 formation is the most favored hydrocarbon over the FT synthesis (temperature ranges 200°C-400°C) although it is the least desired product [20]. Water-gas shift reaction shows very little activity on Co based LTFT. Thus in order to produce the desired products, synthesis can be performed under kinetically controlled conditions [22]. Reactions are also highly exothermic. In order to avoid high temperature which will cause production of lighter hydrocarbons, having sufficient cooling and stable reaction conditions are important aspects of FT [14,21,22].

Table 2.4: FT reactions [19].

Reaction Equation	Reaction
$2nH_2 + nCO \rightarrow -(CH_2)-_n + nH_2O$	Main FT
$(2n+1)H_2 + nCO \rightarrow C_nH_{(2n+2)} + nH_2O$	Formation of Paraffins
$2nH_2+nCO \rightarrow C_nH_{2n} + nH_2O$	Formation of Olefins
$2nH_2+nCO \rightarrow C_nH_{(2n+1)}OH + (n-1)H_2O$	Formation of Alcohols
$CO + H_2O \leftrightarrow CO_2 + H_2$	Water-gas Shift(WGS)
$C + CO_2 \leftrightarrow 2CO$	Boudard Reaction
$3H_2 + CO \rightarrow CH_4 + H_2O$	Methanation

Currently there are two FT operating modes. HTFT synthtesis is operated at 300-350°C with iron-based catalysts. HTFT is suitable for the production of gasoline and linear low molecular mass olefins. LTFT synthesis is operated at 200-240 °C with either iron or cobalt catalysts and it is suitable for the production of high molecular mass linear waxes [16].

For large-scale commercial FT reactors heat removal and temperature control are the most important design features to obtain optimum product selectivity and long catalyst lifetimes. Thus different reactor designs were developed over the years. Four different types of FT reactors are available commercially. These are the multi-tubular fixed bed reactor, the slurry phase reactor and the fluidized bed reactor (with either fixed or circulating bed). Figure 2.6 shows the schematic representation of 4 different reactors that are used in FT synthesis [23].

The fixed bed reactors consist of multiple tubes. Catalyst is placed inside the tubes while cooling water stays on the shell side of the tubes. Short distance between catalyst particles and the tube walls and high gas velocities create turbulent flow inside the reactor. Due to turbulent flow, heat transfer is much easier. It is common practice to recycle some portion of the tail gas in order to gain more velocity and eventually better heat transfer which is crucial for cooling down of the reactor. Still as the tubes are very narrow, it is inevitable to achieve radial and axial temperature gradient. Due to this, it is hard to get steady temperature in the reactor which causes some of the catalyst particles not to achieve optimum temperature. Also due to high velocity and narrow tubes, there is high pressure gradient which causes disintegration of the catalyst bed. Also large fixed bed reactors can have thousands of tubes thus high investment costs are inevitable. Despite of these disadvantages, fixed bed reactors have some advantages. They can be operated more easily. As the catalyst and the products are separated, there is no need to do further separation between them after the operation. Fixed bed reactors are not suitable for HTFT since the temperature control is not easy [23, 24].

In the slurry phase reactors, reactants, products and catalyst are all in one mixture in the reactor. Catalyst is suspended in the slurry mixture. Heavy waxes forms the slurry phase, reagent gases diffuses into the catalyst from gas bubbles and water and lighter products diffuse from the liquid phase to bubbles. Gaseous products leave the reactor from the top. As catalyst is finely suspended into slurry isothermal reaction zone can be achieved in the reactor. Also smaller catalyst particles tend to increase the conversion as diffusion of reagents to catalyst is easier. Main problem with slurry phase design is products and catalyst are mixed in slurry. Separation of this mixture is problematic. Slurry phase reactor designs are suitable for LTFT synthesis as HC of the waxes occur more rapidly at higher temperatures. Despite of these disadvantages, slurry phase reactors only cost 25 % of fixed bed reactors [23-25].

As both fixed bed and slurry phase reactors are not suitable for HTFT, fluidized bed reactors were developed for high temperature conditions. In circulating fluidized bed reactors, catalyst particles move up with the gaseous feed. Any small catalyst particles are recycled by the cyclone. Fixed fluidized bed reactors work very similarly with circulating bed reactors. But higher conversion rates can be achieved as all catalyst particles are exposed to inlet gas [23].

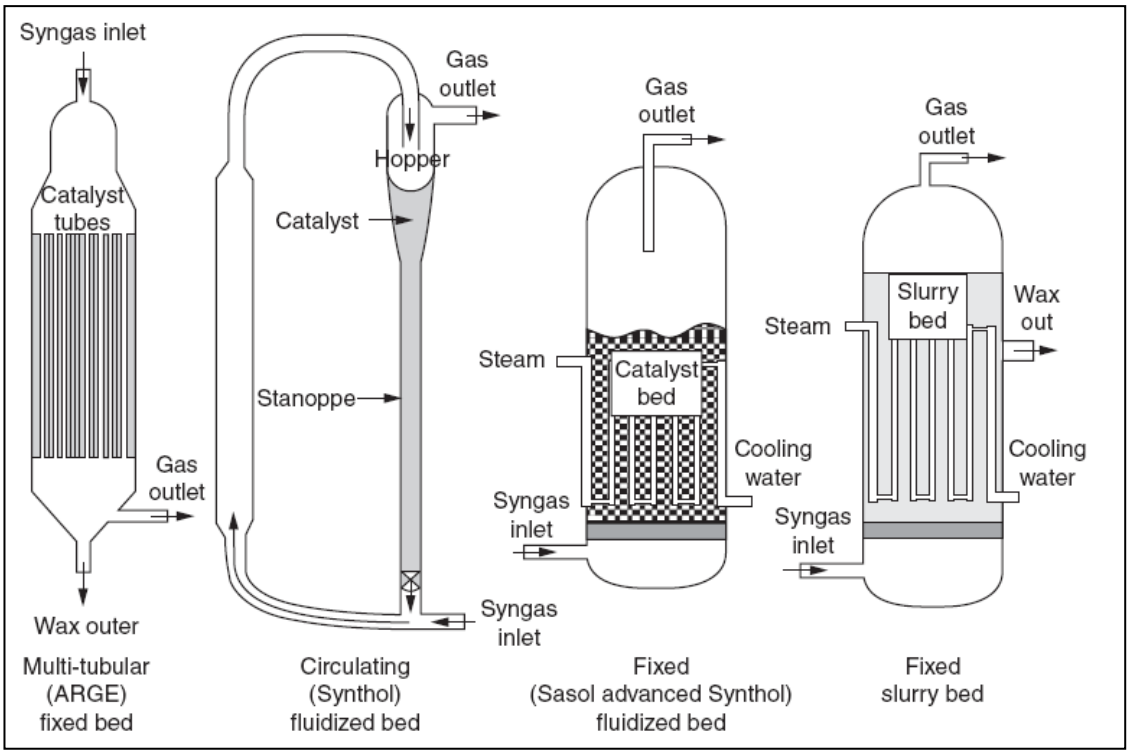

Figure 2.6 : Types of FT Reactors [12,23].

In FT synthesis, catalyst is one of the most important parameter that can change selectivity and conversion. VII transitions metals are active for FT synthesis. However only Co,Ni,Fe and Ru have the sufficient CO hydrogenation activity for commercial use. Table 2.5 shows some properties for different catalysis [17,26].

There are some catalyst characteristics which should be common for possible FT catalyst. First of all they should show hydrogenation activity in order to start FT synthesis. Secondly they should form metal carbonyl groups during the reaction. Last of all, FT synthesis conditions like temperature and pressure should be in range of metal's carbonyl group formation temperature and pressure. As carbonyl group plays a key role during the synthesis. Selection criteria for FT catalyst are not simple as many factors can affect the selection like composition of syngas, desired product, temperature, catalytic life time and availability [17].

Price comparison of FT catalysts eliminates Ru as a commercial catalyst due its high price. It is nearly 30000 times expensive than commercial Fe and 150 times than Co catalyst. Besides Ru is a very rare metal on earth [22,27]. Ni metal produces too much methane under FT standard operation conditions. Also Ni produces highly volatile carbonyls which results in gradual lose of catalytic activity [15,16].

Table 2.5 : Comparison of FT catalysts (plus signs show the increase in the value, minus sign shows the decrease in the value) [27].

Active Metal	Price	FT Activity	WGS Activity
Ni	++++	+	+/-
Fe	+	+	+++
Co	+++	+++	+/-
Ru	+++++	+++++	+/-

With elimination of Ni and Ru for commercial applications, only Fe and Co are practically used in industry. Cobalt is highly active catalyst in comparison with Fe thus any synthesis with Co catalyst should prevent catalyst loss during operation. Also because of the high prices, Co catalyst dispersed into support materials like SiO_2, Al_2O_3 in order to increase surface area of the catalyst. Higher temperatures can increase the yield of methane for Co catalyst. For Fe catalyst temperature tolerance is higher so Co catalyst is not used in HTFT synthesis [16,17].

Fe shows higher WGS reaction activity than the other metals. As a result FT synthesis with Fe catalyst tends to produce more H_2. Thus Fe can be applied to systems where syngas is originated from coal (low H_2 content). On the other hand Co shows little WGS activity. Therefore any application with Co should be in H_2 rich environment [27, 28].

Co has higher yields towards paraffins and longer hydrocarbons due to its higher hydrogenation activity. While Fe catalyst favors the olefinic and aromatic products [17,27].

Also there is a difference between Co and Fe catalyst about their sensivity to impurities such as H_2S. Fe catalysts are more resistant to H_2S than Co catalyst. For this reason Co catalyst must be used for the sulfur-free gas feed [29].

FT process selectivity is affected by several factors. Temperature, partial pressures of H_2 and CO, space velocity, composition and reduction of the catalyst are considered to effect the FT selectivity. Summary of parameters that effect FT are shown in Table 2.6 [30-34].

At higher temperatures, shorter hydrocarbons occur. While H_2/CO ratio can affect the olefin to paraffin ratio. Higher H_2/CO ratio means increase in lighter hydrocarbons and lower olefin content. Also composition and reduction of the

catalyst can affect the selectivity. Figure 2.7 shows different selectivity for the same iron catalyst under different pretreatment conditions. It can be said that higher reduction temperatures and more CO in the pretreatment environment can shift the product distribution to longer hydrocarbons [30,34].

Apart from the effect of different parameters to selectivity, there are some generalizations about the selectivity. Methane selectivity is reported to be higher for Co catalyst in comparison with other hydrocarbons for Fe and Ru. Also olefin selectivity is higher for iron based catalyst while for Co based catalyst product spectrum is more paraffinic [18].

Table 2.6 : Change of FT selectivity with respect to different changing parameters (+: increase with increase in the parameter, -: decrease with the decrease in the parameter, *: complex relation) [28].

Parameters	Chain Length	Chain Branching	Olefin Selectivity	Alcohol Selectivity	Carbon Deposition	Methane Selectivity
Temperature	-	+	*	-	+	+
Pressure	+	-	*	+	*	-
H_2/CO	-	+	-	-	-	+
Conversion	*	*	-	-	+	+
Space Velocity	*	*	+	+	*	-

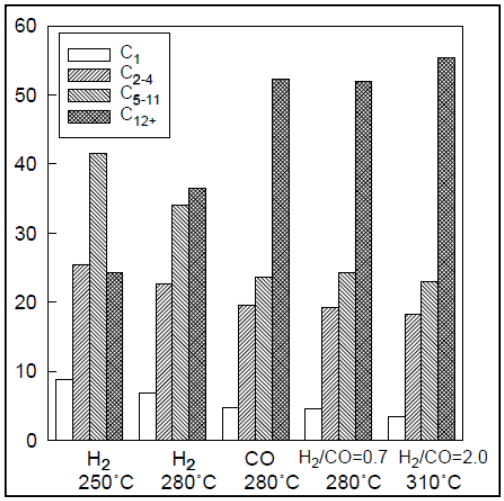

Figure 2.7 : Effect of different pretreatment conditions on selectivity for Fe based FT (x axis: Different pretreatment conditions, y axis: weight fraction of the products) [30].

Widely accepted model for describing the product distribution of FT is Anderson-Shulz-Flory (ASF) model [18]. The ASF model is based on simultaneous chain growth and product desorption where the adsorbed hydrocarbon species either could participate in further chain growth or desorb to form the observed products. The probability of chain growth is referred to as the α value in the ASF polymerization equation which is numbered as 2.2.

$$\log\left(\frac{W_n}{n}\right) = n\log(a) + \log\left(\frac{(1-a)^2}{a}\right) \qquad \textbf{(2.2)}$$

where;

W_n= sum of mass fractions at carbon number n

n= carbon number

a= chain growth probability ranging from 0 to 1

Figure 2.8 shows the weight fraction changes versus chain growth probability. Optimum α values for gasoline cut (C5-C11) is 0.76 and diesel cut (C12-C18) is 0.88. These α values results 48 % and 30 % desired product yield respectively.

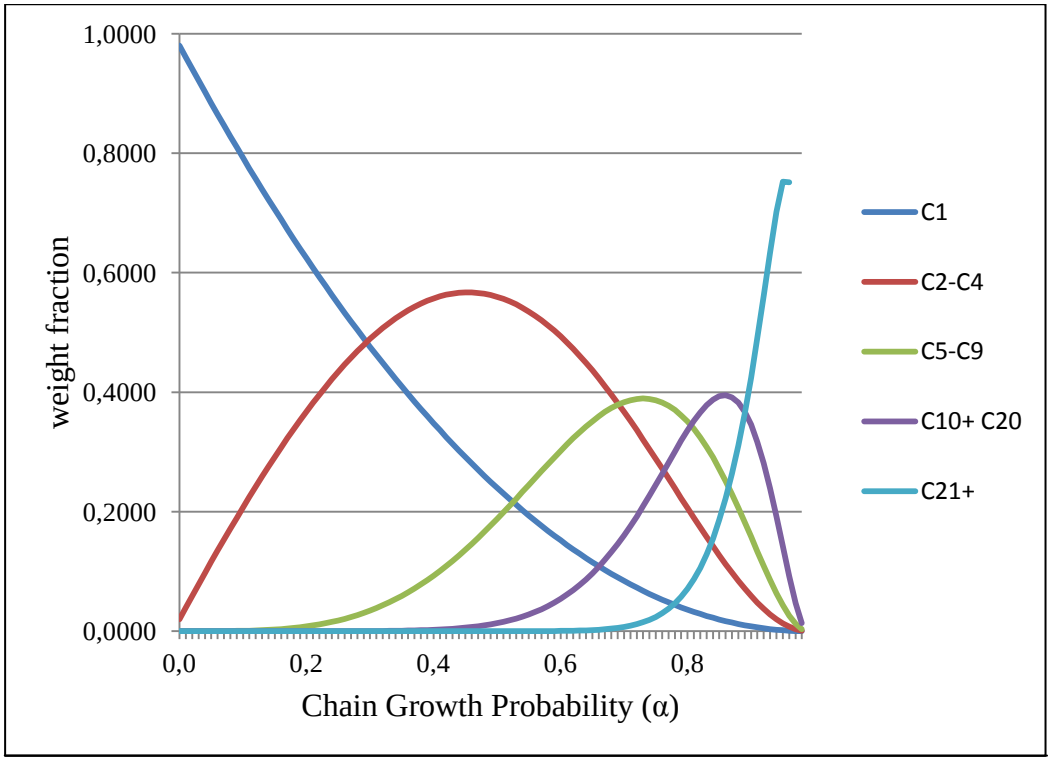

Figure 2.8 : ASF distribution of different hydrocarbon range for different chain growth probability [Drawn from 18].

Products in FT synthesis heavily depend on reaction conditions. One example product distribution for Sasol process is given by the Table 2.7. LTFT processes are generally yield more heavy hydrocarbons. On the other hand HTFT produces more olefins comparing to LTFT.

Table 2.7 : Products comparison between LTFT and HTFT based on SASOL processes [25].

Product	Selectivity (%)	
	LTFT	HTFT
CH_4	4	7
C_2 to C_4 Olefins	4	24
C_2 to C_4 Paraffins	4	6
Gasoline	18	36
Middle Distillate	19	12
Heavy oils and waxes	48	9
Water soluble oxygenates	3	6

For both LTFT and HTFT operation modes, the desired products are not sufficient enough for feasible operation. Thus FT products must be upgraded to desired products after the synthesis. For LTFT, desired products are middle distillates which are the main ingredients of diesel fuel. For HTFT, main aim is to produce gasoline range hydrocarbons.

2.5 Hydrocracking

HC is the process of splitting carbon-carbon bonds in hydrocarbons and putting additional hydrogen molecules for saturating the smaller fragments. For HC of crude oil and FT wax , many types of catalyst are widely used in the industry. One of the most important is bifunctional catalyst. Bifunctional catalyst has two functions, cracking and hydrogenation-dehydrogenation. Cracking on bifunctional catalyst is done by acid sites and hydrogenation-dehydrogenation function is provided by metals. Figure 2.9 shows the acid sites and metal that can be used for bifunctional HC catalyst [35].

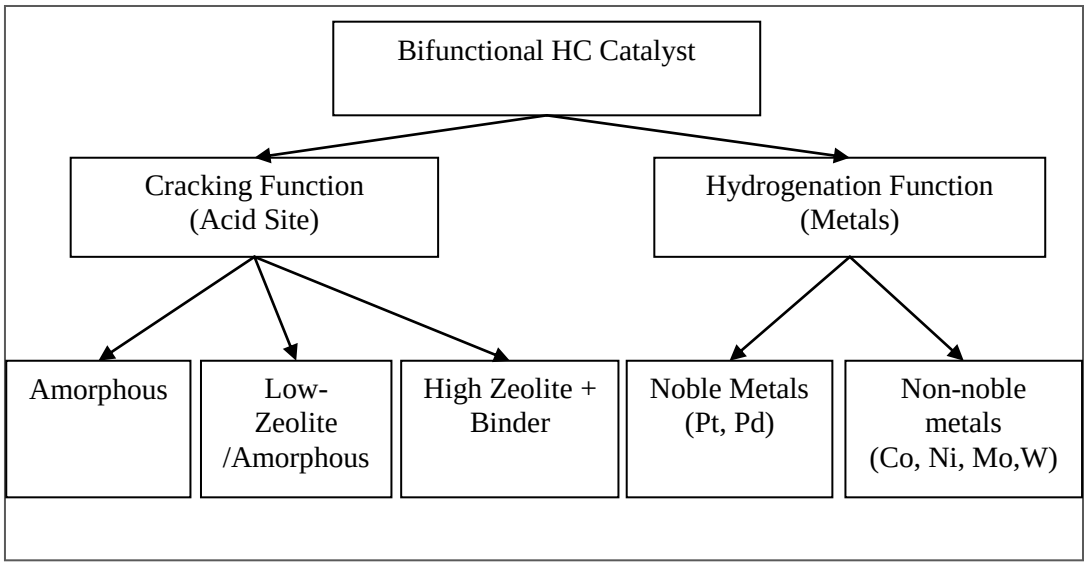

Figure 2.9: Bifunctional HC catalyst and possible acid and metal sites [35].

Currently many choices of catalysts are available for crude oil HC. Thus current commercially available catalysts are optimized for crude oil refinery environment. By considering product spectrum of crude oil and FT synthesis , there are differences in these applications. First of all, FT synthesis product spectrum is free from the sulphur and nitrogen content therefore it can be expected for FTS wax HC will have higher conversion rates as catalyst won't be poisoned by sulphur and nitrogen. Also whereas medium pore sized zeolites have limited application in crude oil HC as pore size limits the HC of large bulky molecules, in FT wax HC it is an advantage as it limits branching and keeps the linear hydrocarbons which will increase cetane number [36].

Zeolites are some of the mainly used acidic sites for the bifunctional HC catalyst. Zeolites are porous crystalline aluminosilicates. SiO_4 and AlO_4 tetrahedra joined together in various arrangements through shared oxygen atoms and zeolite framework is assembled. This arrangement of the atoms forms an open crystal lattice containing pores into which other molecules can penetrate [37].

Silicon is tetravalent and aluminum is trivalent. This causes necessity of charge compensation on aluminum sites in the whole crytalline aluminosilicate network. By introducing cations such as NH_4^+ on the near sites of aluminum after calcination, ammonium form transforms into hydrogen form (H-zeolite). Figure 2.10 shows the representation of acids sites on a sample zeolites. The resulting bridging hydroxyl groups which connects silicon to aluminum in the framework of the zeolite causes

bronsted acidity and catalytic activity, while the oxo-ligands of aluminium that is in interaction with the bridging hydroxyl groups are the corresponding Lewis bases [38].

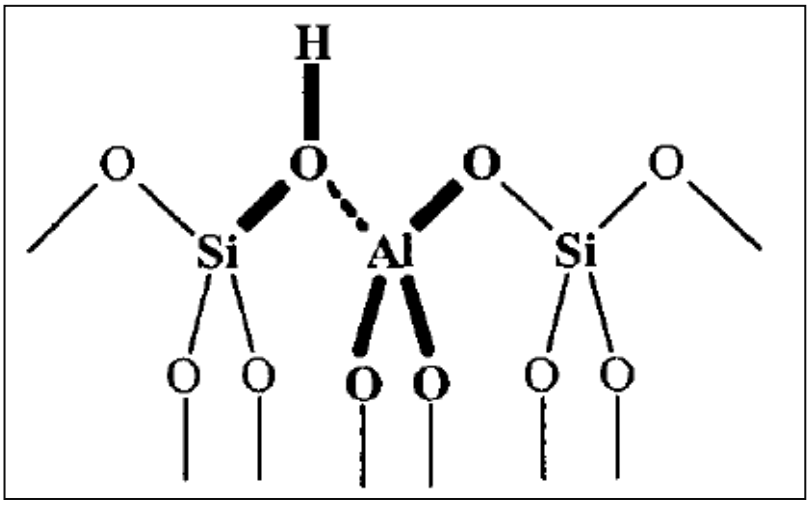

Figure 2.10 : Active sites in hydrogen aluminosilicate zeolites. (The bridging hydroxyl group and the oxo ligands of the Al atom act as bifunctional Bronsted acid - Lewis base sites) [38].

It can be said that lower SiO_2/Al_2O_3 ratio results higher acid sites due to the higher occurance of Al_2O_3 sites but higher SiO_2/Al_2O_3 ratio causes strong acidity as acid sites strength is higher. There is a strong correlation between SiO_2/Al_2O_3 and activity of the zeolites. Figure 2.11 shows butane HC activity for different zeolites and (Al/Si+Al) ratio [39].

Zeolites have extensive use as acid-catalyst for hydrocarbon processes as acid sites are controllable. Because of the porous and shape selective structure of the zeolites, they are also used as molecular sieves for different hydrocarbons.

Three types of shape selectivity mechanism are known [40]. These are;

- Reactant shape-selectivity
- Product shape selectivity
- Transition state selectivity

Reactant shape selectivity occurs when the reactant molecules are too large or too branched to enter through the zeolite pores. Figure 2.12 shows an example of reactant selectivity. 1-methylhexane couldn’t enter through the pore on the other hand n-heptane pass through the pore [41].

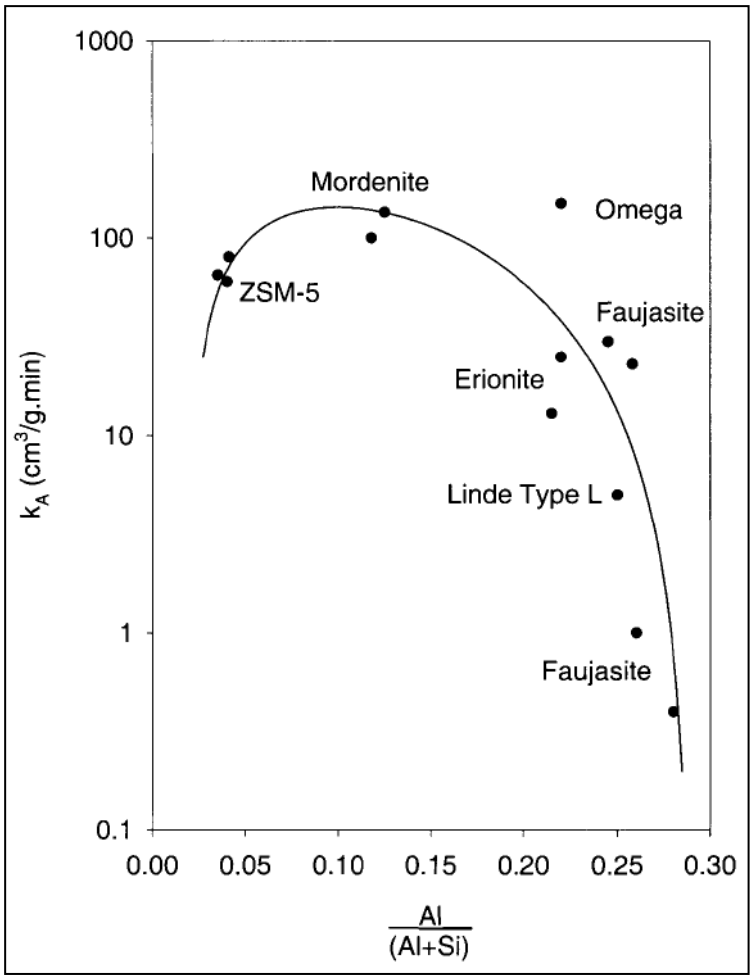

Figure 2.11 : Activity of different zeolites by comparison of Al/Si ratio [39].

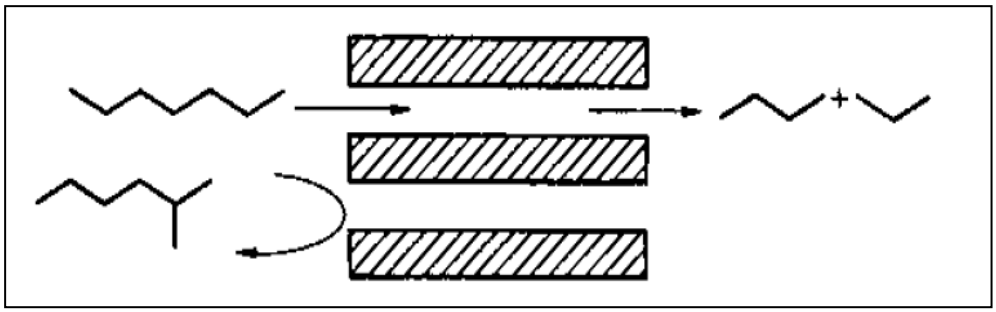

Figure 2.12 : Reactant selectivity [41].

Product shape selectivity takes place when the product in the zeolite pore is too bulky to diffuse out from the narrower channel and causes deactivation of the catalyst by blocking the pore if they are not converted to smaller molecules by cracking or equilibration. Equilibration occurs when the concentration of the bulky product increases inside the pore as the less bulky products diffuse out of the pore which will eventually result equilibrium shift towards to smaller products. This

situation results conversion of bulky products to less bulky products. Figure 2.13 shows these phenomena [41].

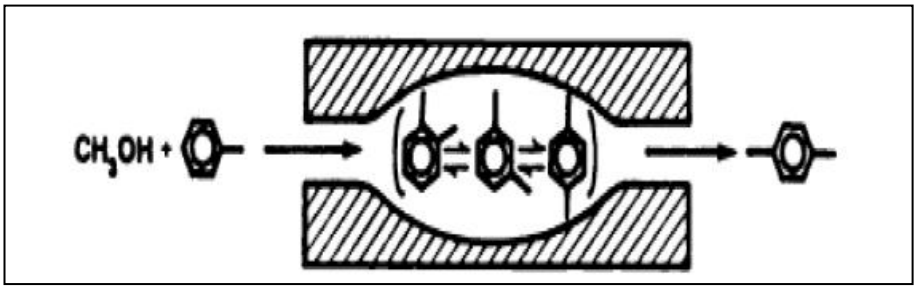

Figure 2.13 : Product shape selectivity [41].

Last of all transition-state shape-selectivity occurs due to the prevention of certain reactions as spatial constraints within the pores. An example of this given in Figure 2.14. It can be said that different transition states of tri-alkylbenzene have an effect on passing through the pore as some transition states are smaller [41].

In some certain zeolites like Zeolite Socony Mobile (ZSM-5) different phenomena is observed. Products diffuse from one channel and reactants diffuse through different channel which prevents counter diffusion [41].

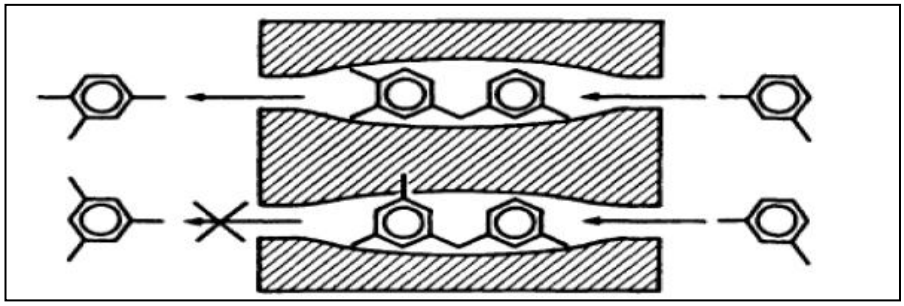

Figure 2.14: Transition state selectivity [41].

There are many types of zeolites that are used in HC processes. Some examples are zeolite beta, faujasite, Mordenite framework inverted (MFI), Mordenite [38]. MFI type zeolites which were used in the experimental work are briefly discussed below. HMFI which is also known as ZSM-5, is based on cages made of 4-, 5-, and 6-MR resulting in two elliptical pores of 5.15.5 and 5.35.6A° normal to each other. Small and intermediate organic molecules can be adsorbed, but not larger molecules. ZSM-5 has SiO_2/Al_2O_3 ratio from around 20 to almost infinity. Representation of the pore structure of ZSM-5 is given in Figure 2.15.

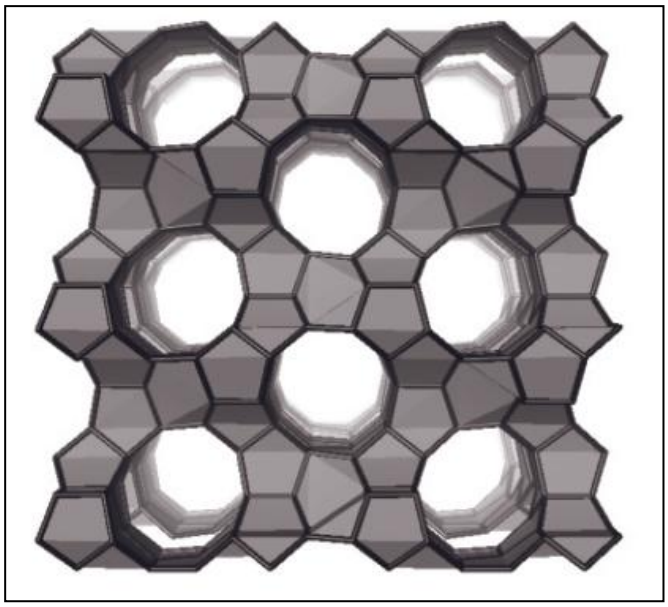

Figure 2.15: Pore structure of ZSM-5 [42].

HMFI catalyst has some advantages against other zeolites in bifunctional HC catalysis. First of all, it shows higher activity for HC of alkanes as it is highly acidic. Secondly due to medium pore size, shape selectivity restricts the HC of bulk molecules and limits branching. Furthermore due to its medium pore size, coke formation on ZSM-5 is very limited [36].

There are three reaction mechanisms proposed for HC on bifunctional catalyst. These are; classical acid-metal HC mechanism, hydrogen spillover mechanism and hydrogenolysis and methanolysis mechanism.

Classical HC mechanism (also named true HC) is the most widely acpected mechanism. HC occurs by the interaction of intermediates between two separately sites, acid and metal. Metal site hydrogenates the n- paraffins to form olefins and these olefins go further by gaseous diffusion to metal site to form carbenium ions after that on the acid sites these carbenium ions isomerizes and continue to be cracked. Olefins that were produced by these isomerizatios migrate to metal site for rehydrogenation. Figure 2.16 shows the mechanism of true HC.

As it can be seen in Figure 2.16, β scission plays a crucial role in the cracking of carbenium ions, which resulst an olefin and a paraffinic carbenium ion. This kind of cracking rate is related to stability of carbenium ions which can be ranked as;

Tertiary>> secondary >> primary [38]

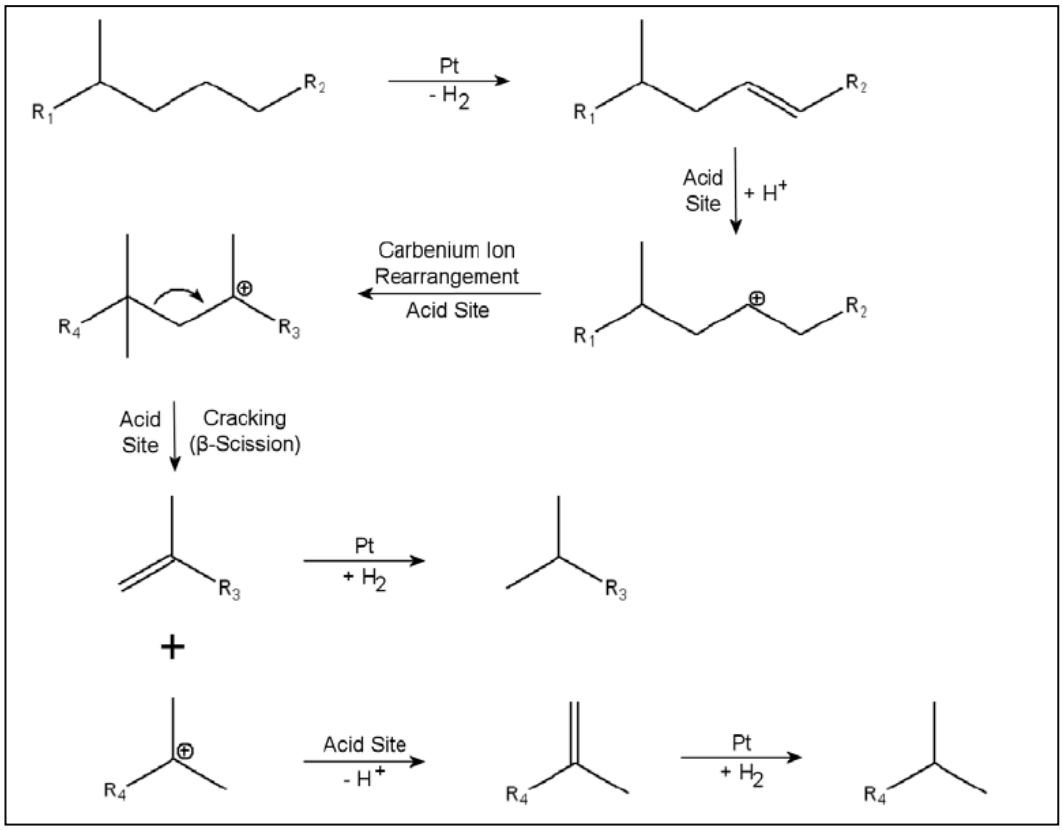

Figure 2.16 : Acid-metal bifunctional catalyst HC reactions [38].

Figure 2.17 shows possible HC mechanisms including tertiary and secondary carbenium ions [43]. Since primary carbenium ions stabilitiy is very low, their possible reactions can be neglected as cracking rate is very low [38].

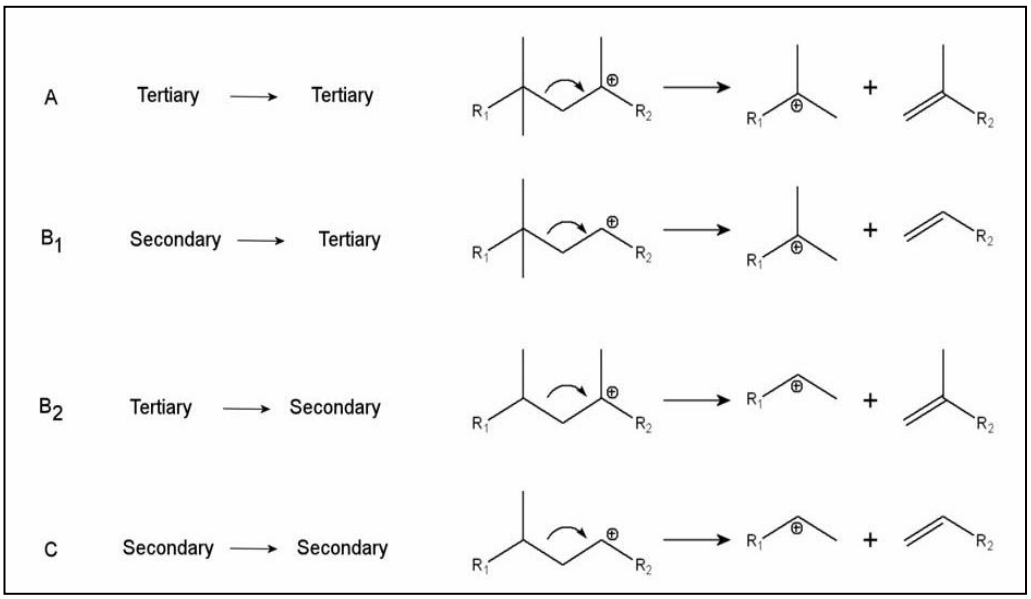

Figure 2.17 : Several HC mechanisms of tertiary and secondary carbenium ions[43].

True HC requires the presence of strong acid and hydrogenation sites, the latter in order to activate the feed paraffins and minimise secondary cracking [36].

Theoretical carbon number distribution and selectivity is given in Figure 2.18**.** Under normal conditions, constant product distribution ranging from C3 to C11 hydrocarbons expected (solid line) but under severe HC conditions, hydrocarbons go to further isomerization and secondary cracking occurs (dashed line) [36].

Not widely accepted and fully understood mechanism as true HC mechanism, hydrogen spillover mechanism was suggested by Steinberg et al. in order to explain the deviation in the selectivity from the true HC mechanism. In true HC mechanism, hydrogen molecules have the duty to hydrogenate the paraffins on the metal site. In suggested hydrogen spillover mechanism H_2 molecules are activated on the metal site and possibly by surface diffusion to acid sites where H_2 can interact with hydocarbon molecules [44].

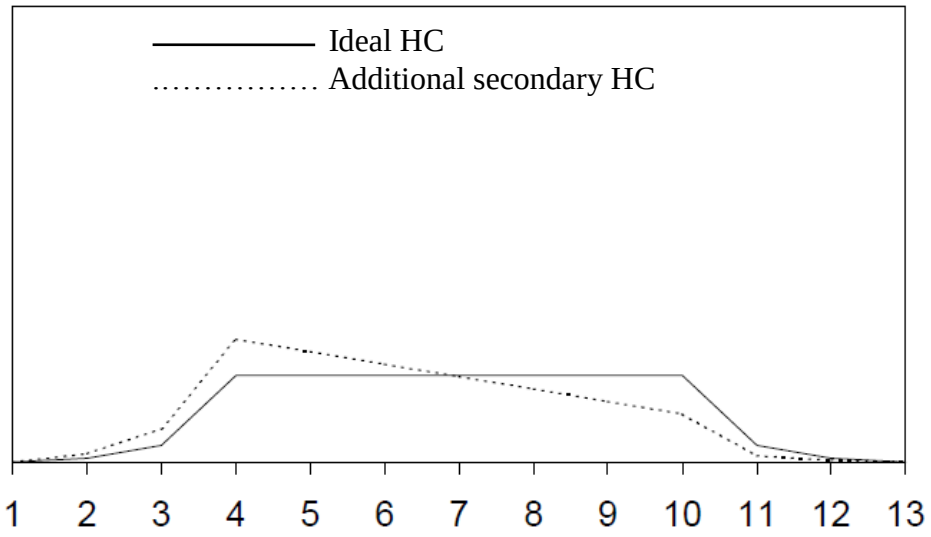

Figure 2.18 : Difference in selectivities for primary and secondary HC (x axis: carbon number, y axis: molar selectivity) [36].

In Hydrogenolysis and Methanolysis mechanism, most favored product is methane in contrary to true HC and hydrogen spillover mechanisms. Main reason for this proposed mechanism is the lack of isomerization on the acid site. Hydrogenolysis proceeds via adsorbed hydrocarbon radical intermediates initially formed through abstraction of a hydrogen radical. These chemisorbed hydrogen-deficient hydrocarbon intermediates undergo C-C scission and the probability of such scission

is almost identical, or non-selective, for all C-C bonds on the hydrocarbon chain. Methanolysis is the special condition of hydrogenolysis Figure 2.19 shows the reaction pathways. This reaction shows the C-C bond cleavage mechanism, α shows the probability of remain adsorbed and demethylated again [36].

Catalyst deactivation is the process of loss or decrease in the activity of the catalyst. There are three major deactivation types. These are; sintering, coking and poisoning.

Sintering occurs when the surface of the catalyst changes. It can occur on both supported and unsupported catalysts. Sintering on unsupported catalyst can be caused by agglomerization of smaller metal particles on larger ones. On supported catalyst sintering can occur due to the migration of metal atoms from crystallite and capture and collision of these metals with other metals.

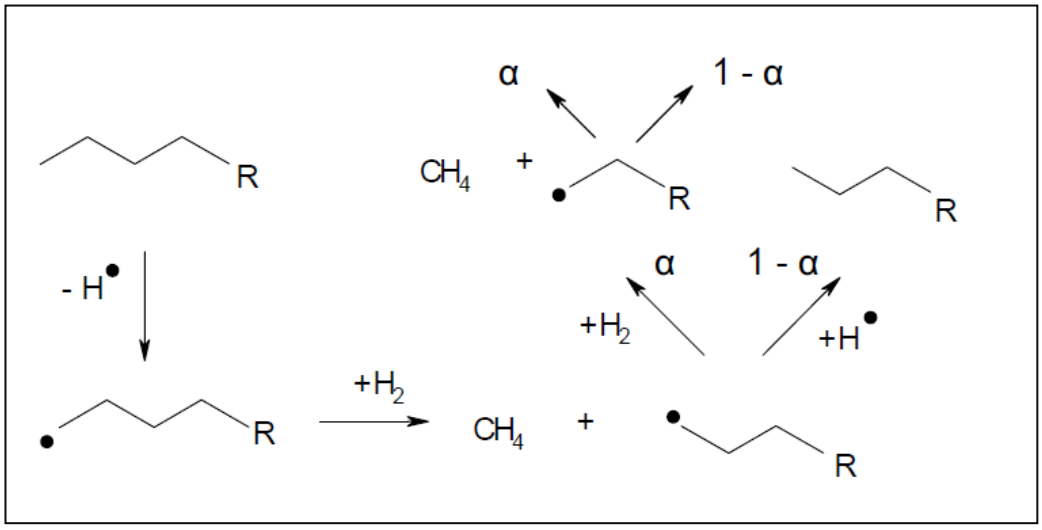

Figure 2.19 : Reaction pathways for methylation [36].

Beside from this, crystallite structure can escape from the support and can be captured by another crystallite. Due to this modification of surface, catalytic activity gradually lost. Sintering is considered to be a physical process which is initiated by thermal effects [35,45].

Coking is the formation of carbonaceous residues on the surface of catalyst due to side reactions of hydrocarbon transformation. Deactivation is caused by either pore blocking or covering of the surface. Coking could occur in macroscopic scale up to 20 % of the catalyst weight. Feedstock type, catalyst composition, reaction temperature and residence time can affect the coke formation rate. Aromatic hydrocarbons tend to produce more coke on the catalyst than aliphatic ones. Higher

temperatures tend to produce less coke while coke formation increases with residence time. Also catalyst composition is very important for controlling coke formation. Different zeolites show different coke formation rate as pore structures and acidities are different. For ZSM-5 catalyst coke formation rate is very low [34,44,45].

Poisoning is the process where chemisorption occurs between impurity and catalyst. Poisoning alters the catalytic activity either blocking the active site or changing the adsorptivity of other materials. Also poisons can change the surface chemistry of catalyst and form new compounds on the surface. Poisoning can be reversible or irreversible. It can be classified as reversible if the chemisorption at the catalyst surface weak which enables desoprtion of the impurity. There are several potential poisons for metal catalysts. Sulphur is widely accepted as poison for metal sites of bifunctional catalysts. Beside from that N,P,As, Pb ; chemicals with proper electronic configuration and chemicals with multiple bonds can be possible poisons for metal sites. Therefore CO can decrease the catalytic activity. Water is also inhibits catalytic activity as it competes with other paraffins for adsorption on the pores of acid sites [35,45-47].

2.6 Literature Review

In this chapter, some of the researches that were done on the topic of Combined FT and HC catalyst are selected and briefly discussed.

Martinez et al. did a research about the deactivation mechanism of hybrid Cobalt and zeolite catalyst. Research was done under typical FT conditions (250°C, 2 MPa H_2/CO:2). C13 represented the whole FT spectrum. They conducted experiments on the deactivation of acid site of the hybrid catalyst with respect to time on stream and coking. Four different type of zeolites were used and according to results, deactivation rate of catalyst is in the order like HZSM-5 < HMOR < HBeta < USY. Beside from controlling the deactivation rates, in their research , water effect on hybrid catalyst was also examined. n-hexadecane was used during these experiments and they concluded that water lowered the activity of catalyst by competing with n-alkane feed molecules [45].

Tsubaki et al. conducted a research about direct synthesis of isoparaffin over hybrid catalyst which is consisting of Co/ZSM-5 and Pd. In their experiments they

examined the effect of Pd loading on selectivity of the combined FT and HC. Results showed that Pd loading suppressed the olefin production. Another result they acquired is by using H_2/CO ratio at 3, they suppressed all olefinic production [48].

Liu et al. conducted a study about producing iso-paraffins over Co/SiO_2 and Pd/beta and Pt/beta catalyst. They used dual fixed bed reactors connected to each other in a line. Operation conditions were 1 MPa and H_2/CO ratio 2. They found out that experiments with Pt/beta produced more iso alkanes. It was suggested that CO affected the acid-metal balance on Pt/beta bifunctional catalyst [49].

Nakamura et al. studied HC of n-dodecane over Pd/ZSM-5. They used continious flow type fixed bed reactor . Reaction conditions were T=503K, P= 10 MPa and H_2/n-dodecane = 9, Pd/ZSM-5= 1:1. They found out that Pd/ZSM-5 showed very high conversion rate around 80 % and also C8-C9 selectivity was realitvely high. They concluded that Pd/ZSM-5 catalyst suppressed secondary HC [50].

In 2003 Li et al. did a research about direct synthesis of middle iso-paraffins from synthesis gas on hybrid catalysts. They tested the performance of six different loadings; β zeolite, Pd/β zeolite, ZSM-5, Pd/ZSM-5, USY and Mordenite zeolites in addition to zeolites, Co/SiO_2 was also loaded. The reaction conditions were , H_2/CO ratio= 2, P= 1 MPa, reaction time : 4 hours, Co/SiO_2 / Zeolite ratio : 4. They found out that additional Pd loading on ZSM-5 increased the CO conversion rate from 35 % to 55 %. They observed a slight change in the methane selectivity and a slight increase in iso-paraffin selectivity [51].

Yoshiriyu et al. studied the direct synthesis of isoparaffin by modified Fischer-Tropsch synthesis using hybrid catalyst of iron and zeolite. In their research, they used Fe/ZSM-5 hybrid catalyst. The ratio of Fe/ZSM-5 was examined during their experiments. Effect of higher ZSM-5 loading was the main effect in the methane selectivity [52].

3. EXPERIMENTAL PART

Aim of the present study is to compare different HC catalysts performance under LTFT synthesis conditions and eventually produce diesel fuel paraffins from CFTH reactions by using the selected catalyst.

Experiments were done in fixed bed dual tube laboratory scale reactor system. All the experiments that were mentioned in this study were done in University of Cape Town (UCT) Chemical Engineering Department Catalyst Research Laboratory. Experimental part consisted of two steps:

- Selection of HC catalyst
- CFTH reactions

Selection of HC catalyst was done by controlling performance of different metal-zeolite catalyst under FT synthesis conditions. Comparison was done for different conditions in the reactor in order to control the performance of the catalyst. These conditions were;

- CO tolerance of metal/zeolite catalyst
- H_2O tolerance of metal/zeolite catalyst

In order to see if the metal loading on the catalyst could overcome the effect of poisoning substances, different metal loadings were used during the experiments.

After the selection of suitable HC catalyst, it was mixed with FT catalyst. Performance of combined catalyst was controlled by checking the following parameters:

- CO Conversion
- Hydrocarbon Selectivities

Four different syngas flow rates were used during the experiments to see the effect of space velocity on conversion and hydrocarbon selectivity.

3.1 Materials and Methods

5% w/w Platinum (Johnson Matthey) was used as the metal site of the catalyst. HMFI90 (Süd-Chemie, SiO_2/Al_2O_3 : 90) was selected for zeolite part of the catalyst [43,50]. All the metal loadings and dispersion rates in this study are given as weight percentage (w/w) and w/w notation won't be further mentioned in this study. Pure n-hexadecane (Sigma Aldrich) was used for representing sole FT product due to the inability of analysis with larger hydrocarbons as they have higher boiling points. H_2 and CO gases were acquired in pure form from the laboratory lines in UCT Chemical Engineering Department Catalyst Research Laboratory. In present study comparison was done between 5 % Palladium and Platinum, as Palladium/HMFI90 catalyst was examined previously by using the same experimental apparatus [53]. During CO and H_2O tolerance experiments, analysis was done by comparing the selectivity and conversion rates. These comparison eventually led to select the suitable catalyst for CFTH synthesis.

After the selection of suitable HC catalyst which is eventually Palladium/HMFI90, it was mixed with 10% Cobalt catalyst which is used commercially for low temperature FT synthesis. 5% Palladium catalyst was acquired from Johnson Matthey. Zeolite part of the HC catalyst was the same material that was used during standard HC experiments. Also H_2 and CO gases were also acquired from the laboratory lines.

10 % Co/SiO_2 catalyst was prepared by incipient wetness impregnation method. First $Co(NO_3)_2.H_2O$ (Johnson Matthey) salt was added into water to get water-salt solution. After that SiO_2 (Sigma Aldrich Silicagel Davisol grade 646) is dried under 350 °C. Then $Co(NO_3).H_2O$ solution and dried silicagel particles are mixed. Then the mixture calcinated for 5 hours under 500 °C [54].

Before starting the experiments Platinum, Palladium, HMFI90 and Co catalyst were pelletized under 10 bar and then crushed in order to get 0.300-0.850 mm particle size. Particle size was a safety measure as smaller particle size could leave the catalytic bed and could cause interruption in the experimental setup.

FT reactions were done under 4 different syngas space velocity in order to examine the effect of space velocity. Three different catalysts loading were used for the comparison of the effect of metal loadings. These are given below;

- 10 % Co/SiO_2
- 10 % Co/SiO_2 + 0.1% Pd/SiO_2 + HMFI90
- 10 % Co/SiO_2 + 1 % Pd/SiO_2 + HMFI90

Both CFTH and HC experiments were conducted in packed bed triple phase dual tube reactors. Details were given in section 3.3.

The catalyst underwent a reductive pretreatment at elevated temperature in hydrogen containing gas, 200 mL/min N_2 with 50 mL/min H_2. The reactor temperature in all four isothermal zones was ramped up from room temperature to 350 °C over a ramp period of 4 hours and held at this temperature for 16 hours. The reactor pressure was set at 20 bar. The main CO supply valve was shut and the line evacuated beforehand to ensure no CO will enter the system. Once the pretreatment was completed the reactor temperature was lowered to the reaction temperature 225 °C.

The feed pumps of n-C16 and H_2O were primed to release any gas bubbles from the intake line which would lead to an interruption of the feed in the middle of the run. The liquid feed flow rate was monitored during the course of an experiment by plotting the weight versus time.

After the laboratory scale reactor was ready for the reactions and pressure and temperature were at desired values, H_2 and C16 were fed to reactor. Analysis was done for sufficient time intervals which were about 120 hours for each run. During the experiments selectivities and conversion were monitored online.

For CFTH experiments, operation procedure was almost same with HC experiments. Only difference was the pretreatment temperature for the catalyst which was 425 °C.

Sample characterization was done by Gas Chromatography (GC)-Flame Ionizer Detector (FID) and micro GC equipments. For HC experiments only GC-FID analysis was used. With GC-FID anaylsis selectivities on carbon basis and conversion rates were found. For FT and HC combined experiments GC-FID analysis is used for observing selectivities on carbon basis, analysis with thermal conductivity detector (TCD) was used to observe conversion.

Reactor effluent was examined by GC Equipment. For examining hydrocarbon selectivity FID was attached to system (Varian GC 3900). And for calculating CO, conversion TCD detector is attached to system.(Varian Micro GC 4900) .

In order to analyze two different reactors, 2 inlet 2 outlet sample valve was attached to the system. Figure 3.1 shows the sample valve that was used during the experiments. Valve was rotated manually during the experiments within the definite time interval.

Schematic representation of the rotating valve is given in Figure 3.2. Figure above shows the valve position one in feed reactor effluent enters the GC line for final analysis. By turning the valve 90 degrees, reactor effluent 2 enters the GC line and eventually reactor effluent 1 enters the vent.

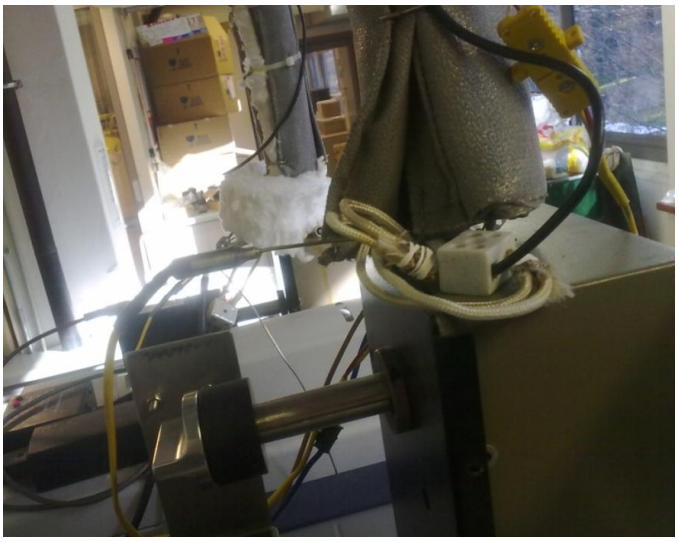

Figure 3.1 : Rotating valve for GC analysis.

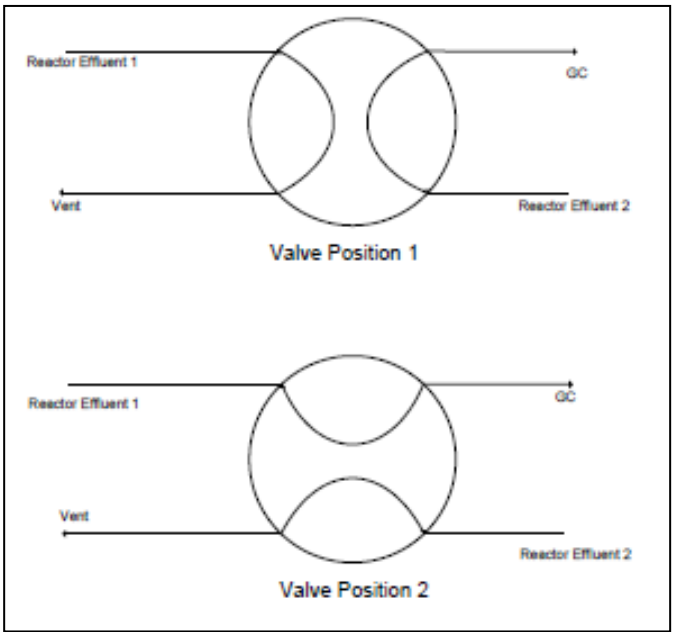

Figure 3.2 : Operation diagram showing two different working positions for rotating valve.

During the experiments analysis in GC equipment was done by same methods for each run. Table 3.1 and Table 3.2 shows the Gas Chromatogram specifications for FID and TCD respectively.

Table 3.1 : FID Operation Mode.

Detector Type		FID(Flame Ionizer Detector)	
Detector Temperature		275 °C	
Injector Temperature		250 °C	
Injector Split Ratio		100	
Gas Flows			
N_2(Make up)		25mL/min	
H_2		30 mL/min	
Air		300 mL/min	
Column Flow		0.7 mL/min	
Owen Temperature		300 °C	
Rate(°C/min)	Step	Time(min)	Total Time(min)
Initial	0 °C	5	5
10	150 °C	0	20
5	300 °C	0	50
Column Type		Capillary Column Varian CP-sil 5 CB 25 mm-0.15mm- 2 μm	

Table 3.2 : TCD Operation Mode.

Model	Varian CP-4900 Micro GC
Detector	Thermal Conductivitiy Detector
Detector Temperature	200 °C
Oven Temperature	80 °C (constant)
	Channel 1
Carrier Gas	Ar
Column Head Pressure	300 kPa
Analysis Temperature	40 °C
Gases Detected	H_2
	Channel 2
Carrier Gas	H_2
Column Head Temperature	200 kPa
Analysis Temperature	40 °C
Gases Detected	CO, CO_2, Ar, CH_4

With FID, every species at the outlet of the system examined by observing the different retention time and peak area. Flame Ionizer detector is mass sensitive so it detects the carbon atoms that were ionized which causes larger of smaller peak area with respect to mass of species.

The peak area in the chromatogram was proportional to the number of reduced carbon atoms in the product peak. The peak area of a product corresponded to the number of carbon atoms in the product peak. Dividing by the total peak area and assuming that all products were detected yields the number of carbon atoms in product peak i as a percentage of the total number of carbon atoms in the entire product spectrum, excluding CO_2 which was quantified using the TCD on the micro-GC, selectivities on a carbon basis were obtained, abbreviated S(Ci). Equation 3.1 shows the equation for the selectivity calculations.

S(Ci) = Selectivity of Ci

Ai = Peak Area of species i

$S(CO_2)$ = Selectivity of CO_2

$$S(Ci) = \frac{A_i}{\sum_i A_i} \times \left(1 - S(CO_2) \right) \quad \textbf{(3.1)}$$

Conversion rate of n-hexadecane was found by the following equation 3.2 ;

$$X_{CO} = \left(\frac{C_{16}}{\sum_i Ai} \right) \times 100 \quad \textbf{(3.2)}$$

By dividing the peak area of n-hexadecane to total peak areas of all species, it was possible to calculate the conversion rate of C16 by finding the reactant/product ratio.

TCD analysis was done by using Micro GC equipment. With TCD analysis CO conversion rate could be determined. By finding the CO conversion rate, conversion rate of reaction could be found.

The TCD is calibrated with the reactor feed stream of known composition. Argon is used as an internal standard since Ar is inert. Ar was acquired from the laboratory lines in UCT Catalyst Research Laboratory. The molar flow rate of Argon was equal for inlet and effluent. Since the concentration of a particular gas in the calibration or sample gas mixture is proportional to the peak area in the chromatogram and the constant of proportionality is a function of the instrument, the ratio of concentration to peak area will be constant in every chromatogram for this particular gas.

Carbon monoxide / Argon proportionality should stay same as Ar inert gas. But due to the reactions occurred in the reactor CO peak area should decrease during the experiments. So with equation 3.3, one can easily calculate the CO conversion rate.

X_{CO} = CO conversion rate

[CO] = Peak Area of CO in the sample

[Ar] = Peak Area of Ar in the sample

$[CO]_c$ = Peak Area of CO in the calibration

$[Ar]_c$ = Peak area of Ar in the calibration

$$X_{CO}=\left(1-\left(\frac{\frac{[CO]}{[Ar]}}{\frac{[CO]c}{[Ar]c}}\right)\right)\times 100 \qquad \textbf{(3.3)}$$

3.2 Experimental Conditions

Cobalt based LTFT synthesis is typically operated at 200-230°C and 10-20 bar. A pressure of 20 bar and temperature of 225°C were used ubiquitously [15,25].

The weight hourly space velocity (WHSV) of the liquid n-hexadecane feed in HC experiments was chosen based on the hypothetical molar formation rate of n-hexadecane in the LTFT. To determine the latter the following assumptions were made; the entire product spectrum of the FT synthesis consists of n-hexadecane, and a syngas conversion of 85% is reached.

Starting from a GHSV (Gas Hourly Space Veolicity) of 90 mL/min·g_{cat} and a H_2/CO ratio of 2 a typical feed gas flow rate and composition found in literature [43, 53], and given 85% conversion, the molar composition of the effluent is calculated with the following reaction equation 3.4 ;

$$2\ H_2 + CO \rightarrow -CH_2- + H_2O \qquad \textbf{(3.4)}$$

At the reactor outlet 0.85 mol $-CH_2-$, 0, 15 mol CO , 0,85 mol H_2O and 0,30 mol H_2 occurred. 90 mL/min.g_{cat} was about 0.0040 mol/min fed into the reactor.

With the formation rate of CH_2, we can conclude that 0.0206 mL C16/min.g_{cat} is required for 0.97h WHSV. Also water formation rate with 85 % is about 0.0205 mL H_2O/min.g_{cat}.

With this calculation 3 important parameters for the experiments can be deduced. The first is WHSV for feeding n-C16 to the HC catalyst on the assumption that FT produces only n-C16. The WHSV in present study was set at 1 h^{-1} for 0.03 mL/min C16 flow rate. In some occasions, C16 feed rate was increased to 0.05 mL/min in order to stabilize the peak area in the GC analysis. The second parameter, the water flow rate, or the water WHSV is almost the same as the n-C16 WHSV. The third and final observation is that the H_2/n-C16 ratio varies depending on the syngas conversion. At 75% conversion of H_2 and CO the remaining molar flow rate of H_2 is approximately 10 times that of the hypothetical n-C16 molar formation rate, at 80% it is down to 8 and at 85% the H_2/n-C16 ratio reduces to 5.7 . H_2/n-C16 ratio was fixed to 10.

For CFTH reactions, same temperature and pressure conditions were also applied. H_2/CO ratio was also 2. During the experiments flow rates were changed in order to change the conversion rate. Four different syngas flow rates in the reactor were used. These are; 120 mL/min, 60 mL/min, 30 mL/min and 15 mL/min.

3.3 Laboratory Scale Experimental Setup

Laboratory scale experimental setup flow diagram can be seen in Figure 3.3. Also detailed process flow diagram (PFD) is given in Appendix A.1 . Reactions occurred in triple phase due to the nature of the FT and HC reactions. Products of FT and HC were in solid, liquid and gaseous phases. Figure 3.4 shows the back and front view of the experimental setup. In this chapter following components of experimental setup are briefly discussed

- Reactor
- Flow Control
- Temperature Control
- Pressure Control
- Vaporizer

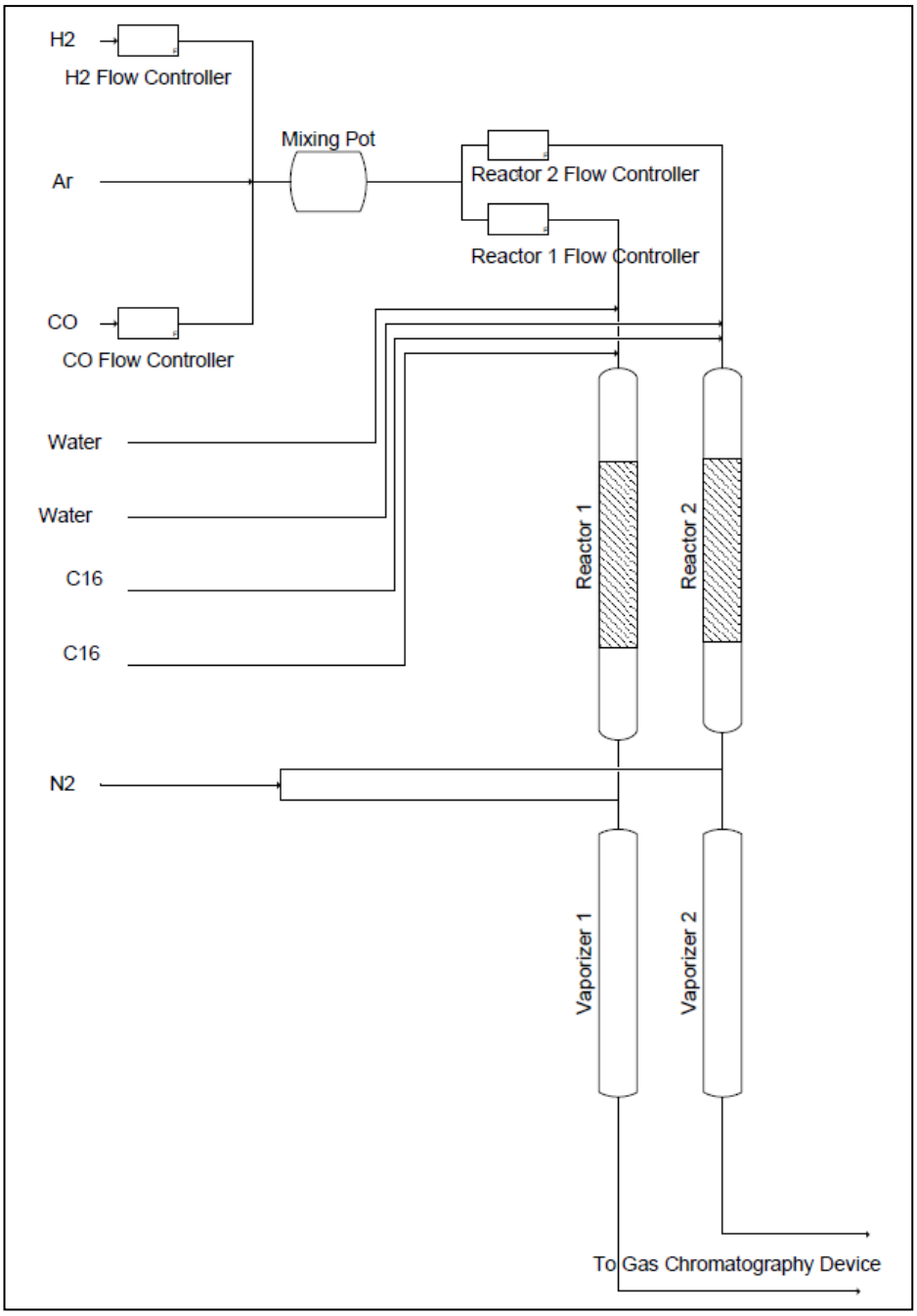

Figure 3.3 : Flow diagram of the laboratory scale experimental setup.

3.3.1 Reactor

Two stainless steel tubular reactors (20 mm (inner radius)- 350 mm (length)) positioned vertically. Reactor tubes are positioned in brass housing with multi zone temperature control equipment in order to achieve steady temperature profile inside the reactor and maintain isothermal zone within the reactor. Figure 3.5 shows the reactors with insulation jacket.

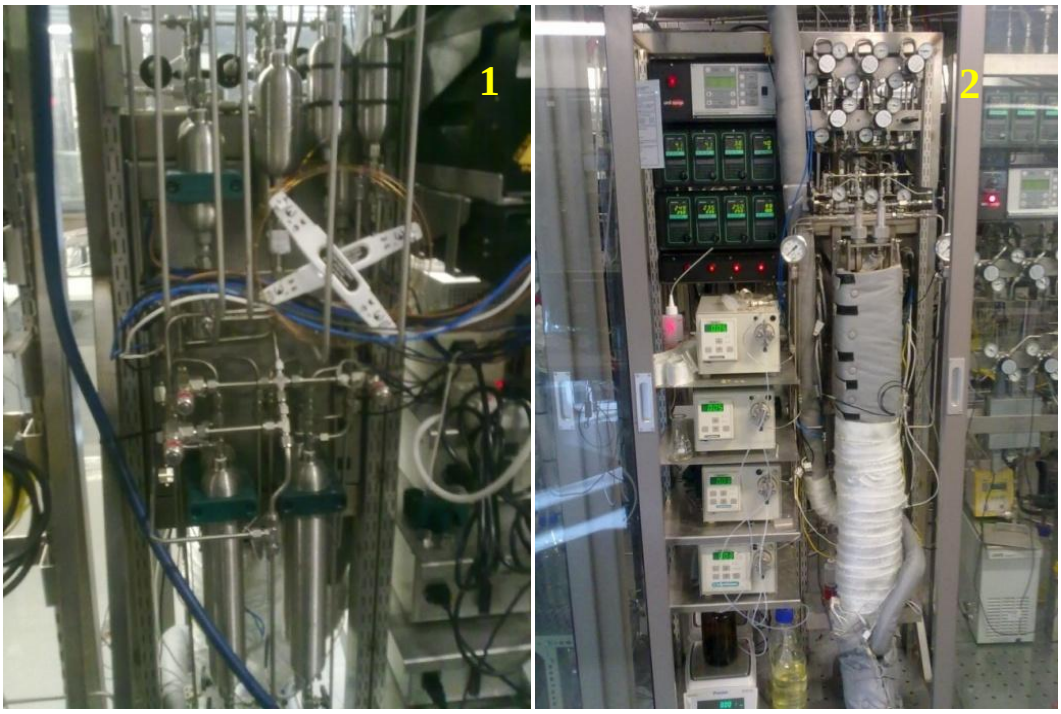

Figure 3.4 : Laboratory scale experimental setup. 1; Back view of experimental setup. 2; Front view of experimental setup.

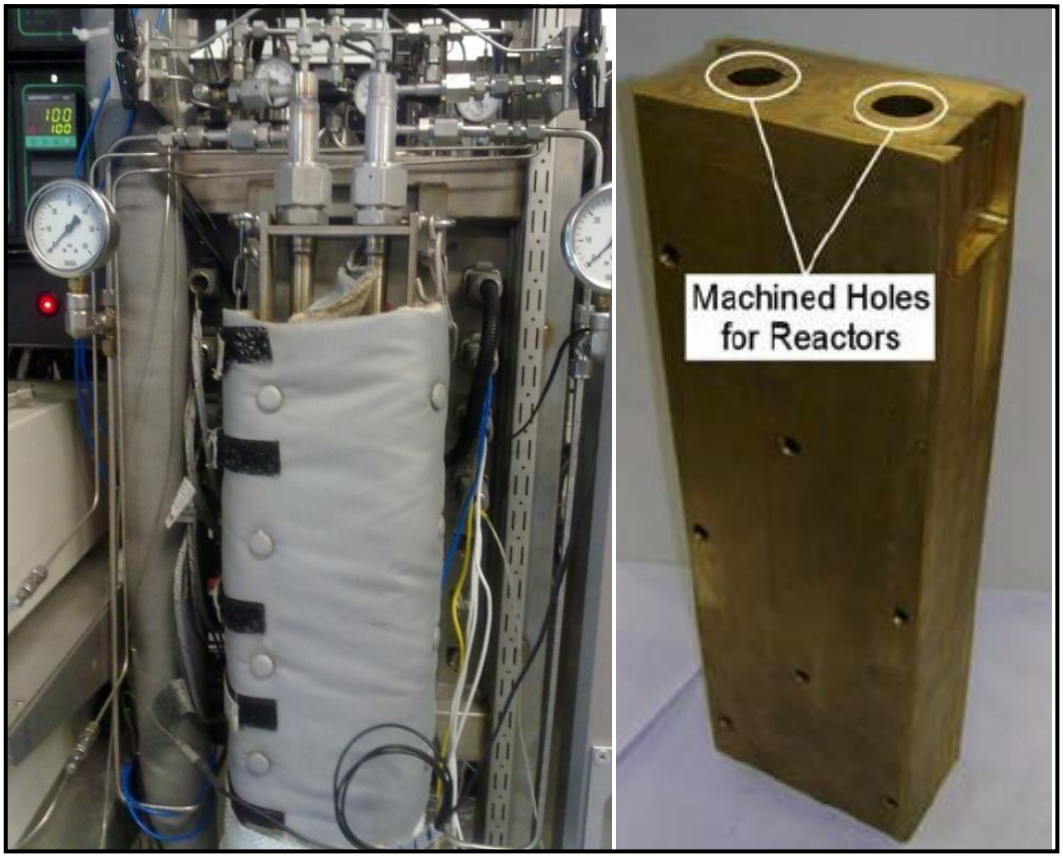

Figure 3.5 : Reactor with insulating jacket and brass housing.

Due to the production of solid and liquid phase products by FT and HC reactions, reaction effluent should be diluted and maintained at specific temperature. This improvement was done by two tubular vaporizer (240 mm lenght-10.2 mm inner radius) which were attached to the exit of both reactors.

After the assumption of achieving only gaseous product spectrum at the effluent of vaporizers, vaporizer bottom stream was sent to GC equipment for selectivity and conversion analysis.

3.3.2 Flow control

In experimental reactor, flow was controlled by different master controllers and pumps. All gaseous inlet mass flow was controlled by 4 different master controllers (Brooks Instrument) which have ranges between 0-500 mL/min. Master controllers are shown in Appendix A.1 PFD diagram as MC1, MC2, MC3 and MC4. Figure 3.6 and Figure 3.7 shows master controllers that were used during the experiments. After flows were regulated for desired mass flow rate, streams were passed through several catch pots in order to prevent liquid feed into reactor.

H_2 and CO gases (which comprise the syngas) were fed to reactor by mixing in a small pot before the inlet of the both reactors.

Liquid inlets C16 and water were fed to reactor by two HPLC piston type pumps for each reactor.

N_2 and Ar gas flows were not controlled by master controllers due to lack of working space and lack of available master controller. N_2 mass flow rate was controlled by 50 m capillary tube for each feed. Figure 3.8 shows the capillary tube that was applied to the system.

After application of capillary tube, mass flow of the N_2 gas was controlled by bubble meter. Flow rate was measured approximately 260 mL/min.

Argon feed was controlled by two orifices in the system. Figure 3.9 shows the orifices that were used in the system.

At the inlet pressure of 46 bar, argon flow through the orifice 7μ(1) was approximately 26 mL/min. This was measured with a bubble flow meter of 100 mL.

Figure 3.6 : Electronic interface of the master controllers.

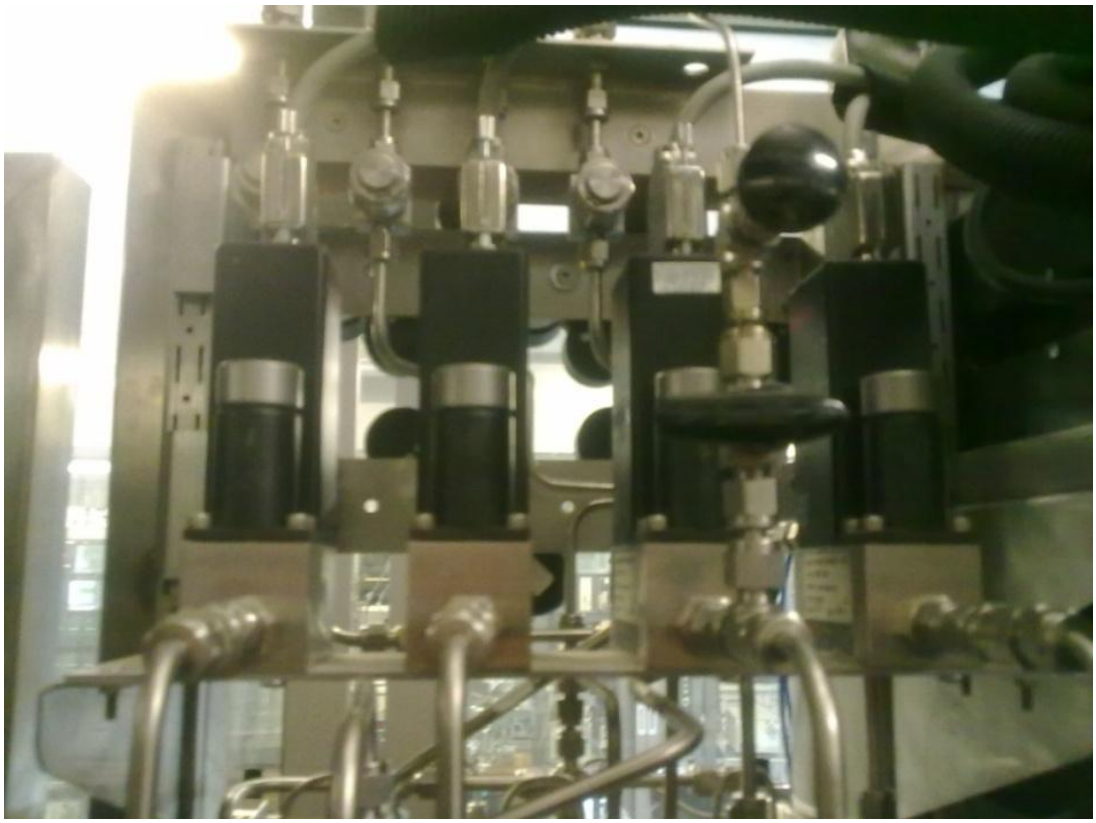

Figure 3.7 : 4 different master controllers for each gaseous stream.

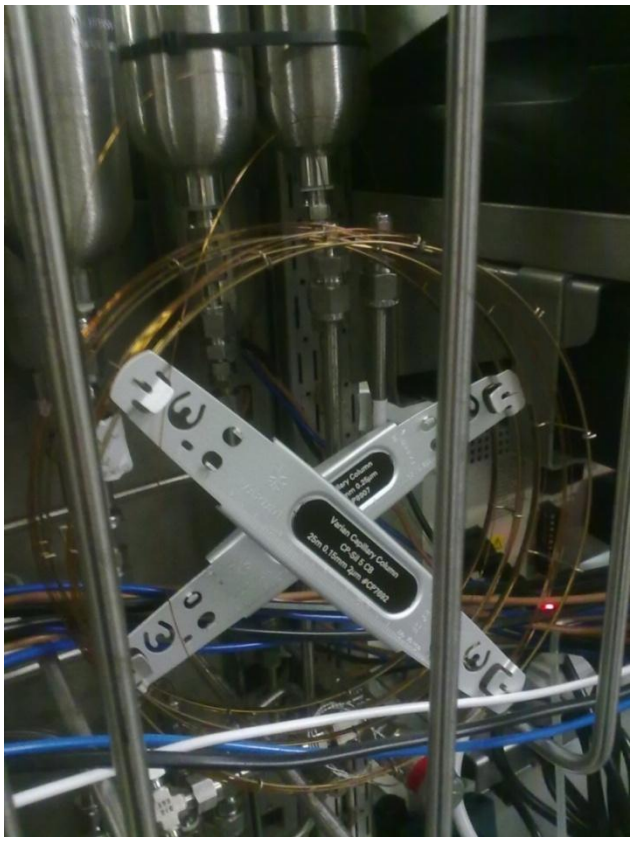

Figure 3.8 : Capillary tubes for N_2 flow control (Each reactor inlets have their own capillary tube).

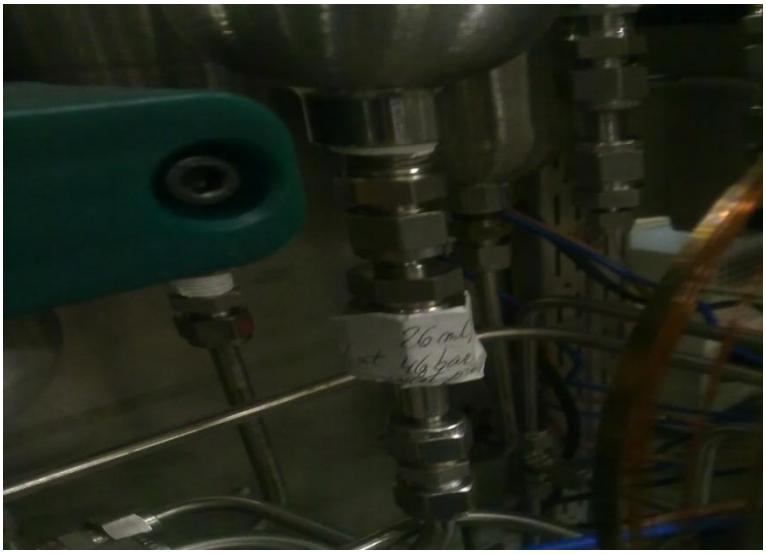

Figure 3.9 : Orifice for mass control of the Ar feed**.**

The bubbles traveled from the bottom to the top in approximately 230 seconds (3 min 50 sec). An alternative orifice (15µ(4)) with a higher flow is available, and taped to the system. This orifice provides an argon stream of 61,2 mL/min (bubble travels 100 mL in 98 seconds).

For water tolerance experiments, water is fed to reactor by HPLC pumps which are exactly same as C16 pumps. But in liquid form, n-hexadecane and water are immiscible. In order to provide mixture to reaction, water is fed to system by deep tube which provided feed 20 cm below from the top of the reactor. Figure 3.10 shows the deep tube which was applied to system. The tube at the top is the water feed tube and it starts from the top of the reactor and ends 20 cm below the top.

Figure 3.10 : Deep tube for water feed.

It can be said that water is in vapor form in that region due to the temperature is sufficient enough to vaporize water.

3.3.3 Pressure control

In order to achieve flow from the mixing pot to reactors, mixing pot pressure was held approximately 5 bar above the reactor. This is done by applying a back pressure regulator to the entrance of the mixing pot which will provide desired pressure. Reactor pressure is controlled by pressure drop regulators which are placed in front of the master controllers which feed the mixture into reactor. Pressure drop regulators were controlled manually.

In order to ensure pressure which is feed to GC from the effluent of the vaporizer correct, back pressure regulator is applied to the bottom of the both vaporizers.

3.3.4 Temperature control

In order to provide steady temperature gradient through the reactor, several heating equipments were applied to system. Both reactors have 4 different temperature zones. Figure 3.11 shows the reactor diagram for 4 different heating zones.

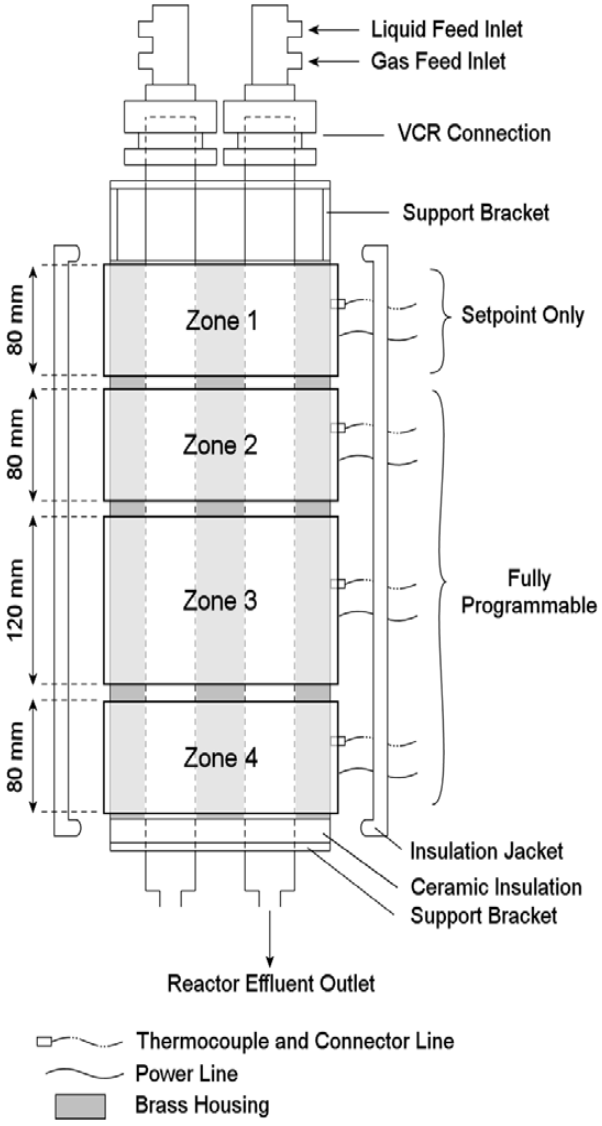

Figure 3.11 : Reactor diagram for four different thermal zones [43].

Except from zone 1, the other three zones are controlled by fully programmable temperature controllers (Gefran 1600).

A thermowell of approximately 3 mm outer diameter runs through the length of the reactor. Four rectangular heating bands surround the brass reactor block by sliding a thermocouple up the thermowell a temperature profile of the reactor was established which shows that the temperature does not vary along the length of the reactor tube except for the bottom 4 cm and the top 10 cm. The brass block apparently conducts heat very well so that the temperature profile is flat. The catalyst is positioned in this flat section by means of SiC filler granulates. The space above the catalyst is also filled with SiC to ensure that the liquid distributes evenly in the radial direction and no channeling occurs. In zone 3 isothermal temperatures were achieved and in that zone catalyst was loaded.

At the reactor outlet, stream was mixed with N_2 or H_2 dilution gas in T junction. From this point to the GC device, all the system was insulated by glass wool in order to avoid heat loss which could possibly cause condensation in the lines. Vaporizer was operated between 160-260 °C. Top of the vaporizer temperature was 160 °C and bottom of the vaporizer 260 °C. Heating was done by heating wires which are more coiled at the bottom of the vaporizer so heating of the vaporizer is achieved by convection and the conduction through vaporizer. Vaporizer is also filled by SiC in order to ensure temperature distribution is flat. Vaporizer outer surface is insulated by glass wool to avoid heat loss.

After exiting vaporizer, in order to avoid condensation, all the line between Vaporizer bottom and GC (contains needle valve) was insulated and heated to 250 °C.

3.3.5 Vaporizer

Vaporization step was crucial for the data analysis and online GC sampling. Due to nature of FT and HC reactions, products are in gaseous, liquid and solid state. In order to achieve a complete analysis in GC, all the reactor effluent should be feed in gaseous form. Vaporizer duty is to vaporize the effluent by diluting the products and heating to the desired temperature.

Two stainless steel tubes, 240 mm in length and with an internal diameter of 10.2 mm, packed with inert SiC. Vaporizers were insulated by glass wool in order to avoid heat loss during operation which is shown in Figure 3.12.

Figure 3.12 : Vaporizer with insulation.

3.4 Experiment Apparatus Blind Test Results

Before starting the analysis with reactor system, some parameters were checked in order to assure the experiment system will work. First of all, vaporizer should vaporize every product. This can be achieved if the vapor pressure of every species is bigger than partial pressure of the every single species and eventually vapour pressure will be higher than the ambient pressure. One way to decrease partial pressure is to add diluents to the reactor effluent. It was planned to use N_2 as a dilution gas but due to non-availability of N_2 gas, in some cases H_2 was used.

Figure 3.13 shows the change of vapour pressure of C16 by temperature. Partial pressure of C16 in the vaporizer was calculated as 0.1628 bar with the respected concentrations for 0.03 mL/min C16, 260 mL/min N_2 and 50 mL/min H_2 flow rates and with the assumption that every species in the vaporizer were in gaseous form. Vapour pressure of C16 at different temperature was found from the literature [55]. In order to vaporize C16 vapor pressure of C16 must exceed the partial pressure of C16 as only liquid compound in the vaporizer was C16. In the Figure 3.13, it can be clearly seen that at above 216 °C vapor pressure exceeded the partial pressure. This shows that C16 would be vaporized completely in the vaporizer which was operated between 160 °C- 260 °C.

Controlling the C16 vapor-partial pressure is necessary for the HC experiments. In order to understand the applicability of CFTH synthesis analysis, every possible FT

product's vapor-partial pressure must be controlled. Procedure was the same with C16 partial pressure control check, only difference was the checking of every species vapor-partial pressure. Figure 3.14 represents the vapor pressure and partial pressure of different hydrocarbons. Figure 3.14 is given in semi-logarithmic scale in order to show which hydrocarbon will vaporize or not.

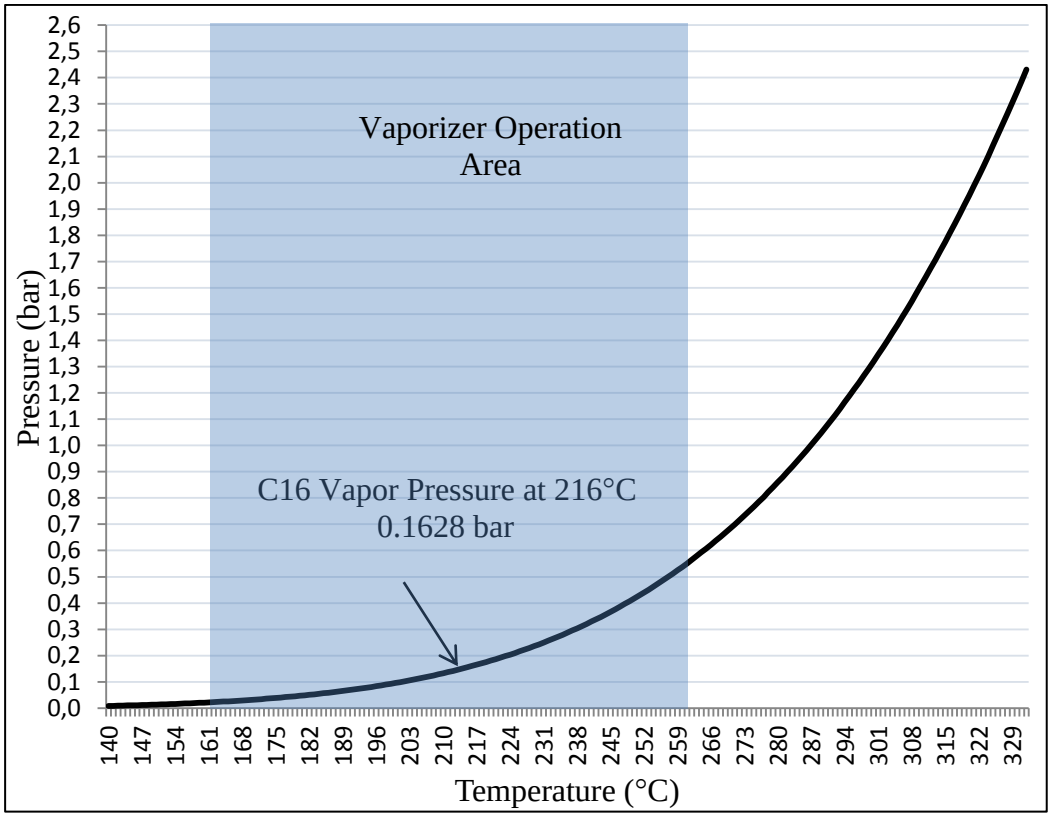

Figure 3.13 : Vapor pressure of C16.

For partial pressure calculations, theoretical 80 % CO conversion rate was selected. By applying equation 3.4, theoretical amounts of $–CH_2–$, CO, H_2 and H_2O can be found. N_2 dilution amount is selected as ten times of CO inlet. Another important calculation was done for ASF chain growth probability value α. α was selected as 0.80 which is common for LTFT synthesis. With α, hypothetical mass fraction of every hydrocarbon can be found. Considering the vaporizer pressure as 20 bar, partial pressure of every species can be found as a fraction regarding their mass fraction in the vaporizer. Vapour pressures of hydrocarbons were found in literature [55].

From the Figure 3.14 it can be clearly seen that above 260 °C for 20 bar every species from C1 to C35 will be vaporized because vapour pressures of every single

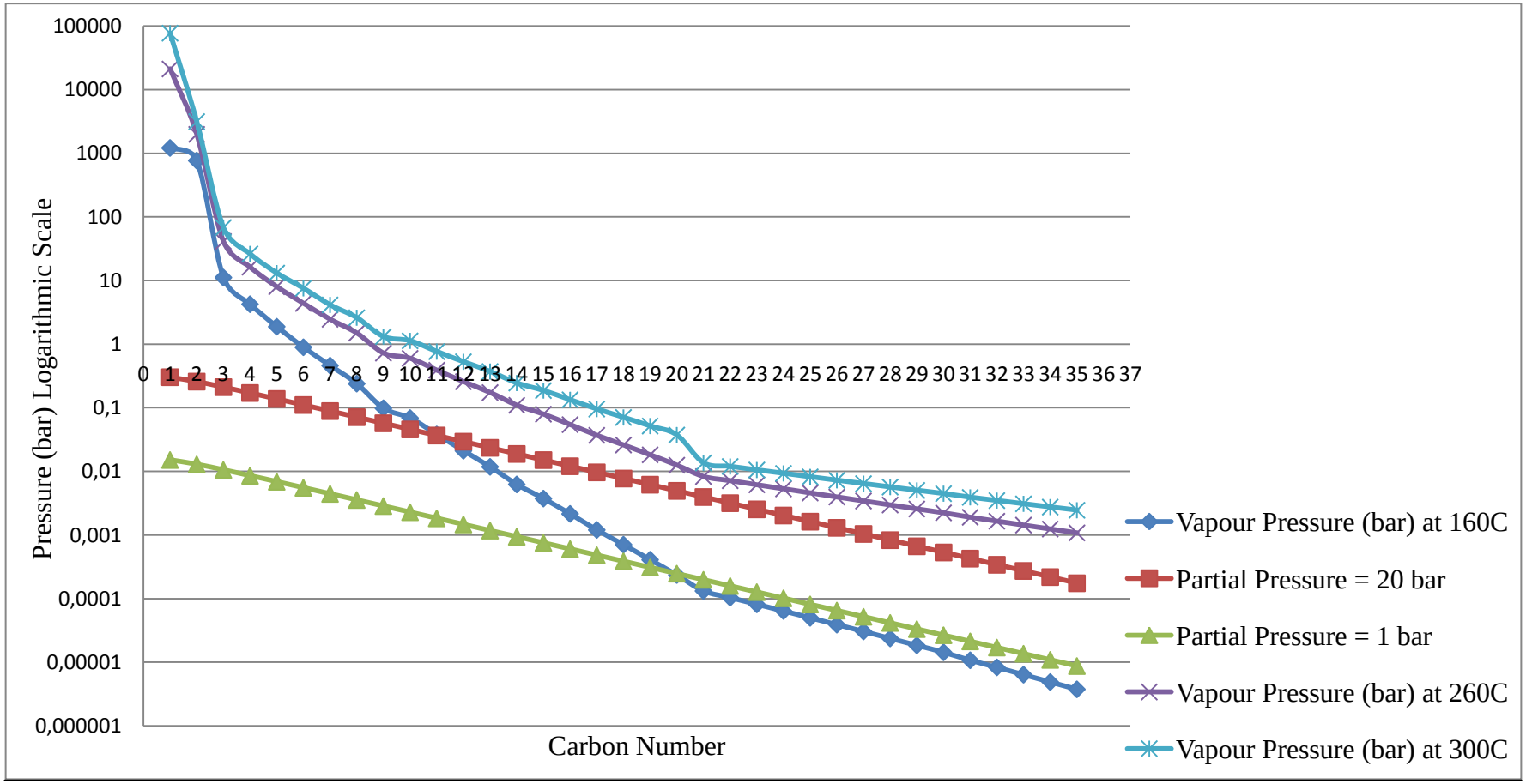

Figure 3.14 : Vapor pressure and partial pressures for different conditions in the reactor and vaporizer.

hydrocarbon will exceed the partial pressure. It can be assumed that hydrocarbons containing more than 11 carbon atoms will be in liquid form at the entrance of the vaporizer. But at the outlet of the vaporizer, all the species that could possibly formed in the reactor will be in gaseous form.

Apart from vaporizer conditions, getting steady peak areas in the GC analysis are also important aspect of pre experiment preparations. This was controlled by online GC analysis. C16 was selected for checking the steady flow rate as it would be used in HC experiments. During these blind experiments, gaps in heating isolations were fixed. Also pressure and flow controllers were observed in order to fix for possible problems. Figure 3.15 shows the last C16 peak height change with time on stream (TOS).

After 410 hours steady peak height was achieved. First 410 hours were spent on fixing the pressure, temperature and flow controllers. By assuring flow will be steady in the GC and vaporizer will do vaporizing step, experimental setup was ready for the analysis.

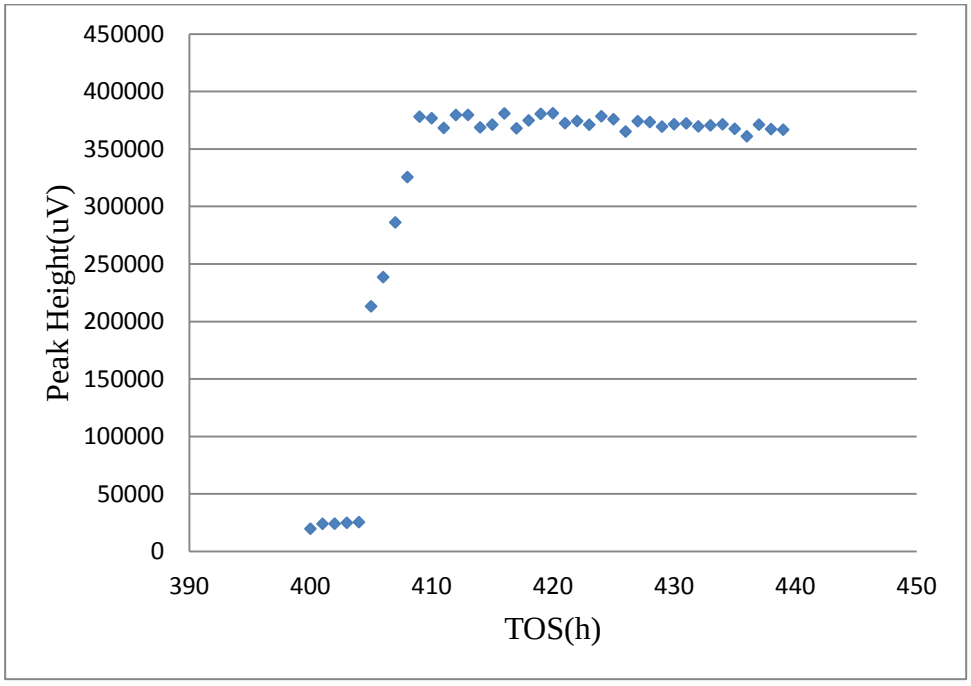

Figure 3.15 : Peak height change during the blind experiment.

4. RESULTS AND DISCUSSION

4.1 Selection of Hydrocracking Catalyst

For selection of HC catalyst, Platinum-HMFI90 catalyst was analyzed. Results were compared with Palladium-HMFI90 results which were acquired from the previous research that had been done in the same laboratory [53]. Selection of bifunctional catalyst was done by comparing the performance of different metal sites on the bifunctional catalyst under FT conditions.

4.1.1 CO tolerance of metal-zeolite catalyst

HC reactions were done in two different metal loadings on Platinum/HMFI90 catalyst. These are 0.1% and 1% for each reactor. Table 4.1 shows the catalyst loading for each reactor in CO tolerance experiments.

Table 4.1 : Catalyst loadings for CO tolerance experiments (Pretreatment temperature: 350 °C).

Catalyst	Reactor 1	Reactor 2
Zeolite	1.286 g	1.286 g
Supported metal (Pt)	0.025 g	0.257 g
Metal loading	0.1%	1.0%

Figure 4.1 shows the C16 conversion rate over time on 0.1% Pt/SiO_2 + HMFI90 which was important for the analysis as getting steady results for each step of the experiments was necessary for calculation of conversion rate. Steady results enable to use mean values for conversion rates. Beside from that calculation of conversion rate, change over time gave insight about catalytic activity over time.

In Figure 4.1 between 15 h and 25 h, reactor is in the stabilization period which changed the conversion drastically. Between 25 h and 50 h, it can be clearly seen that conversion rate was steady. And around 100 h and 120 h, CO deactivation and CO removal steps are shown.

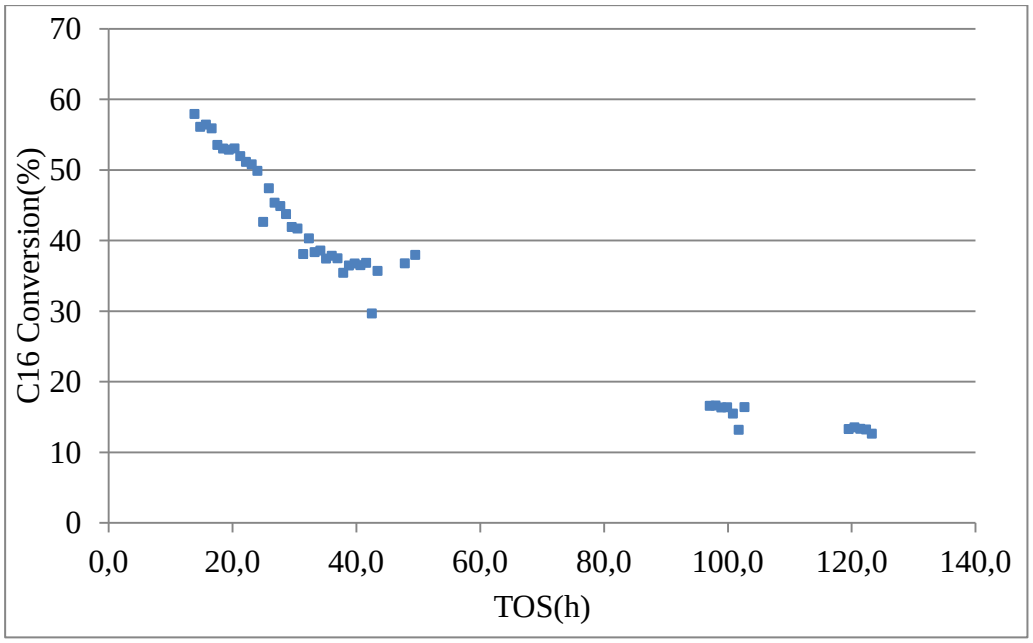

Figure 4.1 : 0.1% Pt/SiO_2 + HMFI90 CO tolerance.

Results are again steady. Progressive deactivation of bifunctional catalyst wasn't observed. This phenomena was expected as ZSM-5 pores have medium size so no coking observed due to the accumulation in the pores [36]. In Table 4.2, summary of conversion change is given for CO deactivation with the standard deviations as the percentage of the average values. It can be clearly seen that CO decreased the conversion rate from 36.46 % to 16.28 %. After the desorption of CO, catalyst lost more activity and conversion rate is 13.20 %. Removal of CO didn't restore the original conversion rate which is evident that CO poisoning on Platinum is irreversible. Since in this work, there was no CO removal from the reactor, reversibility or irreversibility of CO deactivation was not significant.

Further assessment of CO effect on bifunctional catalyst was done by examining the selectivities.

Table 4.2 : CO poisoning on HC catalyst (Metal loading: 0.1 %; Temperature: 225 °C; C_{16} Flow Rate: 0.03 mL/min).

	Conversion (%)	Standard Deviation (%)
Standard HC	36.46	0.70
CO Poisoning	16.28	0.46
CO Desorption	13.20	0.34

In Figure 4.2 and Figure 4.3, effect of CO on selectivity for 0.1% Pt/HMFI90 catalyst is examined. Figure 4.2 shows the standard HC experiment results without any effect of inhibitors. On the other hand Figure 4.3 shows the hydrocarbon distribution and selectivity of HC products in CO environment.

By examining Figure 4.2, Platinum catalyst produced hydrocarbons ranging from C3 to C12, insignificant amount of n-hexadecane about 1% stayed in the reactor without any HC. Products were highly paraffinic. Olefins account for %1 of the total products. Product distribution accumulated around C4-C5-C6 which is evident that secondary cracking occurred and long paraffins further hydrogenated on metal sites.

In Figure 4.3, effect of CO can be seen clearly. CO affected the balance between metal and acid sites. Degree of isomerization is high. Dehydoregantion on the metal site was suppressed by CO effect which caused unsaturated products not to get enough hydrogen to become saturated.

By comparing Figure 4.2 and Figure 4.3, it can be said that CO poisoning didn't change the carbon number distribution much. Products range from C3 to C12 .But olefinic products increased significantly by the effect of CO. It can be said that CO limited the hydrogenate dehydrogenate ability of the metal thus unsaturated hydrocarbons stayed in the products.

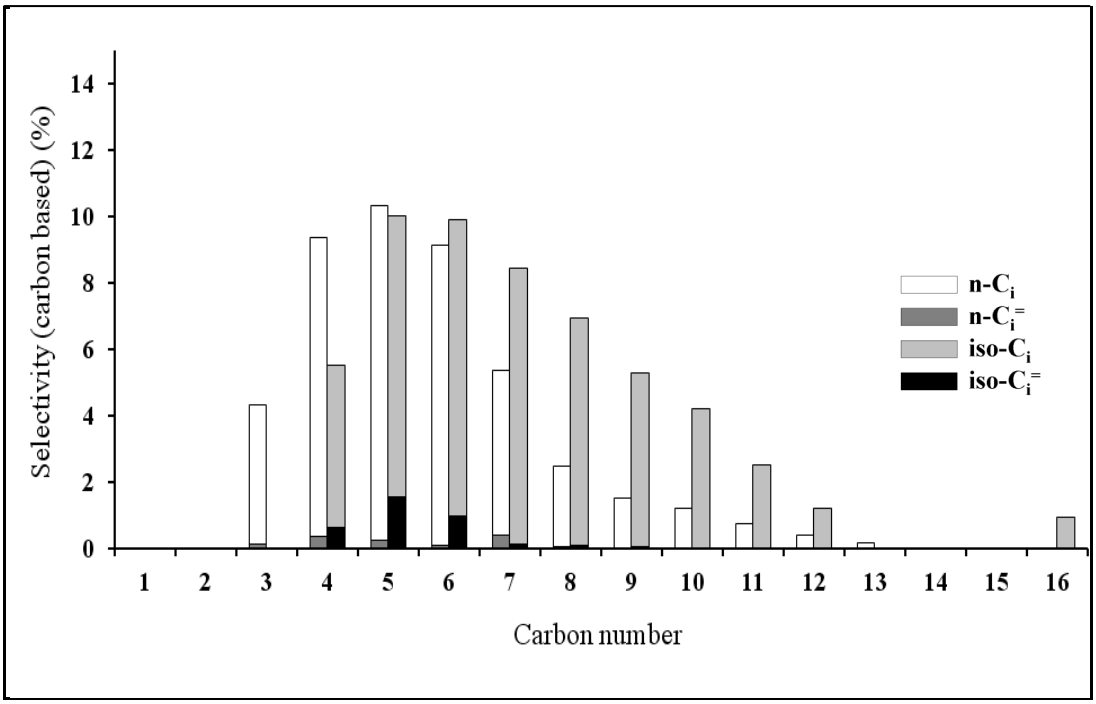

Figure 4.2 : Standard HC selectivity on carbon basis.

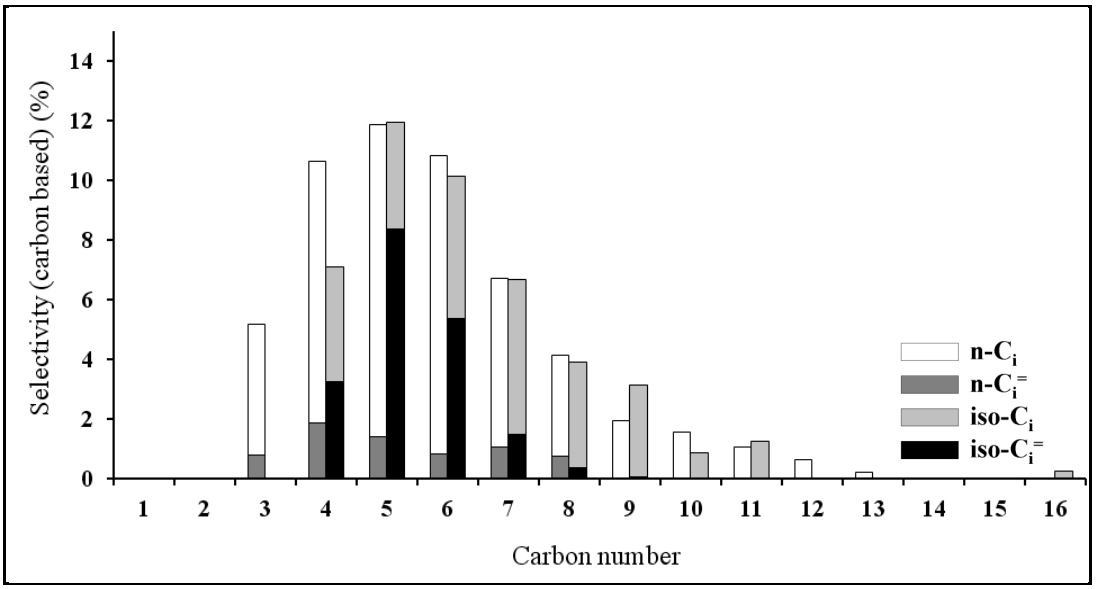

Figure 4.3 : CO deactivation on platinum HC catalyst.

In order to understand the effect of metal loading and in order to examine whether higher metal loading on the bifunctional catalyst can overcome the CO deactivation since CO is thought to affect the metal sites on the bifunctional catalyst. Platinum loading was increased to 1% and same experiment was done again with the same conditions. Catalyst loading and pretreatment temperature is given in Table 4.2.

Figure 4.4 shows the conversion rate changes over time for 1% catalyst. It is clearly seen that conversion rate stayed same for different experiments steps which permits the usage of mean values. Between 25 h and 50 h, standard HC was occurred. Between 83 h and 95 h, CO was fed to reactor. Last data points between 103-120 h shows the CO desorption step.

Progressive deactivation of the catalyst didn't occurred by the time change. For every experimental step, no activity loss was observed.

In Table 4.3, change of conversion rate by CO poisoning on Pt catalyst is examined. 1 % catalyst reached higher conversion rates which are nearly 100 % and as 0.1% CO poisoning affected the catalyst and this interruption is not reversible. Higher conversion rate could be the result of hydrogenation activity which successfully hydrogenates the n-hexadecane which can be caused because of the increased metal sites.

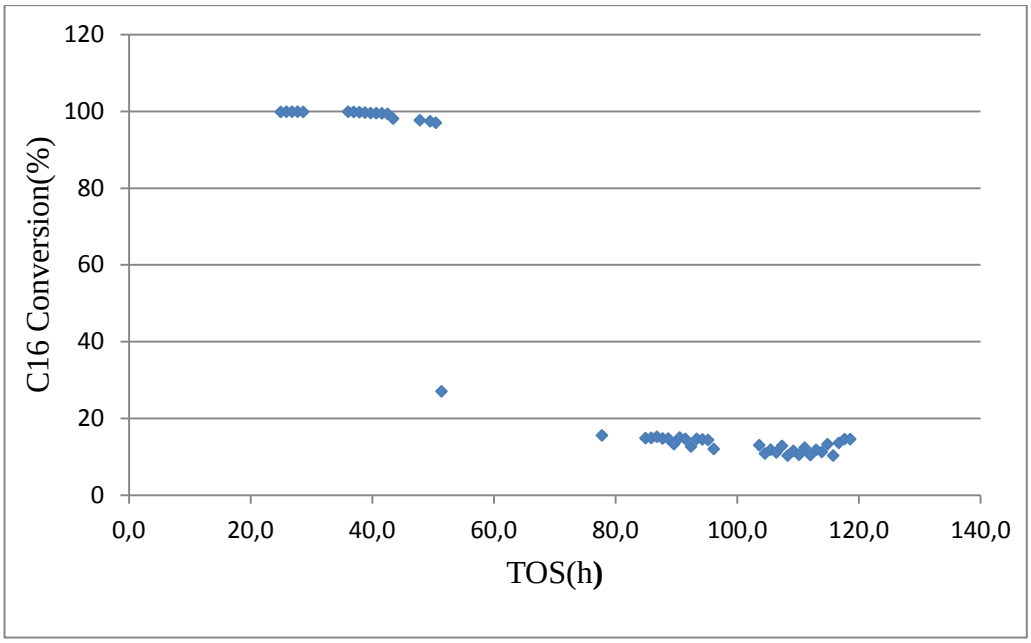

Figure 4.4 : 1% Pt/SiO2 + HMFI90 CO tolerance.

After introducing CO to reactor, catalyst was deactivated significantly. Conversion rate dropped to 14.25 %. Same interpretation can be done as in 0.1 % Pt loading experiments. CO has poisonous effect on bifunctional HC catalyst by disturbing acid-metal balance of the catalyst.

Table 4.3 : Summary of conversion changes for CO poisoning on 1% catalyst. (Temperature: 225 °C; C16 flow rate; 0.05 mL/min).

Experiment	Conversion (%)	Standard Deviation (%)
Standard HC	97.38	0.03
CO Poisoning	14.25	1.01
CO Desorption	13.29	2.03

Figure 4.5 and Figure 4.6 shows the selectivity change over 1% catalyst by CO poisoning. Figure 4.5 shows the standard HC and Figure 4.6 shows the selectivity in CO environment. Results are very identical with 0.1% Pt loading.

As in the 0.1 % metal loading, product spectrum is highly paraffinic for standard HC. Only small amount of olefins were in the product mixture. Also n-hexadecane was completely cracked to shorter hydrocarbons. Figure 4.5 and Figure 4.6 shows that secondary HC reactions occurred for both experiment operations. HC in CO

environment pushed the product range to smaller products. Thus it could be said that even with lower conversions, HC under CO deactivation showed secondary HC.

By comparing Figure 4.5 with Figure 4.6, it can be concluded that olefin selectivity increased by CO poisoning and product spectrum is less paraffinic. CO ceased the hydrogenate-dehydrogenate ability of the metal and because of this disturbance some hydrocarbons stayed unsaturated. And also it can be said that isomerization yields stayed same during two experiments. So CO affected only the metal sites of the bifunctional catalyst.

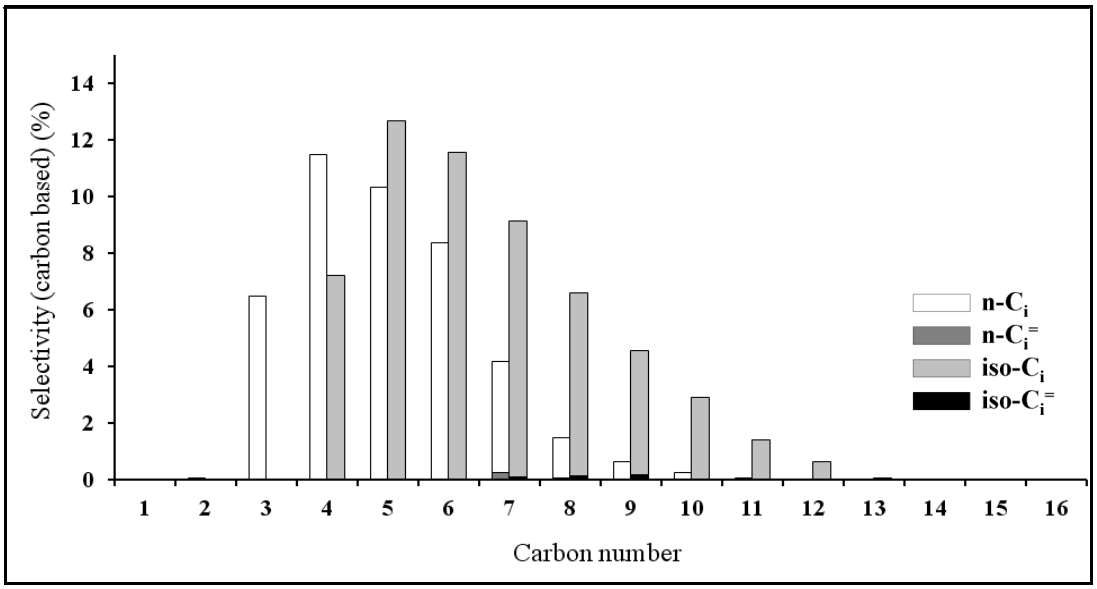

Figure 4.5 : Product selectivity for 1% platinum loading.

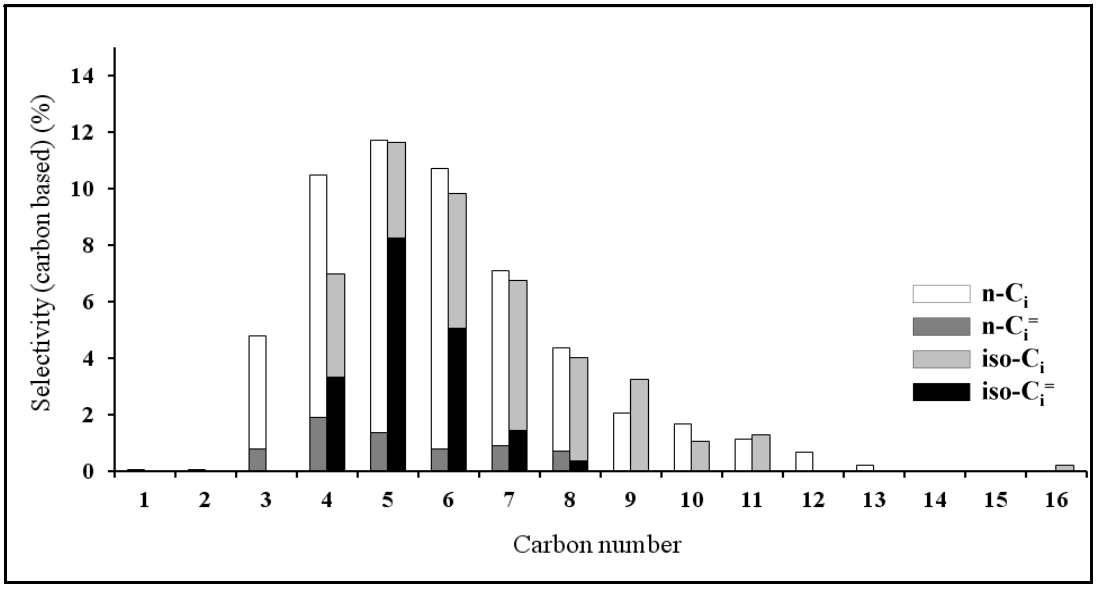

Figure 4.6: Product selectivity for 1% platinum loading during CO feed.

4.1.2 H_2O tolerance on metal-zeolite catalyst

H_2O poisoning experiments are done for 1% metal loading. Table 4.4 shows the catalyst loading for this experiment step.

Table 4.4 : Catalyst loading for H_2O tolerance experiment.

	Weight (g)
Zeolite HMFI90	1.286
Supported Metal (Pt)	0.257
Metal Loading	1%
Pretreatment Temperature	350 °C

Figure 4.7 shows the deactivation of catalyst by H_2O. First 20 hours shows the HC without any inhibition, after 28 hours water was introduced to reactor. It is observed that catalyst lost all its activity in H_2O environment. Last two data point between 60h and 70h shows the H_2O removal step.

In Table 4.5, 1% Pt activity results are summarized. Removal of water from the reactor caused the regain of the catalytic activity. Water poisoning on the Pt catalyst is reversible in contrast to CO poisoning. Water deactivation could be a result of closure in the pores of acid sites. Deactivation by water was observed in a research of Martinez et al. It was proposed that water molecules compete with n-hexadecane on acid site. Since no coking expected on ZSM-5 catalyst and removal of water restored the catalytic activity, deactivation was the result of competition between n-hexadecane and water molecules [47].

Since in H_2O environment Platinum/Zeolite catalyst lost its all activity, it is pointless to show the water effect on selectivities. With nearly no conversion with the catalyst, only little amount of hydrocarbons formed beside from C16 and they were at insignificantly low concentrations.

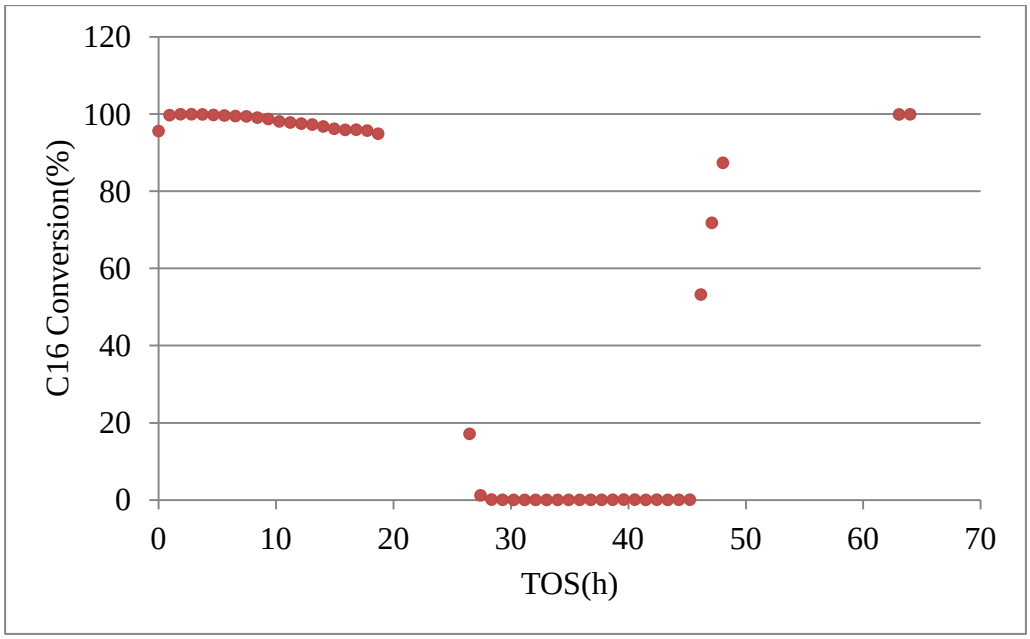

Figure 4.7: 1% Pt/SiO_2 + HMFI90 H_2O tolerance.

Table 4.5 : Water poisoning on 1% Pt/SiO_2 + HMFI90 (T: 225°C, C16 flow rate: 0.05 mL/min).

Experiment Step	Conversion (%)
Standard HC	95.61
H_2O Poisoning	0.01
H_2O Desorption	99.62

4.1.3 Platinum/HMFI90 and Palladium/HMFI90 comparison

In order to do further analyses with combined catalyst, selection of HC catalyst should be done. Selection was done by comparing the conversion values for two different catalysts. Table 4.6 shows the conversion values for different reaction steps and modes.

By comparing Table 4.5 and 4.6, it can be easily said that Palladium is better choice for combined catalyst as it didn't lose all its activity for CO and water deactivation steps. Also it gained some of its activity for 10°C higher temperature. On the other hand, catalyst that was used previously which contains Pt showed no activity under H_2O deactivation, also CO deactivation was more severe.

Table 4.6 : CO and H_2O tolerance for 1% Pd/SiO_2 + HMFI90 catalyst [53].

Temperature	Conversion (%)			
	Standard HC	CO	CO+H_2O	CO desorbed
225 °C	99.91	36.02	4.46	99.82
230 °C	-	45.9	16.95	-
235 °C	-	61.69	42.64	99.88

If the CFTH experiments were done by using Pt as metal site, CO and H_2O would affect the experiments more severely. Thus selection of Pd as metal site was necessary.

4.2 CFTH Reactions

4.2.1 Effect of flow rate on conversion

In order to understand the effect of flow rate on conversion, 3 different experiments were conducted. First experiment was standard FT synthesis which was done for the purpose of base line for combination experiments. Last two experiments were done for two different catalyst loads which are 1% and 0.1 %. Table 4.7 shows the catalyst loadings during the experiments. Figure 4.8, Figure 4.9 and Figure 4.10 show the change of CO conversion against time.

Table 4.7 : Catalyst loadings for CFHT experiments.

Catalyst Loaded	Metal Loading (%)	Co/SiO_2 (g)	Pd/SiO_2 (g)	HMFI90 (g)	Pretreatment Temperature (°C)
Co/SiO_2	-	1.286	-	-	425
Co/SiO_2 + 5 % Pd/SiO_2+ HMFI90	0.1%	1.286	0.025	1.286	425
Co/SiO_2 + 5 % Pd/SiO_2+ HMFI90	1%	1.286	0.257	1.286	350

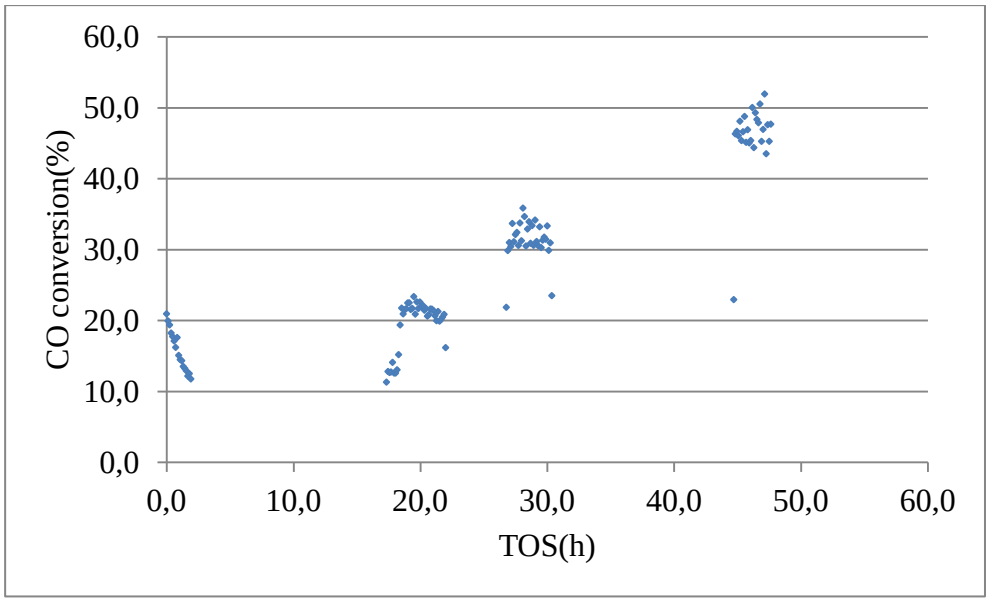

Figure 4.8 : Change of conversion against time for Co/SiO_2 catalyst loading.

Figure 4.8 shows the results for the standard cobalt FT catalyst. This standard FT analysis was done in order to compare the results with combined catalyst. As in the previous HC experiments results should be steady in order to use mean values for the rest of the analysis. It can be clearly seen that results were steady for the conversion rates. Small disturbances in the conversion rates could be resulted as electronic disturbances from the GC which can be neglected.

In Figure 4.9 0.1 % Pd/HMFI90 HC catalyst was added to FT catalyst. Same steady conversion rate is visible.

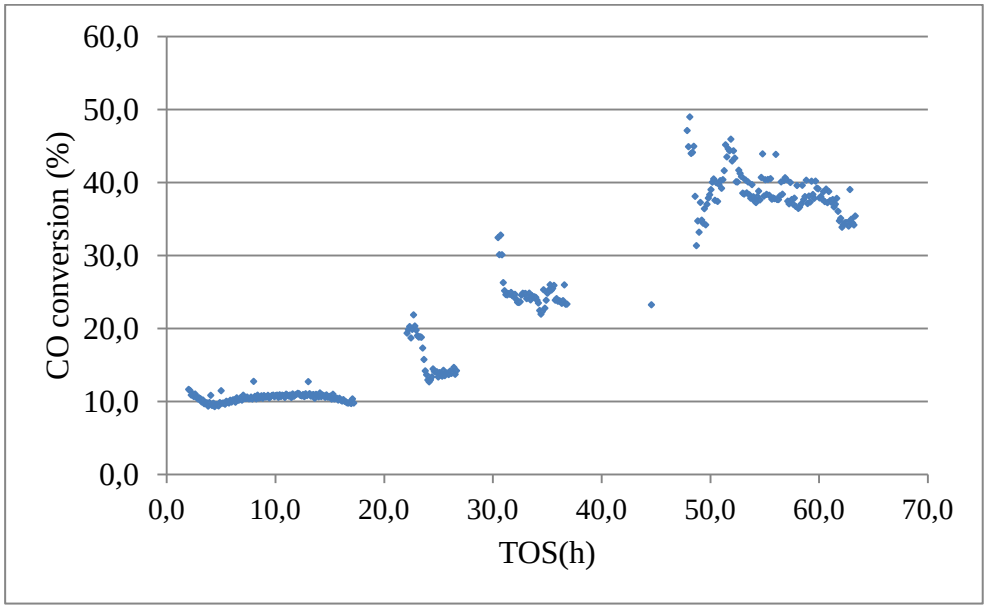

Figure 4.9 : Co/SiO_2 + 0.1% Pd/SiO_2 + HMFI90

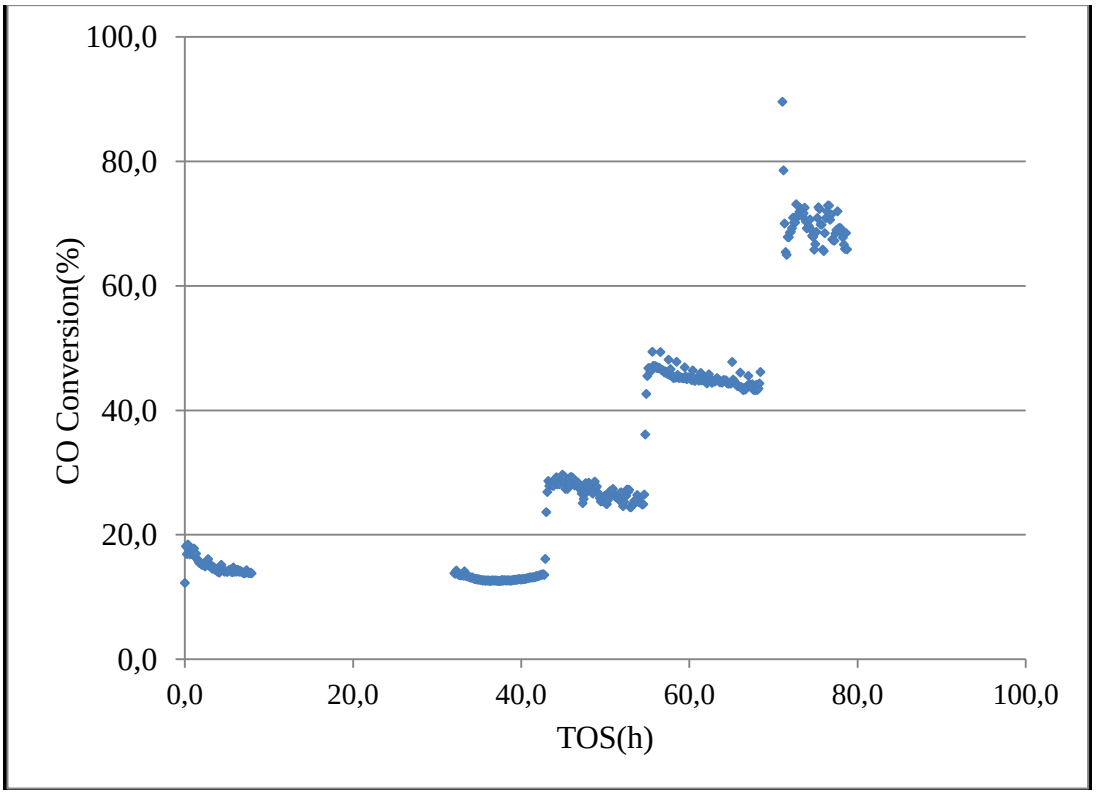

Figure 4.10 : Co/SiO_2 + 1% Pd + HMFI90

Figure 4.10 shows the conversion rate against time for the 1 % Pd/HMFI90 + Cobalt catalyst. Steady conversion rate change is again enabling further analysis. In both Figure 4.8, 4.9 and 4.10, there are four different conversion steps. These steps show the different flow rates 120 mL/min, 60 mL/min, 30 mL/min and 15 mL/min respectively. Table 4.8 summarizes the conversion rates for different catalyst and loadings.

It can be clearly seen that lower flow rates in the reactor which means higher space velocities caused the CO conversion to increase for each different catalyst type and loadings. Another observation can be done from the Table 4.6. 0.1 % metal loading decreased the conversion rates for all flow regimes on the other hand 1 % metal loading could increase the CO conversion from standard FT synthesis. This can be the effect of promotion on the Cobalt catalyst for the FT. It is not clear why 0.1 % metal loading decreased the CO conversion rate. It could be due to adsorption of CO on HC catalyst which prevents CO molecules to reach cobalt catalyst thus lower conversion rate was achieved. Or it could be the result of pretreatment temperature. Relatively higher pretreatment temperature from 1 % Pd catalyst pretreatment could result sintering on the catalyst which results losing some catalytic activity.

Table 4.8 : Conversion rates for different catalyst and different flow rates.

Flow Rate (mL/min)	Conversion (%)		
	10 % Co/SiO_2	0.1 % Pd + HMFI90 + 10 % Co/SiO_2	1 % Pd + HMFI90 + 10 % Co/SiO_2
120	15.5	10.4	13.0
60	21.4	13.8	26.8
30	32.2	24.1	44.8
15	47.1	38.5	69.4

4.2.2 Selectivities for different catalyst

As in the C16 conversion observations, same reactions were also examined for selectivities. Four different flows rates were applied and effects of flow rates on selectivities were examined. Figure 4.11, Figure 4.12, Figure 4.13 and Figure 4.14 shows the selectivities for 120 mL/min, 60 mL/min 30 mL/min and 15 mL/min respectively.

Figure 4.11a shows the standard FT synthesis product distribution. It is noted that methane selectivity was high around 17 %. Beside from that longest hydrocarbon in product spectrum was C18. Figure 4.11b and Figure 4.11c show the selectivities for 0.1 % wt. and 1 % wt. metal loadings respectively. It is clearly seen that higher metal loading lowered the methane selectivity. Beside from that product selectivities showed same patterns for both metal loadings.

High olefin selectivity in both figure 4.11b and 4.11c can be attributed to syngas ratio that was used during the experiments. Since H_2/CO ratio is 2, there was not enough H_2 gases to hydrogenate the paraffins and transform olefins to paraffins on acid site. So olefins that were produced from FT and olefins from HC could be seen in the product spectrum. Still total olefin selectivity was suppressed for both metal loadings. At FT synthesis, total olefin production is 30.33 %. By additional effects of HC catalyst, total olefin product selectivities for %1 and % 0.1 are 23.9 and 25.2 respectively. It can be said that higher metal loading has an effect on olefin selectivity.

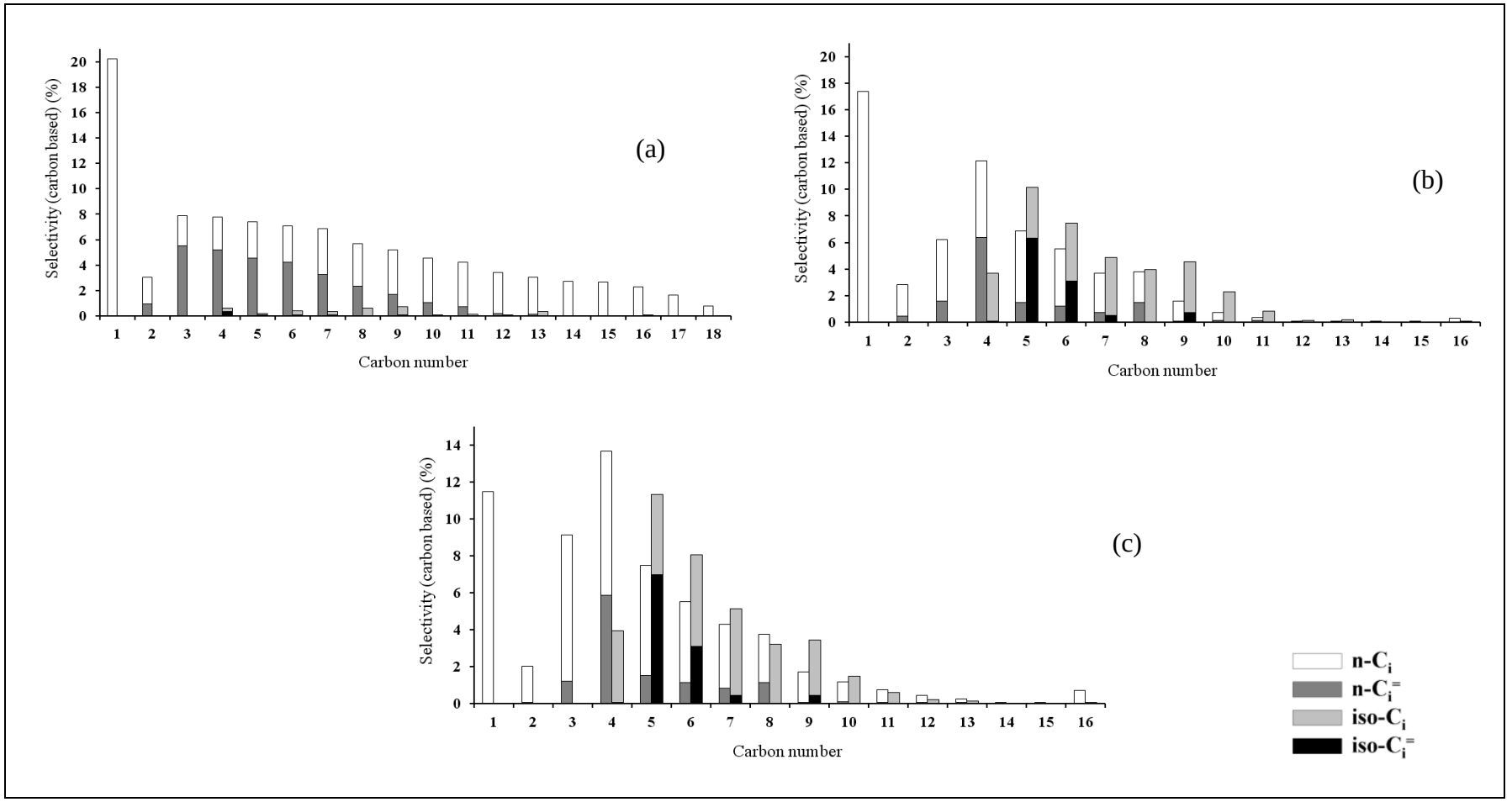

Figure 4.11 : Hydrocarbon selectivities for 120 mL/min flow rate (a) Co/SiO_2, (b) 0.1% Pd/SiO_2 + HMFI90 + Co/SiO_2, (c) 1 % Pd/SiO_2 + HMFI90 + Co/SiO_2. P:20bar; T:225°C; H_2/CO=2.

Since higher metal loading as in % 1 comparing to % 0.1, total active metal sites were increased so there are more free zones for the transformation of olefins to paraffins on metal sites.

Methane selectivities are also significant. While % 0.1wt catalyst loading didn't have any significant effect on selectivity on the other hand 1% Pd loading lowered the methane loading from 17 %to 11 % which can be explained by the lack of olefins in the products of HC due to the effect of Pd which isomerized the olefins further [48].

Paraffin isomerization certainly took placed on combined catalyst. Total Iso-paraffin selectivity increased significantly from 3.10 to 27.62 % for 1 % Pd loading. And for 0.1 % Pd loading, iso-paraffin selectivity was increased to 25.63 % Acid sites of the combined catalyst worked as expected.

In Figure 4.12 carbon selectivity for three different catalyst loadings at 60mL/min flow rate examined. Figure 4.12a shows the standard FT synthesis which has a product spectrum ranging from C1 to C18 with combination HC catalysts which are shown in Figure 4.12b and 4.12c product spectrum was shortened to C13. As in 120 mL/min flow rate product spectrum shows same pattern. There are only no significant differences. Methane selectivity was lower in 1% wt metal loading. Product spectrum becomes more paraffinic as isomerized paraffins were produced by HC.

For 60 mL/min flow rate, Cobalt catalyst produced hydrocarbons ranging from C1 to C18. Product spectrum is consisting of mostly linear hydrocarbons. Total selectivity of n-hydrocarbons is 94 %. Methane selectivity is about 16.24 %. With the combined catalyst in Figure 4.12b and Figure 4.12c isomerization reactions took place. Total iso saturated and unsaturated product selectivity rose from 6 % to 38.2 % for 0.1 % Pd loading and 37.5 % for 1 % Pd loading. Particularly iso-paraffin selectivity is increased for both metal loadings.

For FT base line experiment, iso-paraffin selectivity is 5.16 %. Addition of HC catalyst increased selectivity to 27.46% for 0.1 % Pd loading and 28.57 % for 1 % Pd loading. Isomerization took place on acid sites as different metal loadings didn't change the selectivities significantly which shows that isomerization was done in the pores of zeolite.

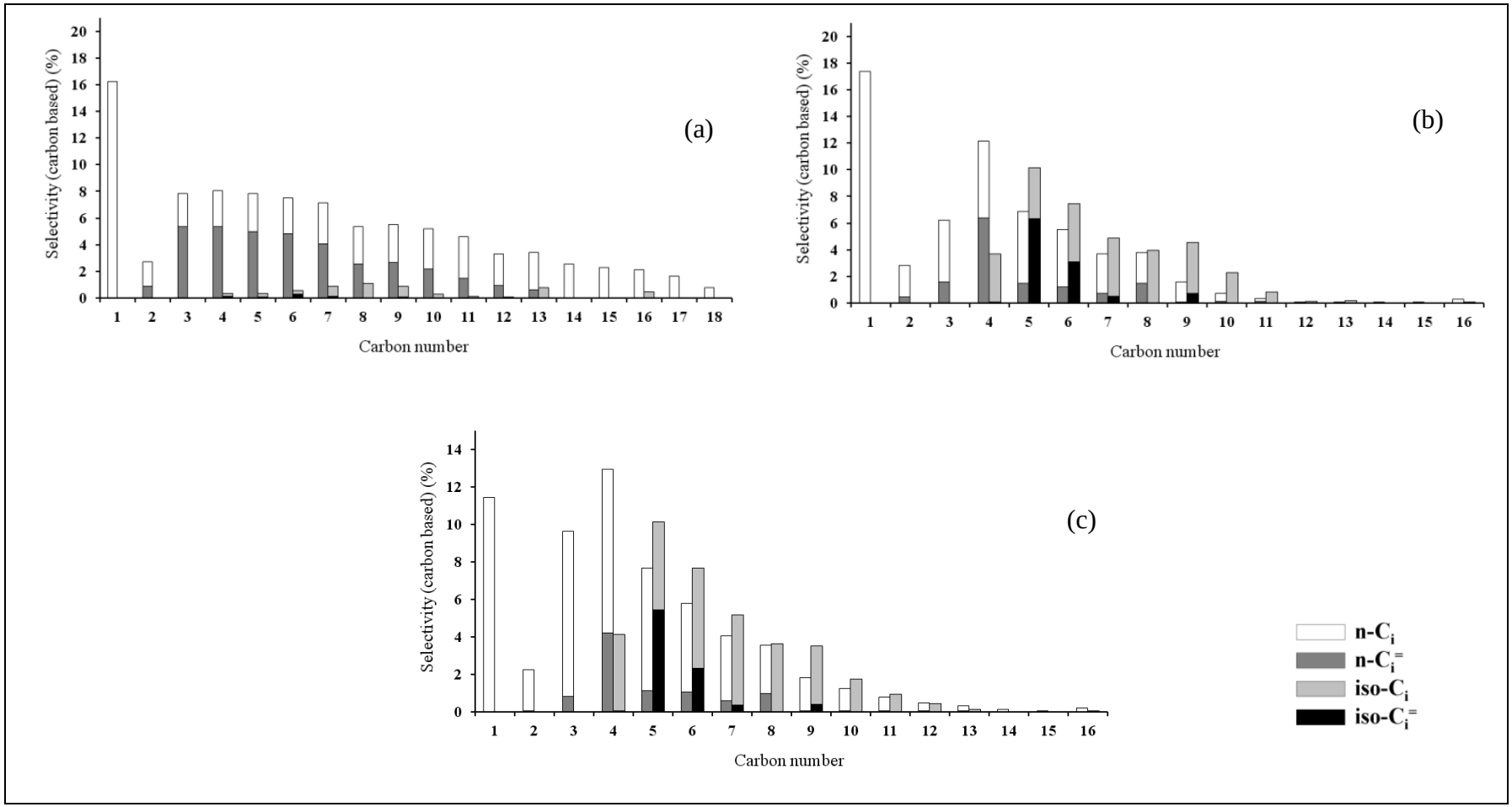

Figure 4.12 : Hydrocarbon selectivity for 60 mL/min flow rate (a) Co/SiO_2, (b) 0.1% Pd/SiO_2 + HMFI90 + Co/SiO_2, (c) 1 % Pd/SiO_2 + HMFI90 + Co/SiO_2. P: 20 bar; T: 225 °C; H_2/CO=2.

Olefin selectivities were also differs for FT and CFTH experiments. For FT experiment, total olefin selectivity was about 36 % which contains mostly linear unsaturated hydrocarbons. On the other hand combined catalyst lowered the olefin selectivities significantly. For 0.1 % Pd loading, total unsaturated product selectivity was about 24 % and for 0.1 % metal loading, olefin selectivity was about 17 %. Increase in the active metal sites could be a reason for lower olefin selectivity for higher metal load since hydrogenation dehydrogenation activity took place on metal site.

Figure 4.13 shows the hydrocarbon selectivity on different catalyst loadings for 30mL/min flow rate. Figure 4.13a shows standard FT synthesis. Figure 4.13b and Figure 4.13c shows CFTH selectivities for 0.1 % and 1 % Pd loadings respectively. Product selectivity ranging from C1 to C18 was limited to C1 to C13 which shows that secondary HC occurred on the combined catalyst. As in the previous flow rates, isomerization took place and iso-hydrocarbon selectivity which was 9 % on Cobalt catalyst was increased to 38 % for 0.1 % Pd loading and 38.3 % for 1% Pd loading. n-paraffins further isomerized on combined catalyst. n-paraffin selectivity is 8 % for cobalt catalyst. It was increased to 29 % for 0.1 % Pd loading and 32 % for 1 % Pd loading. Metal loading didn't change the selectivity much.

Olefins were compromising 32 % of the total products in FT synthesis. Olefin production was suppressed by HC catalyst. For 1 % Pd loading, total olefin selectivity was lowered to 13 % and for 0.1 % Pd loading, it was 20.3 %. As previously observed higher metal loading increased the hydrogenation dehydrogenation function.

Methane selectivity was lowered on 1 % Pd loading. Selectivity lowered from 16 % to 10.72 %. For 0.1 % loading, effect on methane selectivity is insignificant. Methane selectivity was raised to 17.5 %. Little difference between methane selectivities can be negligible.

When the flow rate was lowered to 15mL/min, hydrocarbon selectivities like in Figure 4.14 achieved. Figure 4.14a shows the standard FT synthesis. Product spectrum was ranging from C1 to C18. Figure 4.14b and 4.14c shows the results for combined CFTH selectivities for 0.1 % and 1% Pd loadings respectively.

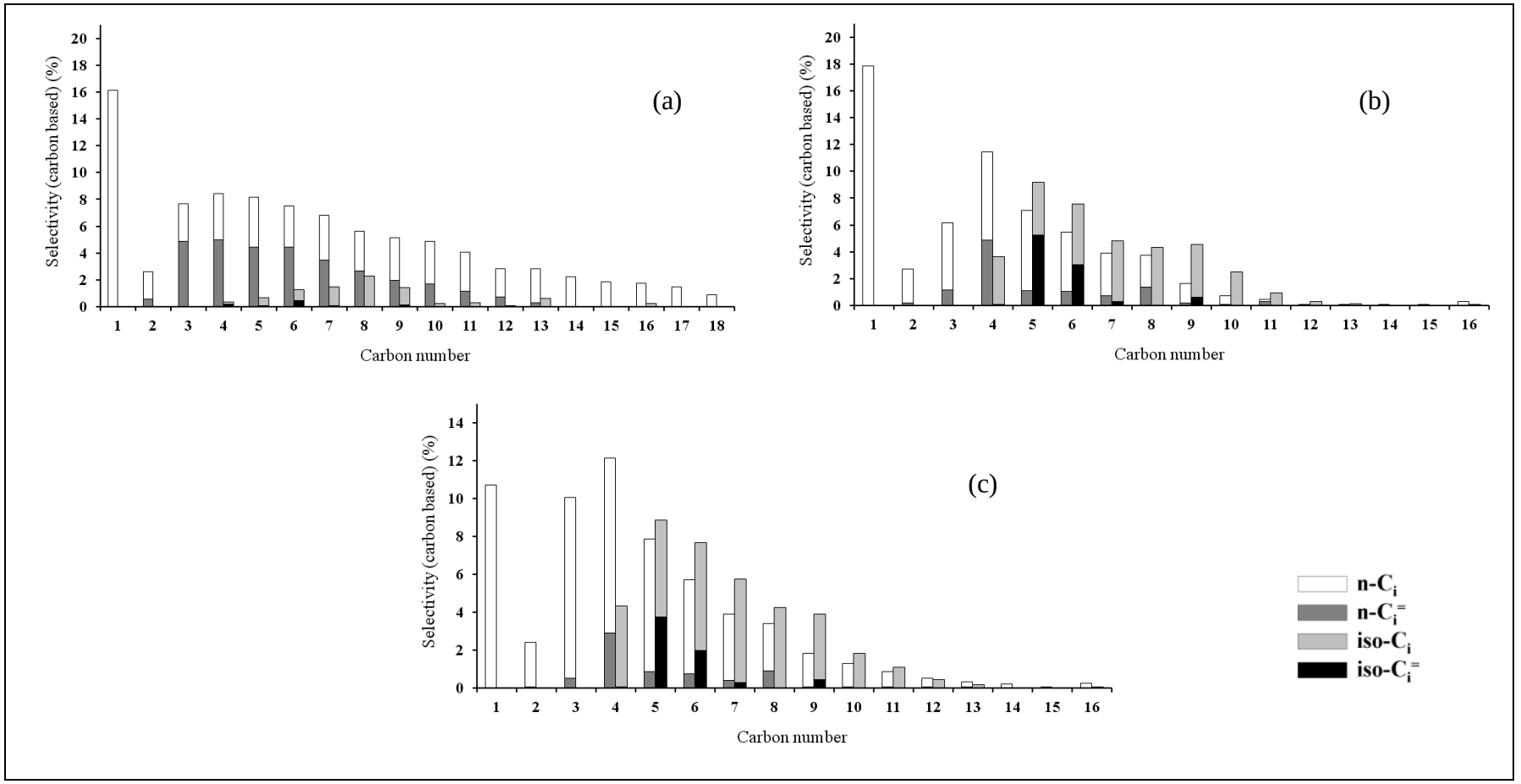

Figure 4.13 : Hydrocarbon selectivity for 30 mL/min flow rate (a) Co/SiO_2, (b) 0.1% Pd/SiO_2 + HMFI90 + Co/SiO_2, (c) 1 % Pd/SiO_2 + HMFI90 + Co/SiO_2, P: 20 bar; T: 225 °C; H_2/CO=2.

Unsaturated products which can be clearly shown in Figure 4.14a make the 29.3 % of the total products. In CFTH experiments, unsaturated product selectivity suppressed to 20.3 % for 0.1% Pd loading and 9.3 % for %1 Pd loading.

Methane selectivity for Cobalt catalyst was 15.3 %. 1 % Pd loading lowered the methane selectivity to 10 % while 0.1 % Pd loading has increased to 19 %. Possible reason for this is at lower metal loading methanoloysis occurred and combined with longer residence time which was ¼ of first experiment; methane selectivity was increased [36].

Iso-products selectivities were increased by the effect of bifunctional catalyst. Total iso products compromise 8.3 % of the total products in FT synthesis. For combined catalyst, iso products in 0.1 % Pd loading experiment was about 35.3 % and in 1 % Pd loading experiment, it was around 39.4 %.

By comparing and examining Figure 4.11, 4.12, 4.13 and 4.14, several results for residence time can be made. Highest conversion rate was achieved at lowest flow rate which is 15 mL/min. There was a steady increase in the n-paraffin selectivity for both metal loadings 0.1% Pd and 1% Pd. Beside from that olefin selectivity decreased as the conversion increased. But changes of selectivity of particular hydrocarbons were not significant so it can be said that conversion rates didn't have important effect on the selectivitties.

Different metal loadings changed the selectivity significantly. While lower metal loading favours more unsaturated products and methane on the other hand higher metal loading favours saturated products which is in line with hydrogenation dehydrogenation function takes place on the metal sites of bifunctional catalyst. Difference in metal loadings didn't alter isomerized products selectivity as isomerization reactions take place on the acid sites.

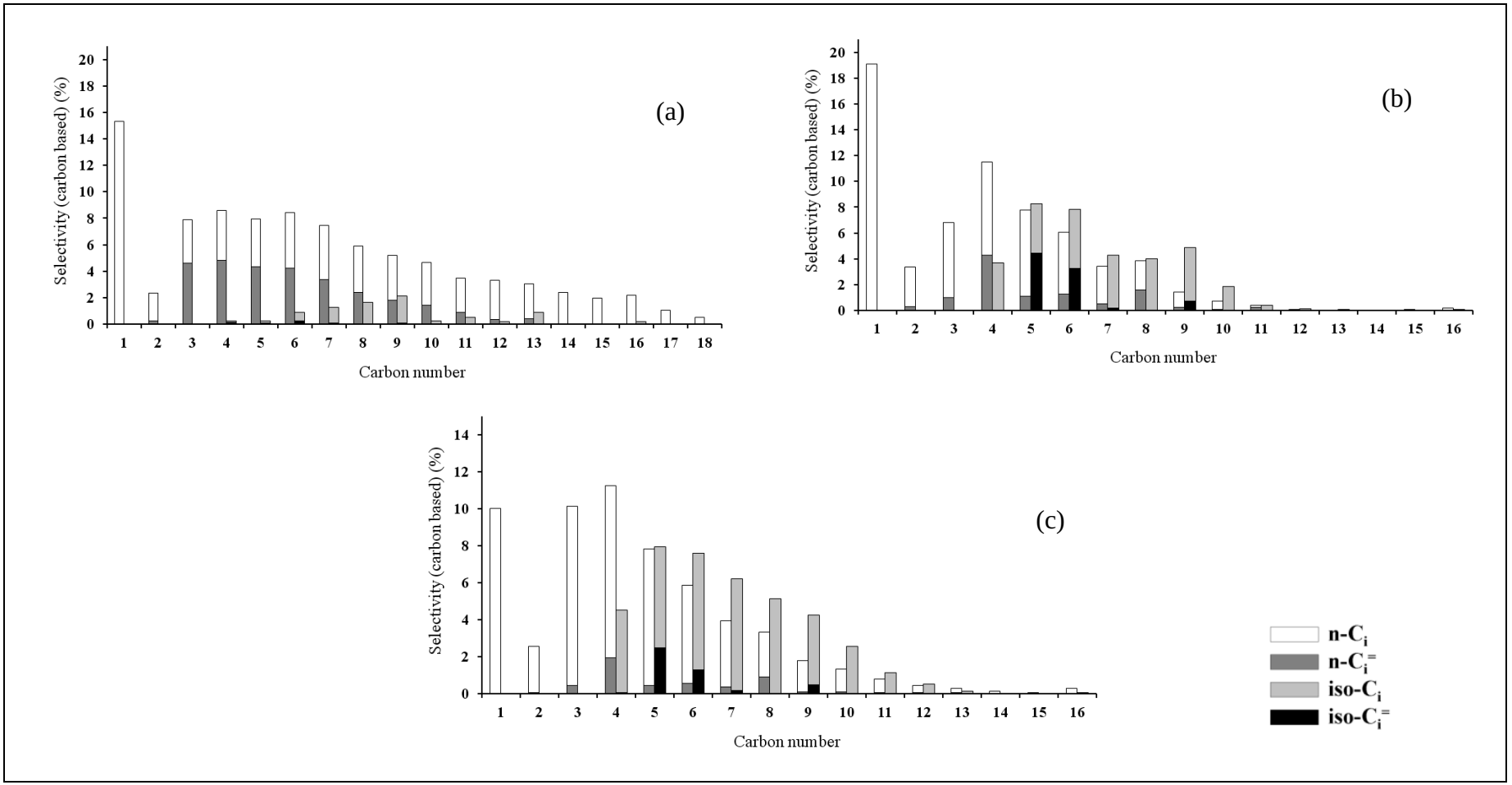

Figure 4.14 : Hydrocarbon selectivity for 15 ml/min flow rate (a) Co/SiO_2, (b) 0.1% Pd/SiO_2 + HMFI90 + Co/SiO_2, (c) 1% Pd/SiO_2 + HMFI90 + Co/SiO_2. P: 20 bar; T: 225 °C; $H_2/CO=2$.

5. CONCLUSIONS AND RECOMMENDATIONS

In this study, performance comparison of Pd/HMFI90 and Pt/HMFI90 bifunctional HC catalysts was done for LTFT synthesis conditions by comparing conversion and selectivities. Pd/HMFI90 was selected as the HC catalyst for the CFTH synthesis experiments. Combination of Pd/HMFI90 and Co catalyst was done and direct synthesis of paraffins from CFTH reactions was achieved. CFTH synthesis was evaluated by examining methane, total paraffin, total olefin and conversion rates.

1. It is possible to combine LTFT synthesis and HC for producing paraffins for diesel fuels. CFTH synthesis shifted the product spectrum to shorter hydrocarbons. Products above C12 have disappeared from the product spectrum. It should be noted that FT catalyst in this study had produced maximum C18. This is due to lower Co content of the catalyst.
2. Pt/HMFI90 catalyst showed poor performance under LTFT conditions. CO and H_2O deactivated the Pt/HMFI90. Higher metal loading on HC catalyst could not overcome the effects of CO and H_2O. For possible future analysis in this field, it is proved that Pt/HMFI90 is not suitable for CFTH processes. In addition, it should be noted that CO deactivation on Pt/HMFI90 was irreversible while H_2O deactivation was reversible.
3. Total olefin selectivity can be reduced by CFTH synthesis. For all flow rates olefins formation rates were suppressed to nearly 40 % of original values. In addition, isomerization of n-paraffins occurred in CFTH synthesis. This result was expected for ZSM-5 catalyst as HC on ZSM-5 favored the isomerization of both paraffin and olefins.
4. Methane selectivity was lowered by increasing the metal loading on HC catalyst. Nearly 50 % of methane produced in FT synthesis was disappeared from the product mixture of CFTH synthesis. 0.1 % Pd loading increased the methane formation rate at longer residence times. This could be a result of loss of hydrogenation property of the catalyst.

5. Residence time altered conversion rates significantly. Higher residence time can increase the conversion rate. On the other hand, effects on the selectivities are negligible.
6. It is observed that CFTH synthesis can be applied to produce gasoline range hydrocarbons as isomerization process occurred on the combined catalyst. Further analysis can be applied by using different catalyst and targeting gasoline range hydrocarbons like aromatic compounds.
7. Further analysis should be made with higher Co content FT catalyst which will enable any research to analyze the results with longer hydrocarbons. In addition to that, different syngas composition can be used in order to suppress total olefin selectivity that will result in deeper analysis of iso paraffin selectivities. Also cetane number comparison between CFTH and commercial oil based diesel fuels can be done in order to measure the success of CFTH.
8. Further research in CFTH area is crucial in optimization for economical feasibility analysis and life cycle assessment for environmental concerns. Different metal and zeolites should be examined and their performance should be tested. Acidity is important factor in isomerization of the hydrocarbons. Effect of acidity should be further analyzed for the isomerization characteristics of different zeolites.
9. For commercial application of synthetic engine fuels production from coal in Turkey, national coal reserves of Turkey should be examined for their applicability in FT operations.

REFERENCES

[1] **International Energy Agency**, (2011). Key world energy statistics, France, http://www.iea.org

[2] **International Energy Agency**, (2010). World energy outlook, France, http://www.iea.org

[3] **Bundestalt für Geowissenschaften und Rohstostoffe**, (2011). Reserven ressourcen und verfügbarkeit von energierohstoffen, Deutschland, http://www.bgr.bund.de

[4] **Republic of Turkey Ministry of Energy and Natural Resources Official Website**, (2011), http://www.enerji.gov.tr

[5] **World Energy Council Turkish National Commitee Official Website**, (2011). http://www.worldenergy.org

[6] **Kural, O.**, (1998). Kömür Özellikleri, Teknolojisi ve Çevre İlişkileri, İstanbul

[7] **Türkiye Kömür İşletmeleri**, (2010). Yıllık Faaliyet Raporu, Ankara, http://www.worldenergy.org/

[8] **Türkiye Taş Kömürü Kurumu,** (2010). Yıllık Faaliyet Raporu, Ankara, http://www.taskomuru.gov.tr

[9] **World Coal Association,** (2011). Coal and Steel Facts, London, http://www.worldcoal.org

[10] **Verein der Kohlen Importeure,** (2011). Annual Report, Germany, http://www.verein-kohlenimporteure.de

[11] **Fossil Energy study guides.** (2011). In United States Department of Energy Office of Fossil Energy website. Date retvieved: 15.07.201, adress: http://fossil.energy.gov/education/energylessons

[12] **Higman, C., & van der Burght, M.**, (2007). Gasification Second Edition, Gulf Professional Publishing, United States.

[13] **World Coal Association**, (2009). Coal: Liquid Fuels, London, http://www.worldcoal.org

[14] **Speight, J.**, (2008). Synthetic Fuels Handbook Properties, Process and Performance, Mc Graw Hill Hanbooks, United States of America

[15] **Dry, M.E.,** (2001). High quality diesel via Fischer-Tropsch process-a review, *Journal of Chemical Technology and Biotechnology*, **77**, 43-50

[16] **Dry, M.E.,** (2002). The Fischer Tropsch Process 1950-2000, *Catalysis Today*, **71**, 227-241

[17] **Schulz, H.,** (1999). Short history and present trends of Fischer-Tropsch synthesis, *Applied Catalysis A: General*, **186**, 3-12

[18] **Dry, M.E.**, (1999). Fischer-Tropsch reactions and the environment, *Applied Catalyst A: General*, **189**,185-190

[19] **Dry, M.E.**, (2004), Chemical concepts used for engineering purposes, *Studies in Surface Science and Catalysis*, **152**, 196-257

[20] **Hussain, S. T., Mazhar, M., & Nadeem, M. A.**, (2009). Suppression of methane formation during Fisher-Tropsch synthesis using manganese-cobalt oxide supported on H-5A zeolite as a catalyst, *Journal of Natural Gas Chemistry*, **18**, 187-190

[21] **Steynberg, A.P, Espinoza, R.L., Jager, B., Vosloo, A.C.**, (1999). High temperature Fischer–Tropsch synthesis in commercial practice, *Applied Catalysis A: General* , **186**, 41- 54.

[22] **Subiranas, A. M.**, (2009). Combining Fischer-Tropsch synthesis and hydrocarbon reactions in one reactor, Universitat Verlag Karlsruhe, Germany.

[23] **Steynberg, A.P., Dry, M.E., Davis, B.H., & Breman, B.B.**, (2004). Fischer-Tropsch Reactors, *Studies in Surface Science and Catalysis*, **152**, 64-195

[24] **Espinoza, R.L., Steynberg, A.P., Jager, B., & Vosloo, A.C.**, (2004). Low temperature Fischer–Tropsch synthesis from a Sasol perspective, *Applied Catalysis A: General* **186** 13-26

[25] **Jager, B.**, (1997). Developments in Fischer-Tropsch technology, *Natural Gas Conversion IV*, **107**, 219:224

[26] **Dry, M. E.**, (2004). FT Catalysts, *Studies in Surface Science and Catalysis*, **152**, 533-600

[27] **Dokun, T. B. A.**, (2010). Fischer-Tropsch Catalyst Structures and Process Design for JP-5 fuel integrated wirh MFEC, UMI Dissertation Publishing, United States

[28] **van der Laan, G. P.**, (1999). Kinetics Selectivity and Scale up of the Fischer-Tropsch Synthesis, Cip-Gegevens Koninklijke Bibliotheek, Nethertlands

[29] **Tsakoumis, N. E., Rønning, M., Borg, Ø., Rytter, & E., Holmen, A**., (2010). Deactivation of cobalt based Fischer–Tropsch catalysts: A review, Catalysis Today,**154**,162-182

[30] **Bukur, D.B., Koranne, M., Lang, X., Rao, & Huffman, G.P.**,(1995). Pretreatment effect studies with a precipitated iron Fischer-Tropsch catalyst, *Applied Catalysis A*, 126, 85–113.

[31] **Dry, M.E.,** (1981). The Fischer-Tropsch synthesis, *Catalysis Science and technology*, **1**, 160-255

[32] **Dictor, R.A.**, **& Bell, A.T.**, (1986). Fischer-Tropsch synthesis over reduced and unreduced iron oxide catalysts, *Journal of Catalysis*,**97**, 121-136

[33] **Iglesia, E., Reyes, S.C., & Madon, R.J.** , (1991). Transport-enhanced E -olefin readsorption pathways Ru-catalyzed hydrocarbon synthesis, *Journal of Catalysis*,**129**, 238-256

[34] **Donnelly, T.J., & Satterfield, C.N.**, (1989). Product distributions of the Fischer-Tropsch synthesis on precipitated iron catalysts, *Appied. Catalysis A,* **52**, 93- 114.

[35] **Scherzer, J., & Gruia, A.**, (1996). Hydrocracking Science and Technology, CRC Press, United States

[36] **Böhringer, W., Kotsiopoulos, A., de Boer, M., Knottenbelt, C., & Fletcher, J.C.Q.** , (2007). Selective Fischer-Tropsch wax hydrocracking – opportunity for improvement of overall gas-to-liquids processing Fischer Tropsch Synthesis, *Fischer-Tropsch Synthesis Catalyst and Catalysis*, **163**, 345-365

[37] **Ruthven, D. M.**, (1984), Principles of Adsorption and Adsoprtion Processes, John Wiley and Sons, US

[38] **Martens, J., & Jacobs, P.A.**, (2001). Introduction to acid catalysis with zeolites in hydrocarbon reactions, *Studies in Surface Science and Catalysis*, **137**, 633-672

[39] **Jentys, A., & Lercher, J.A.**, (2001), *Techniques of zeolite characterization, Studies Surface Science and Cataly*sis, **137**,345-386

[40] **Csicsery, S.**, (1986). Catalysis by shape selective zeolite – science and technology, *Pure and Applied Chemistry*, **58**, 841-856

[41] **Maxwell, I.E., & Stork, W.H.J.**, (1991). Hydrocarbon Processing with zeolites, *Introduction to Zeolite Science and Practice*, **58**, 571-630

[42]**Broach, R. W.**, (2010), Zeolite Types and Structures, Zeolites in Industrial Seperation and Catalysis, 27-60

[43] **Kukard, R.S.**, (2008). The Effect of Zeolite Type on the Hydrocracking of Long n-Paraffins, Department of Chemical Engineering University of Cape Town, South Africa

[44] **Steinberg, K., Mroczek, U. & Roessner, F.**, (1990). Aromatization of Ethane on Platinum Containing ZSM-5 Zeolites. *Applied Catalysis*, **66**, 37-44

[45] **Martínez, A., Rollán, J., Arribas, M. A., Cerqueira, H.S., Costa, A.F., & Aguiar, E.F.S.**, (2007). A detailed study of the activity and deactivation of zeolites in hybrid Co/SiO2- zeolite Fischer–Tropsch catalysts, *Journal of Catalysis*, **249,**162-173

[46] **Mirth, G., Cejka, J., Krtil, & Lercher, A.J.**, (1994). Deactivation and coking of HZSM5 catalysts during alkylation reactions, *Studies in Surface Science and Catalysis*, **88**, 241-248

[47] **Li, J., Zhan, X, Zhang, Y, Jacobs, G, Das, T., & Davis, B. H.**, (2002). Fischer–Tropsch synthesis: effect of water on the deactivation of Pt promoted Co/Al2O3 catalysts, *Applied Catalysis A:General*, **228**, 203-212

[48] **Tsubaki, N., Yoneyama, Y., Michiki, K., & Fujimoto, K.**, (2003). Three-component hybrid catalyst for direct synthesis of isoparaffin via modified Fischer Tropsch synthesis, *Catalysis Communications*, **4**, 108–111

[49] **Liu, Z.W., Li, X.,Asami, K., & Fujimoto, K.**, (2005), Iso-paraffins synthesis from modified Fischer-Tropsch reaction- Insights into Pd/beta and Pt/beta catalysts *Catalysis Today*, **104**, 41–47

[50] **Nakamura, I., & Fujimoto, K.**, (1996). Hydrocracking of paraffinic hydrocarbons over hybrid catalysts containing H-ZSM-5 zeolite and supported hydrogenation catalyst, *Catalyst in Petroleum Refining and Petrochemical Industries*, 235-242

[51] **Li, X., Luo, M., & Asami, K.**, (2004). Direct synthesis of middle iso-paraffins from synthesis gas on hybrid catalysts , *Catalysis Today*, **89**, 439-446

[52] **Yoneyama, Y. , He, J., Morii, Y., Azuma, S., &Tsubaki, N.**, (2005), Direct synthesis of isoparaffin by modified Fischer–Tropsch synthesis using hybrid catalyst of iron catalyst and zeolite, *Catalysis Today*, **104**, 37–40

[53] **Brosius R.**, (2010). Pd/HMFI90 Hydrocracking Catalyst Performance under Low Temperature Fischer Tropsch Conditions experiment notes, Cape Town

[54] **Kraum, M., & Baerns, M.**, (1999). Fischer–Tropsch synthesis: the influence of various cobalt compounds applied in the preparation of supported cobalt catalysts on their performance, *Applied Catalysis A: General*, **186**, 189-200

[55] **Dykyj J., Svoboda J., Wilhoit R.C., Frenkel M., & Hall K.R.**, (1999). Vapor Pressure and Antoine Constants for Hydrocarbons, and Sulfur, Selenium, Tellurium, and Halogen Containing Organic Compounds, Springer-Verlag, 1999

APPENDICES

APPENDIX A.1: Process flow diagram of the experimental setup

APPENDIX A.1

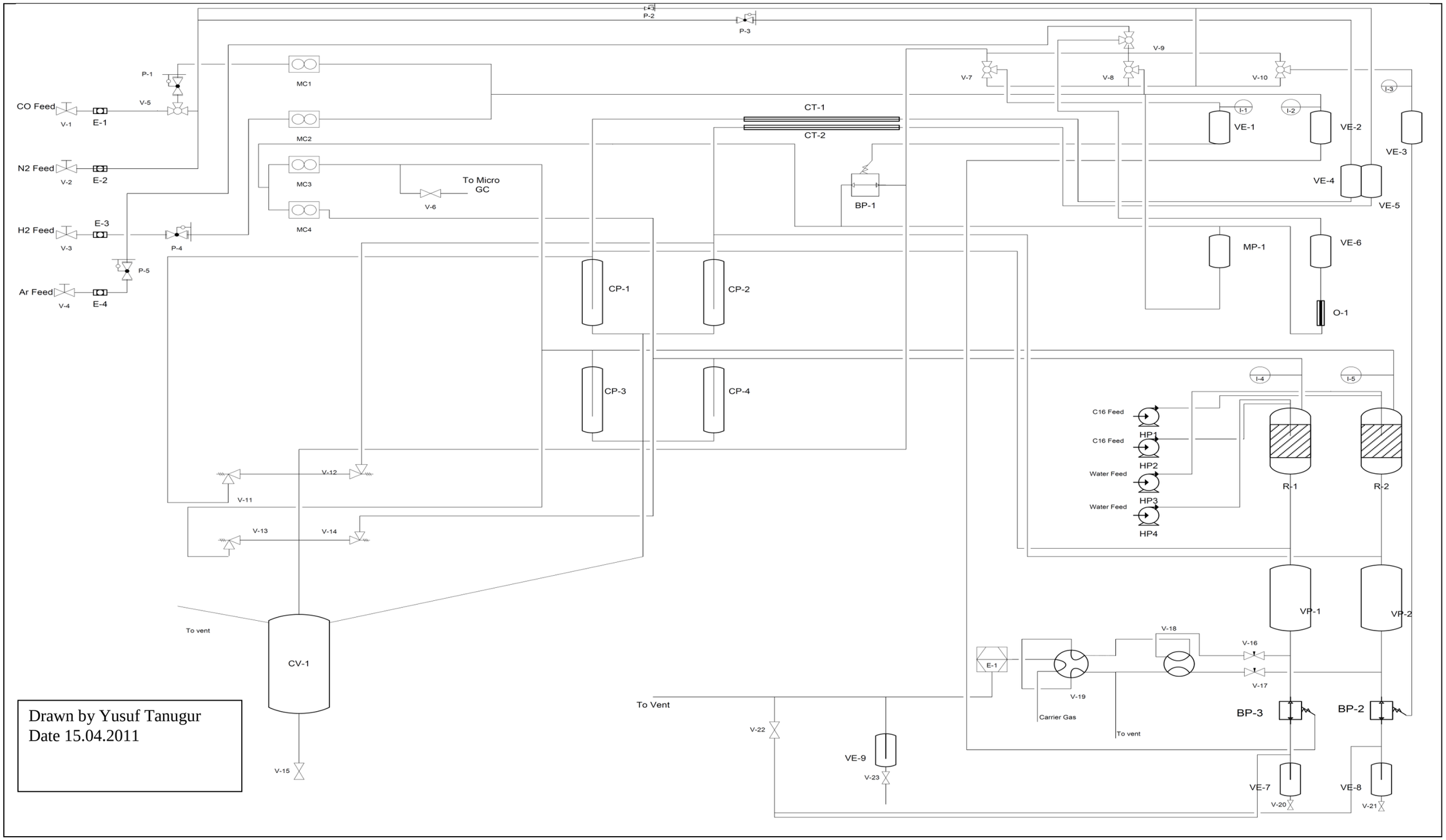

Figure A.1 : Process flow diagram of the experimental setup.

Table A.1 : Equipment list for PFD.

Unit Name	Description	Unit Name	Description
V-1	CO Feed Valve	CP-1	Vaporizer Catch Pot
V-2	N2 Feed Valve	CP-2	Vaporizer Catch Pot
V-3	H2 Feed Valve	CP-3	Reactor Catch Pot
V-4	Ar Feed Valve	CP-4	Reactor Catch Pot
E-1	CO Feed Filter	CT-1	Capillary Tube
E-2	N2 Feed Filter	CT-2	Capillary Tube
E-3	H2 Feed Filter	MP-1	Mixing Pot
E-4	Ar Feed Filter	O-1	Orifice
P-1	Pressure Drop Regulator	V-16	Needle Valve
P-2	Pressure Drop Regulator	V-17	Needle Valve
P-3	Pressure Drop Regulator	V-18	Rotating Valve
P-4	Pressure Drop Regulator	V-19	Sample Valve
P-5	Pressure Drop Regulator	E-1	Gas Chromatograhy Equipment
MC -1	CO/N2 Flow Controller	VE-1	Pressure Control Vessel
MC -2	H2 Flow Controller	VE-2	Pressure Control Vessel
MC -3	Reactor 2 Flow Controller	VE-3	Pressure Control Vessel
MC -4	Reactor 1 Flow Controller	VE-4	N2 Vessel
V-5	3 Way Valve	VE-5	N2 Vessel
V-6	Bypass line valve	VE-6	Ar Vessel
V-7	3 Way Valve	VE-7	Reactor 1 Outlet Collecting Vessel
V-8	3 Way Valve	VE-8	Reactor 2 Outlet Collecting Vessel
V-9	3 Way Valve	V-20	Gate Valve
V-10	3 Way Valve	V-21	Gate Valve
BP-1	Mixing Pot Back Pressure Regulator	V-22	Gate Valve
BP-2	Reactor 2 Back Pressure Regulator	V-23	Gate Valve
BP-3	Reactor 1 Back Pressure Regulator	VE-9	Collecting Vessel
R-1	Reactor 1	I-1	Mixing Pot Pressure Indicator
R-2	Reactor 2	I-2	Reactor Outlet Pressure Indicator
VP-1	Vaporizer 1	I-3	Reactor Outlet Pressure Indicator
VP-2	Vaporizer 2	I-4	Reactor Inlet Pressure Indicator
HP-1	C16 feed HPLC Pump	I-5	Reactor Inlet Pressure Indicator
HP-2	Water feed HPLC Pump		
HP-3	C16 feed HPLC Pump		
HP-4	Water feed HPLC Pump		
V-11	Pressure Relief Valve		
V-12	Pressure Relief Valve		
V-13	Pressure Relief Valve		
V-14	Pressure Relief Valve		
CV-1	Collecting Vessel		
V-15	Gate Valve		

CURRICULUM VITAE

Name Surname: Yusuf Tanuğur

Place and Date of Birth: Istanbul 08.05.1987

Address: Icadiye Mah. Cemil Meric Sok No: 46/10 Uskudar/ Istanbul

E-Mail: ytanugur@yalova.edu.tr

BSc: Chemical Engineering-Istanbul Technical University Chemical and Metalurgical Engineering Department

Professional Experience and Rewards:

2010 January - : Research and Teaching Assistant, Yalova University, Energy Systems Engineering Department

2011: YOK (The Council of Higher Education) – 6 month Abroad Master Research Scholarship for the Research Topic 'Low Temperature Co Based Fischer Tropsch Sythesis and Hydrocracking', University of Cape Town Chemical Engineering Department, South Africa

PUBLICATIONS/PRESENTATIONS ON THE THESIS

- Başakçılardan Kabakcı S., **Tanugur Y.**, 2010: Waste in the Renewable Energy Legislations of European Union, United States and Turkey, *10. International Conferance on Clean Energy (ICCE 2010)*, June 15-17, 2010 Famagusta, Cyprus

- **Tanuğur Y.**, Mersin İ.E., Başakcılardan Kabakcı, S., 2011 : Örnek Bir Gençlik Projesi: Genç Neslin Gözünden Enerji Verimliliği ,*8.Ulusal Temiz Enerji Sempozyumu*, 1-5 December, 2010 , Bursa, Turkey